Ingeniería e Investigación
Journal
Abbreviated Journal Title: **Ing. Investig.**

Editor-in-chief
Andrés Pavas, Ph.D.

Editorial Assistants
Fabián Hernando Ríos, B. Eng.
Jennifer Zuluaga Tapia B. Eng.

Frequency
Quarterly, 3 issues per year
April, August and December

Cover Layout
Carlos Andrés Ortiz Valle

Proofreader
Janeth Alejandra García

Layout Artist
Patricia Chavez R.

Photography
Courtesy of the Dept. of Electrical and Electronic Engineering (Anonymous Author)

Printing
Corcas Editores S.A.S.

For additional information contact
revii_bog@unal.edu.co
Bogotá - Colombia
April - 2019

Table of Contents

Editorial 3

Chemical Engineering / Food Engineering / Environmental Engineering

Analysis and modeling of the hydraulic behavior of EGSB reactors with presence and absence of granular biomass at different hydraulic retention times 6
Yudy Andrea Londoño, Laura Victoria Castrillón, Nancy J. Pino, Edwin Lenin Chica, and Gustavo A. Peñuela

Process simulation for xylitol production from brewer's spent grain in a Colombian biorefinery. Part 1: Xylose production from arabinoxilans extracted by the alkaline pretreatment of BSG 15
Andrés A. Gil-Montenegro, Juan S. Arocha-Morales, Lilia C. Rojas-Pérez, and Paulo C. Narváez-Rincón

Study of coagulating/flocculating characteristics of organic polymers extracted from biowaste for water treatment 24
Brenda Buenaño, Edwin Vera, and María B. Aldás

Civil Engineering / Sanitary Engineering

Assessment of groundwater level variations using multivariate statistical methods 36
Fausto Molina-Gómez, Lenin A. Bulla-Cruz, Luis Á. Moreno-Anselmi, Juan C. Ruge, and Carol Arévalo-Daza

Electrical Engineering / Telecommunications Engineering

Support for incident management in optical networks through critical points identification 43
Aminadabe B. Sousa, Alberto S. Lima, Neuman de Souza, and J. A. B. Moura

Industrial Engineering

Procedure for the continuous improvement of human resource management 53
Germán Gemar, Ana M. Negrón-González, Carlos J. Lozano-Piedrahita, Vanesa F. Guzmán-Parra, and Norberto Rosado

Mechanical Engineering / Materials Engineering

Modeling and simulation for mechanical behavior of modified biocomposite for scaffold application 63
Jenan S. Kashan, and Saad M. Ali

Instructions for Authors 77

Papers published in *Ingeniería e Investigación journal* are abstracted/indexed in

- Science Citation Index Expanded (SciSearch®), Clarivate Analytics
- Scopus - Elsevier
- Scientific Electronic Library Online - SciELO, Colombia
- Chemical Abstract
- Índice de Revistas Latinoamericanas en Ciencias Periódica
- Dialnet
- Sistema Regional de Información en Línea para Revistas Científicas de América Latina, El Caribe, España y Portugal - Latindex
- Ebsco Publishing
- DOAJ - Directory of Open Access Journals
- Redib - Red Iberoamericana de Innovación y Conocimiento Científico

Ingeniería e Investigación journal was created in 1981. This is an entity in charge of spreading the teaching, scientific and technical research developed in the Universidad Nacional de Colombia's Engineering Faculty and other national and international institutions. *Ingeniería e Investigación journal* deals with original, unedited scientific research and technological developments in the various disciplines related to engineering. *Ingeniería e Investigación journal* contributes towards the development of knowledge, generating a global impact on academia, industry and society at large, through an exchange of knowledge and ideas maintaining a set of serious and recognized quality standards.

Ingeniería e Investigación journal publications are developed for the academic community who is interested in research and engineering knowledge development. We invite readers to be part of this Journal and participate either as authors, peer reviewers or subscribers.

For additional information contact:
www.revistas.unal.edu.co/index.php/ingeinv
E-mail: revii_bog@unal.edu.co
Tel: 57(1) 3 16 5000 Ext. 13674

Tabla de Contenido

Editorial 3

Ingeniería Química / Ingeniería de Alimentos / Ingeniería Ambiental

Análisis y modelación del comportamiento hidráulico de reactores EGSB en presencia y ausencia de biomasa granular a diferentes tiempos de retención hidráulica 6
Yudy Andrea Londoño, Laura Victoria Castrillón, Nancy J. Pino, Edwin Lenin Chica y Gustavo A. Peñuela

Simulación de proceso para la producción de xilitol a partir de bagazo de cebada en una biorrefinería en Colombia. Parte 1: producción de xilosa a partir de arabinoxilanos extraídos en el pretratamiento alcalino de BSG 15
Andrés A. Gil-Montenegro, Juan S. Arocha-Morales, Lilia C. Rojas-Pérez y Paulo C. Narváez-Rincón

Estudio de las características coagulantes/floculantes de polímeros orgánicos extraídos de residuos para el tratamiento de agua 24
Brenda Buenaño, Edwin Vera y María B. Aldás

Ingeniería Civil / Ingeniería Sanitaria

Evaluación de cambios en el nivel freático mediante métodos estadísticos multivariados 36
Fausto Molina-Gómez, Lenin A. Bulla-Cruz, Luis Á. Moreno-Anselmi, Juan C. Ruge y Carol Arévalo-Daza

Ingeniería Eléctrica/ Ingeniería de Telecomunicaciones

Soporte de gestión de incidentes de redes ópticas a través de la identificación de puntos críticos 43
Aminadabe B. Sousa, Alberto S. Lima, Neuman de Souza y J. A. B. Moura

Ingeniería Industrial

Procedimiento para la mejora continua de la gestión de recursos humanos 53
Germán Gemar, Ana M. Negrón-González, Carlos J. Lozano-Piedrahita, Vanesa F. Guzmán-Parra y Norberto Rosado

Ingeniería Mecánnica / Ingeniería de Materiales

Modelado y simulación para el comportamiento mecánico de un biocompuesto modificado para la aplicación de andamios 63
Jenan S. Kashan y Saad M. Ali

Instrucciones para Autores (Inglés) 77

Editorial

Español

Actualización de los posicionamientos de revistas 2018 y los indicadores bibliométricos

La presente nota editorial resume los resultados más recientes del posicionamiento de la revista *Ingeniería e Investigación* en índices bibliográficos mundiales. Además, se muestran novedades sobre la inclusión en uno de los índices bibliográficos de alcance latinoamericano.

Novedades

La revista *I&I* comparte el espíritu de la "Declaración de San Francisco sobre Evaluación de la Investigación" – DORA[1]. Sin embargo, la Universidad Nacional de Colombia aún no ha abordado la discusión sobre algunos aspectos puntuales definidos en DORA y no ha tomado una determinación acerca de su compromiso institucional con esta iniciativa. La revista I&I no es ajena a los lineamientos institucionales de la Universidad Nacional de Colombia, pero está comprometida con el acceso abierto y la evaluación responsable. También consideramos fundamental el respeto por la autonomía y la independencia de los autores, los lectores y las instituciones en definir sus políticas y visiones. Por lo tanto, la Revista I&I no cumple uno de los requerimientos recientes exigidos por Redalyc para la evaluación e inclusión de revistas en sus índices[2] y, en consecuencia, ha sido excluida de este espacio. Lamentamos profundamente la afectación que el requerimiento de Redalyc y la consecuente exclusión de la revista puedan causar a nuestros autores.

A continuación, siguiendo las recomendaciones de la Declaración de San Francisco, presentamos un resumen de los indicadores de citación en diferentes sistemas de indexación y citación con fines informativos.

Avances

La Revista I&I mantiene su presencia en los principales índices comprometidos con el acceso abierto, como se ha mencionado en ocasiones anteriores (Pavas, 2018a; Pavas y Arzola, 2018). Las publicaciones de I&I permanecen visibilizadas a través de DOAJ y SciELO. En notas editoriales previas, se han presentado análisis sobre las posibilidades de mejorar los indicadores y posicionamiento en los índices bibliográficos (Pavas, 2017; Pavas, 2018b), resaltando que una política editorial clara y un trabajo continuo pueden facilitar el mejoramiento de la visibilidad y el posicionamiento. A continuación, se

[1]https://sfdora.org/read/es/
[2]https://www.redalyc.org/redalyc/editores/evaluacionCriterios.html

English

Update of 2018 journal rankings and bibliometric indicators

This editorial note summarizes the most recent results of the ranking of the *Ingeniería e Investigación* journal in world bibliographic indexes. In addition, it shows news about the participation of the journal in one of the bibliographic indexes of the Latin American scope.

News

The *I&I* journal shares the spirit of the San Francisco Declaration on Research Assessment – DORA[1]. However, the Universidad Nacional de Colombia has not yet addressed the discussion on some specific aspects defined in DORA and has not made a determination about its institutional commitment to this initiative. The *I&I* journal is not exempt of to the institutional guidelines of the Universidad Nacional de Colombia, but is committed to open access and responsible evaluation. We also consider as fundamental the respect for the autonomy and independence of authors, readers and institutions in defining their policies and visions. Therefore, the *I&I* Journal does not meet one of the recent requirements demanded by Redalyc for the evaluation and inclusion of journals in its indexes[2] and, consequently, it has been excluded from this network. We deeply regret the inconveniences that the requirement of Redalyc and the consequent exclusion of the journal may cause to our authors.

Next, following the recommendations of the San Francisco Declaration, we present a summary of the citation indicators in different indexing and citation systems for information purposes.

Advance

The *I&I* journal maintains its presence in the main indexes committed to open access, as mentioned on previous occasions (Pavas, 2018a; Pavas and Arzola, 2018). Besides, *I&I* publications remain visible through DOAJ and SciELO. Previous editorial notes have presented analyses on the possibilities of improving indicators and the rank in bibliographic indexes (Pavas, 2017; Pavas, 2018b), highlighting that a clear editorial policy and continuous work can facilitate the improvement of visibility and ranking. Below are the results achieved by the *Ingeniería e Investigación* journal.

[1]https://sfdora.org/read/es/
[2]https://www.redalyc.org/redalyc/editores/evaluacionCriterios.html

muestran los resultados alcanzados por la Revista Ingeniería e Investigación.

Indicadores en SciELO

Los indicadores de impacto más recientes de la Revista en SciELO[3] se presentan en la Tabla 1.

Tabla 1. Indicadores de citación de la Revista Ingeniería e Investigación en SciELO

Año	2015	2016	2017	2018
Artículos	59	43	42	34
Total citas	90	122	79	84
Factor de impacto (3 anos)	0,1484	0,2199	0,1781	0,2014

Fuente: Los autores

Indicadores en Google Scholar

Los resultados de la Tabla 2 fueron obtenidos de la página web de Google Scholar y a partir del software Publish or Perish.

Tabla 2. Indicadores de citación de la Revista Ingeniería e Investigación en Google Scholar

Año	2015	2016	2017	2018
Artículos	62	44	44	37
Citas desde el ano en cabecera hasta ano 2019	450	255	120	47
Documentos hasta 2019	187	125	81	37
Citas/Documento	2,41	2,04	1,48	1,27
h5	7	7	8	10
mediana h5	9	8	12	14

Fuente: Los autores

Indicadores en el *Scimago Journal Rank* – SJR

La medición más reciente del SJR arrojó un nuevo posicionamiento para la revista *Ingeniería e Investigación*, que alcanzó el cuartil 2. En la Tabla 3, se resumen los valores que la revista ha obtenido en el ranking del grupo Scimago.

Tabla 3. Indicadores de citación de la Revista Ingeniería e Investigación en el *Scimago Journal Rank*

Año	2015	2016	2017	2018
Artículos	61	44	44	28
Citas 3 anos	57	77	83	90
Citas/Documento	0,456	0,562	0,589	0,643
SJR	0,159	0,204	0,189	0,164
Cuartil	Q3	Q3	Q3	Q2

Fuente: Los autores

[3] shorturl.at/swST1

Indicators in SciELO

The most recent impact indicators of the Journal in SciELO are presented in Table 1.

Table 1. Citation indicators of the *Ingeniería e Investigación* journal in SciELO

Year	2015	2016	2017	2018
Articles	59	43	42	34
Total citations/cites	90	122	79	84
Impact factor (3 years)	0,1484	0,2199	0,1781	0,2014

Source: The authors

Indicators in Google Scholar

Results in Table 2 were obtained from the Google Scholar website and from the Publish or Perish software.

Table 2. Citation indicators of the *Ingeniería e Investigación* journal in Google Scholar

Year	2015	2016	2017	2018
Articles	62	44	44	37
Citations from the year on top to 2019	450	255	120	47
Documents until 2019	187	125	81	37
Citations/Document	2,41	2,04	1,48	1,27
h5	7	7	8	10
h5 median	9	8	12	14

Source: The authors

Indicators in the Scimago Journal Rank - SJR

The most recent SJR measurement showed a new ranking for the *Ingeniería e Investigación* journal, which reached quartile 2. Table 3 summarizes the values that the journal has obtained in the SJR.

Table 3. Citation indicators of the *Ingeniería e Investigación* journal in the Scimago Journal Rank

Year	2015	2016	2017	2018
Articles	61	44	44	28
Citations (3 years)	57	77	83	90
Citations/Document	0,456	0,562	0,589	0,643
SJR	0,159	0,204	0,189	0,164
Quartile	Q3	Q3	Q3	Q2

Source: The authors

Posicionamiento en *Journal Citation Report* - JCR

Los indicadores de citación del JCR muestran una tendencia creciente de las citas de la revista, como se ve en la Tabla 4.

Tabla 4. Indicadores de citación de la Revista Ingeniería e Investigación en el *Journal Citation Report*

Año	2015	2016	2017	2018
Artículos	43	41	41	34
Total citas	72	108	162	219
Factor de impacto de la revista	0,278	0,28	0,455	0,575

Fuente: Los autores

Referencias

Pavas, Andrés (2017). Are there chances of improving Colombian engineering journals rankings? *Ingeniería e Investigación*, *37*(3), 3-7, DOI: 10.15446/ing.investig.v37n3.69519

Pavas, Andrés (2018a). Novelties in the 2017 SJR for Engineering journals ranking. *Ingeniería e Investigación*, *38*(2) 3-8, DOI: 10.15446/ing.investig.v38n2.73400

Pavas, Andrés (2018b). What are the differences between engineering journal performances? *Ingeniería e Investigación*, *38*(1) 3-7, DOI: 10.15446/ing.investig.v38n1.71250

Pavas, Andrés y Arzola, Nelson (2018). Gestión Editorial de la Revista Ingeniería e Investigación. *Ingeniería e Investigación*, *38*(3) 3-7, DOI: 10.15446/ing.investig.v38n3.76946

ANDRÉS PAVAS
Director Revista *Ingeniería e Investigación*
Profesor Asociado
Departamento de Ingeniería Eléctrica y Electrónica
Universidad Nacional de Colombia
http://orcid.org/0000-0002-0971-0725

NELSON ARZOLA DE LA PEÑA
Editor Asociado Revista *Ingeniería e Investigación*
Profesor Titular
Departamento de Ingeniería Mecánica y Mecatrónica
Universidad Nacional de Colombia
https://orcid.org/0000-0002-5004-113X

Ranking in the *Journal Citation Report* - JCR

The citation indicators of the JCR evidence a growing trend in the citations of the journal, as shown in Table 4.

Table 4. Citation indicators of the *Ingeniería e Investigación* journal in the Journal Citation Report

Year	2015	2016	2017	2018
Articles	43	41	41	34
Total citations	72	108	162	219
Journal Impact Factor	0,278	0,28	0,455	0,575

Source: The authors

Reference

Pavas, Andrés. (2017). Are there chances of improving Colombian engineering journals rankings? *Ingeniería e Investigación*, *37*(3), 3-7. DOI: 10.15446/ing.investig.v37n3.69519

Pavas, Andrés. (2018a). Novelties in the 2017 SJR for Engineering journals ranking. *Ingeniería e Investigación*, *38*(2) 3-8. DOI: 10.15446/ing.investig.v38n2.73400

Pavas, Andrés. (2018b). What are the differences between engineering journal performances? *Ingeniería e Investigación*, *38*(1) 3-7. DOI: 10.15446/ ing.investig.v38n1.71250

Pavas, Andrés and Arzola, Nelson. (2018). Gestión Editorial de la Revista Ingeniería e Investigación. *Ingeniería e Investigación*, *38*(3) 3-7. DOI: 10.15446/ing.investig.v38n3.76946

ANDRÉS PAVAS
Head Editor of *Ingeniería e Investigación*
Associate Professor
Department of Electrical and Electronic Engineering
Universidad Nacional de Colombia
http://orcid.org/0000-0002-0971-0725

NELSON ARZOLA DE LA PEÑA
Associate Editor of *Ingeniería e Investigación*
Full Professor
Department of Mechanical and Mechatronics
Universidad Nacional de Colombia
https://orcid.org/0000-0002-5004-113X

Ingeniería e Investigación vol. 39 No. 1, April - 2019 (6-14)

DOI: http://dx.doi.org/10.15446/ing.investig.v39n1.76753

Analysis and modeling of the hydraulic behavior of EGSB reactors with presence and absence of granular biomass at different hydraulic retention times

Análisis y modelación del comportamiento hidráulico de reactores EGSB en presencia y ausencia de biomasa granular a diferentes tiempos de retención hidráulica

Yudy Andrea Londoño[1], Laura Victoria Castrillón[2], Nancy J. Pino[3], Edwin Lenin Chica[4], and Gustavo A. Peñuela[5]

ABSTRACT

The efficiency of biological wastewater treatment systems is linked fundamentally to the hydraulic performance of each treatment unit. These units should guarantee an adequate contact between the microorganisms and the residual water, and the compliance with the hydraulic retention time established, in order to decrease the number of dead zones or short circuits that may exist inside the reactors. In this work, hydraulic performance was evaluated in seven Expanded Granular Sludge Bed (EGSB) reactors with a useful volume of 3,4 L and constructed in acrylic. The analysis was carried out through the stimulus-response test, using bromide as tracer. Two hydraulic retention times (8 and 24 h) and the effect of the presence of granular biomass were considered. Results were analyzed qualitatively through the construction of curves C, E and F, and quantitatively through the construction of a mathematical model of axial dispersion. The results of the hydraulic performance of the reactors revealed a marked tendency to a complete mix flow pattern, with a low effect of HRT or the presence of granular biomass on their operation.

Keywords: Distribution of residence times, EGSB, Tracers, Mathematical modeling.

RESUMEN

La eficiencia de los sistemas biológicos de tratamiento de aguas residuales está vinculada fundamentalmente al rendimiento hidráulico de cada unidad de tratamiento. Estas unidades deben garantizar un contacto adecuado entre los microorganismos y el agua residual, y el cumplimiento del tiempo de retención hidráulico establecido, con el fin de disminuir el número de zonas muertas o cortocircuitos que puedan existir dentro de los reactores. En este trabajo, se evaluó el rendimiento hidráulico de siete reactores EGSB (del inglés *Expanded Granular Sludge Bed*) con un volumen útil de 3,4 L y construido en acrílico. El análisis se llevó a cabo a través de la prueba de estímulo-respuesta, utilizando bromuro como indicador. Se consideraron dos tiempos de retención hidráulica (8 y 24 h) y el efecto de la presencia de biomasa granular. Los resultados se analizaron de forma cualitativa a través de la construcción de las curvas C, E y F, y cuantitativamente a través de la construcción de un modelo matemático de dispersión axial. Los resultados del desempeño hidráulico de los reactores revelaron una marcada tendencia a un patrón de flujo de mezcla completo, con un bajo efecto en su operación por parte de la TRH o la presencia de biomasa granular.

Palabras clave: Distribución de tiempos de residencia, EGSB, Trazadores, Modelación matemática.

Received: December 10th, 2018
Accepted: April 29th, 2019

Introduction

The operation of wastewater treatment systems has been based mainly on the optimization of the biological

[1]Sanitary Engineer, Universidad de Antioquia, Colombia. M.Sc. and Ph.D. in Environmental Engineering, Universidad de Antioquia, Colombia. Affiliation: GDCON Research Group, Faculty of Engineering, Universidad de Antioquia, Colombia. Email: yudyandrea@gmail.com.
[2]Microbiologist and Bioanalyst, Universidad de Antioquia, Colombia. M.Sc. in Biology, Universidad de Antioquia, Colombia. Affiliation: GDCON Research Group, Faculty of Engineering, Colombia. Email: lauravictoria2c@gmail.com.
[3]Microbiologist and Bioanalyst, Universidad de Antioquia, Colombia. M.Sc. in Environmental Sciences, Universidad de Antioquia, Colombia. Ph.D. in Biotechnology, Universidad de Antioquia, Colombia. Affiliation: Associate professor, Universidad de Antioquia, Colombia. Email: nancy.pino@udea.edu.co.
[4]Mechanical Engineer, Universidad de Antioquia, Colombia. M.Sc. in Engineering, Universidad EAFIT. Ph.D. in Industrial Engineering, Universidad de Valladolid, España. Affiliation: Associate professor, Universidad de Antioquia, Colombia. Email: edwin.chica@udea.edu.co.
[5]Chemist, Universidad Nacional de Colombia, Colombia. M.Sc. in Chemical Sciences, Universidad Nacional de Colombia, Colombia. Ph.D. in Environmental Chemistry, Universitat de Barcelona, España. Affiliation: Full-Professor, Universidad de Antioquia, Colombia. Email: gustavo.penuela@udea.edu.co.

How to cite: Londoño, Y. A., Castrillón, L. V., Pino, N. J., Chica, E. L., and Peñuela, G. A. (2019). Analysis and modeling of the hydraulic behavior of EGSB reactors with presence and absence of granular biomass at different hydraulic retention times. *Ingeniería e Investigación*, *39*(1), 6-14.
DOI: 10.15446/ing.investig.v39n1.76753

and physicochemical processes that are involved in the degradation of a large number of organic pollutants (Pérez-Pérez et al., 2017). However, the efficiency of these systems is fundamentally linked to the hydraulic behavior of each treatment unit (Karim et al., 2005). In these units there should be an adequate contact between the microorganisms and the residual water, and operation within an optimum hydraulic retention time (HRT) to achieve the required efficiency levels and those proposed during the design of the treatment system (Odriozola, López and Borzacconi, 2016). However, the fluid tends to deviate from this ideal hydraulic behavior (Mao, Feng, Wang and Ren, 2015), due to factors such as the shape of the system, the scale, the hydraulic characteristics of the input and output structures, the presence of biomass, and environmental conditions (Nicolella, van Loosdrecht and Heijnen, 2000). These factors produce unfavorable hydraulic conditions or flow channels, such as dead zones, inertial currents and hydraulic short circuits (Fuentes, Scenna, and Aguirre, 2011), which reduce the HRT and decrease the efficiency of the system (Pérez-Pérez, Pereda-Reyes, Pozzi, Oliva-Merencio and Zaiat, 2018).

These hydraulic difficulties are currently subject to great interest, which has led to an increase in studies to modify or optimize biological technologies in order to enhance their ability to deal with the global problem of wastewater treatment (Batstone, Puyol, Flores-Alsina,and Rodríguez, 2015). Water pollution is an increasingly complex problem due to the presence of a large number of pollutants with different physical and chemical properties that are recalcitrant and present low degradation. For this reason, it is necessary to achieve an adequate performance of the systems used for the water treatment (Ahmed and Rodríguez, 2018). Many of these pollutants are part of the composition of domestic and industrial wastewater, which must be treated before being discharged to natural water bodies, in order to minimize harmful impacts on aquatic environments and human health.

The study of different hydraulic conditions of treatment systems, mainly with regard to biological technologies (Barrera et al., 2015), is a contribution towards improved bioremediation of wastewater. This aims not only to decrease parameters such as COD and BOD, but also to remove microcontaminants such as pesticides, pharmaceutical and personal care products.

Regarding systems using anaerobic processes, some hydraulic improvements have been made. For example, the modification of the sludge mantle reactor with upward flow (UASB) has been applied to an expanded mud blanket with upward flow (EGSB) (Fuentes et al., 2011). This reactor is characterized by operation at flow rates > 4 m/h (Hwu, van Lier and Lettinga, 1998), which are achieved due to the high height/diameter ratio and the high rate of recirculation of the effluent. This favors mixing inside the reactor and optimizes the contact between the biomass and the substrate to be degraded. As a result, efficiency is improved in the removal process of organic matter and the EGSB system becomes an attractive form of technology for the treatment of wastewater (Wang, Zhang, Zhang, Qaisar and Zheng, 2007).

Studies on the hydraulics of EGSB reactors have reported complete mixing conditions for these systems. However, few researchers have tried to ascertain in detail the hydraulic behavior of these reactors under different operating conditions, for example with extreme values of HRT and the presence of granular biomass. An alternative to better understand the hydraulics of these systems is through the analysis of the residence time distribution (RTD). In RTD, the time that the elements of a fluid remain inside the reactor is evaluated through the stimulus-response test or dispersion studies using tracers (De Nardi, Zaiat and Foresti, 1999).

Meanwhile, mathematical analysis and simulation models are used to understand the quantitative behavior of biological systems, in addition to predict the overall performance of a reactor. These can help in the start-up, operation, and characterization of the dynamics and control of reactors, as well as in the estimation of the times required to reach stable states when disturbances occur (Pérez and Torres, 2008).

In the literature, few models to characterize the non-ideal flow of EGSB reactors have considered the recirculation effect. These are often limited to black box models, where only the input and output of the system are considered (Pereda Reyes et al., 2014). In order to improve the knowledge about the hydrodynamics of this kind of reactor, it is necessary to include the study of the convective or diffusive phenomena that predominate in the expansion zone and the separator. For this purpose, the Peclet number is calculated for each condition by applying an axial dispersion model, which allows to model the hydrodynamics of the reactor with greater precision. This type of model has been used to describe the non-ideal flow patterns of the liquid phase of upstream reactors at pilot scale (Bhattacharyya and Singh, 2010). The objective of this study was to evaluate the distribution of the retention time in different EGSB anaerobic reactors, in order to elucidate the way in which the liquid mass has been subjected to the treatment system. We evaluated the influence of various factors such as the geometry of the reactor, the presence of granular biomass, and different HRT values in the operation of the systems. For this purpose, the stimulus-response test was used, as well as the construction of a mathematical model that fits and describes the hydraulic performance of each reactor.

Materials and Methods

General assembly of EGSB reactors

The reactors were constructed using transparent acrylic sheet. They were formed by three main units that highlighted the most important characteristics of the system (Figure 1): an upper part that favored solid-liquid-gas separation; a body formed by a thin cylinder that allowed the expansion of the mud; and a support formed by a perforated plate for the uniform entry of the feed flow. The diameter of the cylinder was 4,4 cm, with a total height of 85 cm. An effective volume of 3,4 L and an expansion volume of the sludge mantle of 1 L were obtained.

The gas collection hood (Figure 1) located inside the structure of EGSB systems was supported by two partitions that allowed water to rise at the outlets of both the effluent and the recirculation ducts. Gases were led by hoses to plastic bags, where they were stored. Additionally, this hood helped to retain the sludge that had not settled.

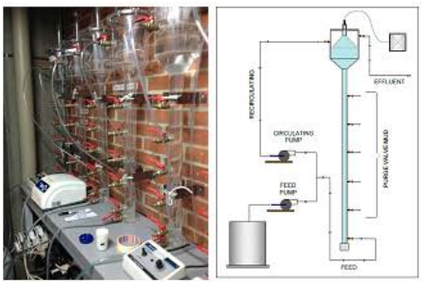

Figure 1. General scheme of the sampling valves and the flow and recirculation system.
Source: Authors

The operation of each reactor consisted of the tributary inputs through the lower part, where it was evenly distributed by means of a perforated plate. There were two output devices in the upper part.: one responsible for the recirculating part of the effluent and another for evacuating the excess flow. This system was installed in a closed space, avoiding maximum exposure to ambient conditions.

Stimulus-response test for the determination of RTD

Analysis of the hydraulic behavior of the seven EGSB systems was carried out using potassium bromide as tracer substance. The total concentration of the tracer within each reactor was calculated as approximately 150 mg/L Br-, assuming a predominance of complete mixing in the system.

The tests were carried out independently for each system. The pulse preparation was carried out in 25 mL of distilled water with a Br- concentration of 20 400 mg/L. It was injected into the affluent of the reactors, which were subsequently operated continuously for a period of 3 times the HRT with an up-flow velocity of 3 m/h. In the test, two fundamental parameters were evaluated: the effect of the presence or absence of granular biomass; and the two hydraulic retention times used (8 and 24 h). For this purpose, the experimentation was set up in accordance with the description in Table 1.

Analysis and quantification of bromides

RTD analysis using the stimulus-response method was carried out by monitoring the concentration of the bromide in the effluent of each EGSB system at different time intervals. The quantification was carried out by ion chromatography using a Dionex ICS-1000 ion chromatograph. The operating conditions were as follows: equipment pressure of 1 500-2 100 psi, workflow of 1 milliliter/minute and conductivity below 30 µs. The column used was a Thermo Scientific Dionex IonPac AS14A of 0,25 meters length and 4 millimeters diameter, with a 7-micrometer film. The pH range was between 2,0-10,0. A Dionex standard was used. The retention time of the bromide was approximately 5,5 min.

Table 1. Distribution of HRT and biomass in each EGSB system for the tracer test

Reactor	HRT	Biomass
EGSB 1	8 hours	Yes
EGSB 2	8 hours	No
EGSB 3	8 hours	Yes
EGSB 4	8 hours	No
EGSB 5	24 hours	Yes
EGSB 6	24 hours	Yes
EGSB 7	24 hours	No

Source: Authors

Mathematical modeling for the actual flow: Hydraulic behavior of an EGSB system

Axial dispersion model. The most used and simplest model to describe flow systems, where both convection and diffusion are important, is the axial dispersion model (Aris, 1999; Danckwerts, 1953; Taylor, 1953) with the Danckwert boundary conditions. The model is based on the following equation:

$$\frac{\partial C}{\partial t} = -v\frac{\partial C}{\partial z} + D\frac{\partial^2 C}{\partial z^2},\ z\in\ (0, L),\ t\in\ (0, T) \qquad (1)$$

which in its dimensionless form becomes:

$$\frac{\partial C}{\partial t} = -\frac{\partial C}{\partial z} + \left(\frac{D}{vL}\right)\frac{\partial^2 C}{\partial z^2} \qquad (2)$$

where $C(z,t)$ is the concentration of the tracer, a function of time t and the coordinate of axial position of the system z; D is the axial dispersion coefficient; and v is a constant average axial velocity, which does not depend on z. The first terms on the right side of Eq. (1) characterize the dispersive term and L, which is the length of the reactor (length of the tube plus length of the separator). The second term determines a convective transport of component C in the vertical direction. The Danckwerts-type boundary conditions (Danckwerts, 1953) are:

$$D\frac{\partial C}{\partial z} = v\left(C_{i(z=0)} - C_{i,\ in}\right),\ z=0 \qquad (3)$$

$$\frac{\partial C}{\partial z} = 0, z = L$$

$$C_{in} = \frac{C_a Q_a + C_r Q_r + C_{tr} Q_{tr}}{Q_a + Q_r + Q_{tr}}$$

where $C_{i,in}$ is the input concentration, Q_a is the influent flow, C_a is the influent concentration, Q_r is the recirculation flow, C_r is the concentration of recirculation, Q_{tr} is the flow rate of the tracer and C_{tr} is the concentration of the tracer. Q_{tr} and C_{tr} can be calculated from the time of injection and the volume injected.

Originally, Danckwerts boundary conditions were formulated for mass balance equations in discontinuity interfaces between piston flow and dispersive flow in chemical reactors (Danckwerts, 1953). They were then expanded to describe the effects of axial dispersion due to maldistribution of the flow in the heat exchanger. The group without dimensions $\left(\frac{vL}{D}\right)$ is the Peclet number (Pe), i.e. the parameter that quantifies the extension of the axial dispersion. It has the following limits: for the ideal mixed flow, the Peclet number is 0; and for an ideal pulse flow, it is infinite.

$\frac{D}{vL} = \frac{1}{Pe} \rightarrow 0$ Minimum dispersion, therefore plug-flow.

$\frac{D}{vL} = \frac{1}{Pe} \rightarrow \infty$ Large dispersion, therefore mixed flow.

For the solution of the model equation, we used the finite central difference method of order 2. The aim of using finite difference methods to solve Eq. (1) is to replace spatial and temporal derivatives by appropriate approximations, and then to solve the equations of the resulting differences numerically.

The first step in the discretization procedure is to replace the domain $[0, L] \times [0, T]$ with a set of mesh points.

$$z_i = i\Delta z, \quad i = 0, \ldots, N_z \tag{4}$$

$$t_n = n\Delta t, \quad n = 0, \ldots, N_t \tag{5}$$

In addition, C_i^n denotes the approaching mesh function $C(x_i, t_n)$ for $i = 0, \ldots, N_z$ and $n = 0, \ldots, N_t$. Requiring Eq. (1) to be fulfilled in a mesh point $(x_i,\ t_n)$ leads to the equation:

$$\frac{\partial C(x_i,\, t_n)}{\partial t} = -v\frac{\partial C(x_i,\ t_n)}{\partial z} + D\frac{\partial^2 C(x_i,\ t_n)}{\partial z^2},\ z \in (0,\ L),\ t \in (0,\ T) \tag{6}$$

The next step is to replace the derivative with approximations of finite differences. The simplest computational methods arise from the use of a direct difference in time and a central difference in space.

$$\frac{C_i^{n+1} - C_i^n}{\Delta t} = -v\frac{C_{i+1}^n - C_{i-1}^n}{2\Delta z} + D\frac{C_{i+1}^n - 2C_i^n + C_{i-1}^n}{\Delta z^2} \tag{7}$$

$$D\frac{C_{i+1}^n - C_{i-1}^n}{2\Delta z} = v\left(C_{i(z=0)} - C_{i,\,in}\right),\ z = 0$$

$$\frac{C_{i+1}^n - C_{i-1}^n}{2\Delta z} = 0, \rightarrow C_{i+1}^n = C_{i-1}^n\ z = L$$

We have turned the Eq. (1) into algebraic equations, also often called discrete equations. The key property of the equations is that they are algebraic, which makes them easy to solve. As usual, we anticipate that C_i^n is already calculated, so that C_i^{n+1} is the only term unknown in Eq. (7). To resolve with respect to this unknown, Eq. (8) is used:

$$C_i^{n+1} = \left(-v\frac{C_{i+1}^n - C_{i-1}^n}{2\Delta z} + D\frac{C_{i+1}^n - 2C_i^n + C_{i-1}^n}{\Delta z^2}\right)\Delta t + C_i^n \cdots \tag{8}$$

The derivative of the boundary condition was also replaced by finite difference approximations.

$$D\frac{C_{i+1}^n - C_{i-1}^n}{2\Delta z} = v\left(C_i - C_{i,\,in}\right),\ z = 0 \tag{9}$$

$$\frac{C_{i+1}^n - C_{i-1}^n}{2\Delta z} = 0, \rightarrow C_{i+1}^n = C_{i-1}^n\ z = L$$

When solving equation (8), the domain was divided into two regions. These were two tubular reactors in series: the first the region of the tube and the region of the separator. The length of each region is divided into small elements of length equal to Δz. The computational algorithm pseudocode was developed using MATLAB software.

Results and Discussion

Distribution curves

Curve C(t). The distribution of tracer concentration in the effluent of the EGSB systems over time (curves C) are presented in Figure 2.

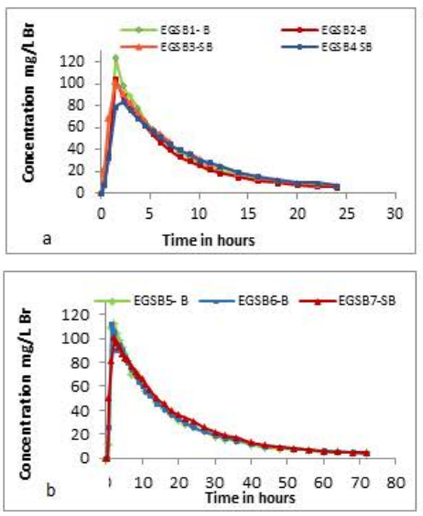

Figure 2. Tracer Behavior through EGSB systems applying a hydraulic retention time of a) 8 hours and b) 24 hours.
Source: Authors

The results of the C curves obtained for each test showed a similar and defined trend of the tracer within each EGSB reactor. For the theoretical HRT of 24 hours, the behavior was more uniform, while for the HRT of 8 hours, the peaks of maximum concentration presented some differences. This may be linked to failures at the moment of application of the pulse, which in some cases takes more time to enter than others. However, no significant effect of the biomass was observed on the behavior of the tracer distribution in the effluent of the operated systems at a HRT of 8 h. These results seem to indicate that the presence of the granular sludge did not prevent the homogeneous distribution of the flow

within these reactors. In addition, it should be considered that the maximum concentration peak of the bromide within the systems could have occurred when samples were not taken, since monitoring was not second by second, but at longer time intervals.

In the graphs, the first-time values showed that the concentration of the tracer was increasing progressively from zero to the peak of maximum concentration. This behavior has been reported as characteristic of real reactors with a combination of piston flow and complete mixing (Arroyave, González Arteaga and Gallego, 2005). Additionally, for the majority of the systems that operated with HRT of 8 h, a single peak of maximum concentration was observed, independently of the presence or absence of granular biomass. This condition allows the nonexistence of short circuits in the hydraulic performance of the EGSB systems to be inferred and was not observed only in the cases of EGSB reactors 5 and 6, which operated with a HRT of 24 h and with the presence of biomass. After the maximum concentration peak, another peak with a slight increase was observed, which theoretically indicates the presence of short circuits in these systems and, consequently, an effect of the biomass combined with the high value of HRT.

Curve E(t). Curve E represents the distribution of the ages of the fluid that leaves a system or a container, in this case, corresponding to the time required by the tracer to pass through the EGSB reactors. This is presented in Figure 3.

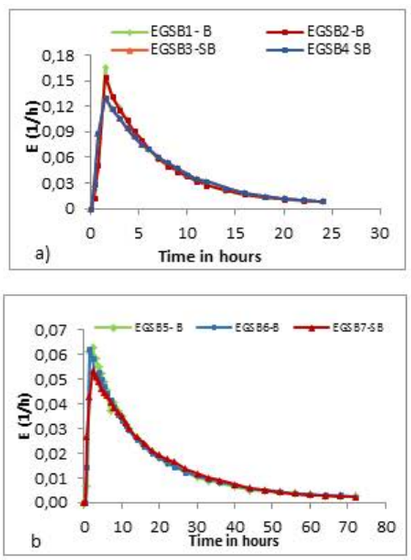

Figure 3. Curves E applying a hydraulic retention time of a) 8 hours and b) 24 hours.
Source: Authors

According to the trends reported, the normalized behavior of the tracer within the reactors reflected a hydraulic performance with a tendency similar to complete mixing flow. This condition will be discussed later in the analysis of the F graphs that are illustrated below.

Curve F. Curve F is used to describe the cumulative concentration of the tracer at the outlet by measuring the concentration in the reactor in relation to the initial one (C/C_o).

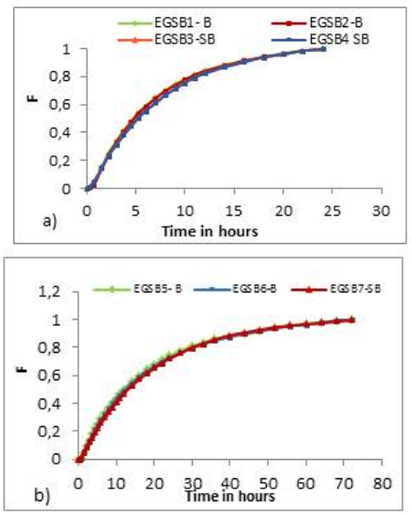

Figure 4. Curves F: a) Applying a hydraulic retention time of 8 hours and b) 24 hours.
Source: Authors

Curve F shows an increase in the bromide concentration in the output current of each reactor evaluated. The behavior in the distribution of the remnant tracer is shown in Figure 4a. At the beginning of the curves, there is a small upward concave tendency, and subsequently a concave downward curve. It should be noted that initially the curve has a steep slope, which softens after the equilibrium state. The nature of this curve indicates a strong tendency to a complete mixing flow pattern, but the possibility of a combination with piston flow is not ruled out. In Figure 4b, the behavior of the curve is completely concave downward, without sharp increases or decreases. This suggests that for these conditions the reactors behave like full mix reactors.

Figure 5 logically presents a behavior that is analogous to curve F (Figure 4). For this trend, a homogeneous behavior is evident without the apparent presence of hydraulic problems such as short circuits, dead zones or recirculation that impede the effective performance of each reactor.

Qualitative analysis of the trend of the tracer concentration curve in the reactors

When applying the stimulus-response test in a reactor, analysis of the samples obtained in the effluent of the system reveals that concentration increases with time, until reaching a maximum and then decreasing progressively. This results in a curve showing the behavior of the concentration of the tracer vs. the time, which is also known as curve C. This graphical representation can be analyzed qualitatively according to the criteria described in Table 2.

Table 2. Values of the experimental times obtained for each of the EGSB systems used for the qualitative analysis of the curves trend

Parameter	EGSB 1	EGSB 2	EGSB 3	EGSB 4	EGSB 5	EGSB 6	EGSB 7
t_i = initial time since the tracer is applied until it appears in the effluent.	0,33	0,33	0,33	0,33	0,75	0,75	0,75
t_p = modal time, time for the presentation of the maximum concentration	1,50	1,50	1,50	2,25	2,25	1,50	2,25
t_o = average retention time or theoretical holding time = V/Q.	8	8	8	8	24	24	24
t_m = medium time, time until the 50 % of the tracer crosses the reactor.	7,00	7,10	7,40	7,90	18,40	19,00	19,20
T_c = time in which the concentration is greater than Cp 2.	4,5	5,25	6,00	7,00	11,00	10,00	12,00
t_b = time in which the concentration is greater than Cp/10	14	18	22	22	36	40	40
C_p = maximum concentration at the exit.	124	104	102	84	111	113	101
t_f = time until the tracer crosses the entire reactor.	24	24	24	24	72	72	72

Source: Authors

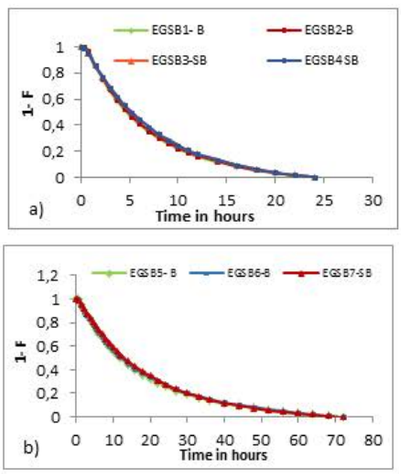

Figure 5. Curves 1-F applying a hydraulic retention time of a) 8 hours and b) 24 hours.
Source: Authors

Table 3 exposes the results of the qualitative analysis for each of the EGSB systems using the criteria presented in Table 2.

The results of the qualitative analysis of the tracer test are consistent with the behavior described in the analysis of the DTR curves. In this analysis, the hydraulic performance of the EGSB systems was evaluated, demonstrating a tendency towards a complete mixing flow pattern with little or no presence of dead zones or short circuits within the treatment units (Table 4).

Table 4. Application Results of the axial dispersion model for each of the EGSB systems

Reactor	$HRT_{theoretical}$ (h)	HRT_{Real} (h)	% death zones	σ_2	$\sigma\theta_2$	D/uL	Pe (vL/D)
EGSB 1		7,0	12,5	18,4	0,4	0,19	5,3
EGSB 2	8	7,1	11,1	18,6	0,4	0,18	5,4
EGSB 3		7,4	7,6	20,2	0,4	0,18	5,4
EGSB 4		7,9	0,9	21,1	0,3	0,17	6,0
EGSB 5		18,4	23,2	140,5	0,4	0,21	4,8
EGSB 6	24	19,0	20,7	149,5	0,4	0,21	4,8
EGSB 7		19,2	19,9	147,1	0,4	0,20	5,0

Source: Authors

Figure 3. Relations between experimental times and theoretical time for the trend analysis of the tracer distribution curve [8, 10]

Relation	EGSB 1	EGSB 2	EGSB 3	EGSB 4	EGSB 5	EGSB 6	EGSB 7	Description
t_i/t_o	0,04	0,04	0,04	0,04	0,03	0,03	0,03	if = 1 - piston flow if = 0 - mixed flow if > 0,3 - short circuits presence
t_m/t_o	0,88	0,89	0,93	1,0	0,77	0,79	0,80	if < 1 - hydraulic short circuits if > 1 - error in measurement or stagnation in sludge
t_p/t_o	0,19	0,19	0,19	0,28	0,09	0,06	0,09	if = 1 - there is only piston flow if = 0 - completely mixed flow if > 0,5 piston flow predominates if < 0,5 mixed flow predominates
t_c/t_o	0,56	0,66	0,75	0,875	0,46	0,42	0,50	For a fully mixed reactor this ratio is 0,693 or higher.
e	2,67	2,67	2,67	2,48	2,84	2,91	2,84	The value of E is equal to 0 for piston flow and greater than 2,3 for mixed flow

Source: Authors

Validation of mathematical model

Figures 6 to 9 present the results of the experimental curves and the adjustment obtained with the proposed model.

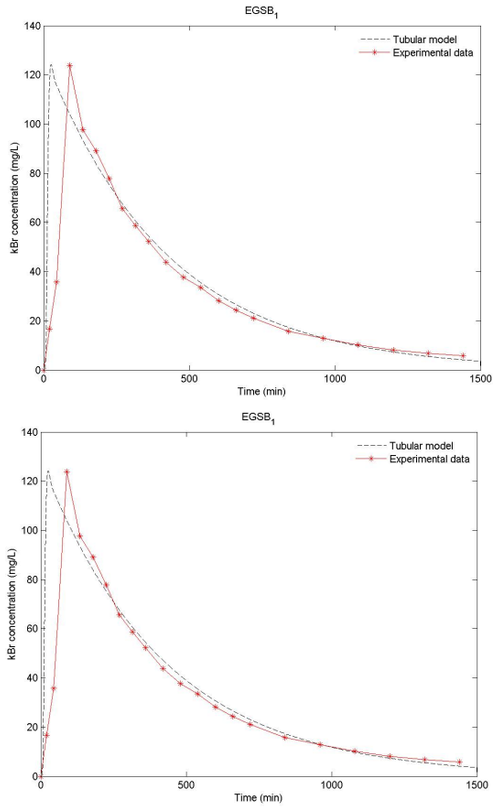

Figure 6. Distribution functions of residence times, experimental and theoretical, for the EGSB operated with HRT of 8h and with the presence of granular biomass.
Source: Authors

Figures 6 to 9 show the results of the tracer at the exit of each system and it is evident that the model developed presents a good adjustment to the behavior of the reactor. It is worth mentioning that the injection of the tracer was performed simultaneously to each system. However, small variations in time and pulse inflow could occur during the execution of the test, which may cause differences between the peak and the experimental model. Another possible cause of this difference in the peak is the starting point of the data collection. In the experimental test, time zero was considered immediately after the injection of the tracer, while for modeling, time zero should be considered as the start of the injection (Pereda Reyes et al., 2014).

Results of the tracer test analysis allowed the real HRT values for each EGSB system to be obtained. This allowed to define, with regard to the four reactors that operated with an HRT of 8 h, that the spaces or dead zones within each system were small, ranging between 0,9-12,3 %, without a significant effect on the part of the granular biomass. In the case of reactors operated with a HRT of 24 h, a small increase in dead zones was observed, varying in a range of 19,9-23,2 %. This behavior was verified independently of the presence and/or absence of granular biomass.

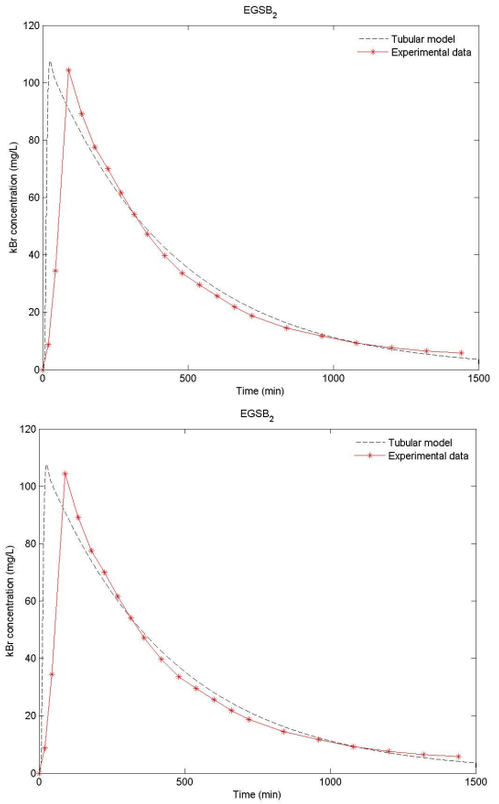

Figure 7. Distribution functions of residence times, experimental and theoretical, for the EGSB operated with HRT of 8h and without the presence of granular biomass.
Source: Authors

The values of the high number dispersion $\frac{D}{vL} > 0 > 0,01$ correspond to a fast dispersion of the tracer, indicating the presence of a mixed flow. Values $\frac{D}{vL} < 0,01$ indicate a slow dispersion, while $\frac{D}{vL} = 0$, means that there is no dispersion, hence piston flow predominates. The results of the dispersion number for each of the reactors evaluated in this study showed values higher than 0,01. This condition indicates a high degree of dispersion and a marked tendency towards mixed flow, which is consistent with the analysis of the curves presented above. Other studies carried out to analyze the hydraulic performance of EGSB reactors have reported flow characteristics congruent to those obtained in this test. Bhattacharyya evaluated. Reference was corrected the performance of EGSB systems with different rates of ascensional flow and HRT values. The results reported through these studies were under conditions of completely mixed flow with low percentages of dead zones.

Based on the foregoing, it is clear that the complete mix flow pattern governs the hydraulic performance of EGSB systems, under various operating conditions. This is related to the high dispersion values obtained inside the treatment unit.

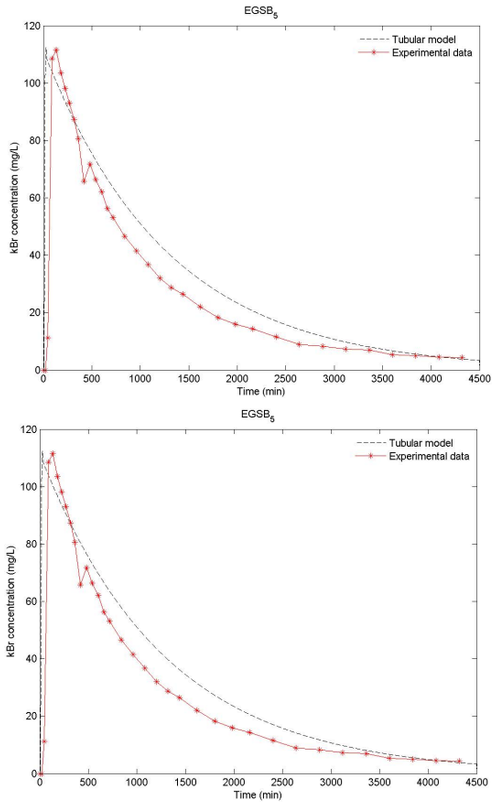

Figure 8. Distribution functions of residence times, experimental and theoretical, for the EGSB operated with HRT of 24h and with the presence of granular biomass.
Source: Authors

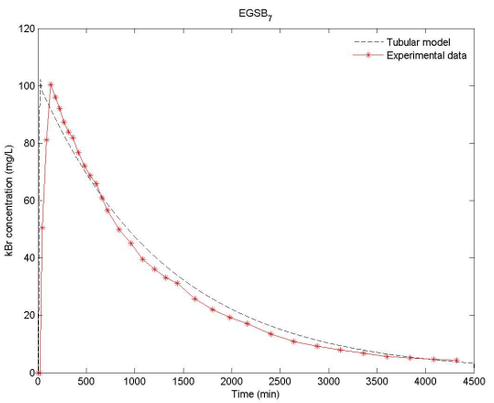

Figure 9. Distribution functions of residence times, experimental and theoretical, for the EGSB operated with HRT of 24h and without the presence of granular biomass.
Source: Authors

Conclusions

The hydrodynamic analysis of the EGSB systems allowed them to be characterized as completely mixed reactors, regardless of the HRT evaluated and/or the presence or absence of granular biomass. However, the best performance was obtained by the reactors evaluated with an HRT of 8 h, since they seem to contain no short circuits and, additionally, presented lower percentages of dead zones.

The reactors evaluated with an HRT of 24 h presented dead zone percentages of around 20 %, which were not very large but were higher than for the HRT of 8 h. Additionally, for these reactors, the presence of short circuits (EGSB 5 and 6), the combined effect on hydraulic performance of the existence of granular biomass and the high HRT value cannot be ruled out.

The axial dispersion model used for the flow behavior inside the EGSB reactors presented a good fit to the experimental data. This indicates an accurate selection of the model. Additionally, this indicates that the configuration of the systems presented a complete mixing flow pattern, which is in contrast with the analysis performed through curves C, E and F.

Acknowledgements

The authors thank the Colombian Administrators of the Department of Science, Technology and Innovation - COLCIENCIAS, the GDCON group and the Committee for the Development of Research (CODI) of the University of Antioquia for supporting this project.

References

Ahmed, W., and Rodríguez, J. (2018). Modelling sulfate reduction in anaerobic digestion: Complexity evaluation and parameter calibration. *Water Research*, 130, 255-262. DOI: 10.1016/J.WATRES.2017.11.064

Aris, R. (1999). On the Dispersion of A Solute in A Fluid Flowing Through A Tube. *Process Systems Engineering*, *1*, 109-120. DOI: 10.1016/S1874-5970(99)80009-5

Arroyave, D., González Arteaga, M., and Gallego, D. (2005). *Evaluación del comportamiento hidráulico un reactor UASB utilizado para el tratamiento de aguas residuales*. Paper presented at the VIII Congreso Peruano de ingeniería química, Lima, Confederación Interamericana de Ingenieros Químicos - CIIQ. Retrieved from: http://www.ciiq.org/varios/peru_2005/Trabajos/III/3/3.3.11.pdf.

Barrera, E. L., Spanjers, H., Solon, K., Amerlinck, Y., Nopens, I., and Dewulf, J. (2015). Modeling the anaerobic digestion of cane-molasses vinasse: Extension of the Anaerobic Digestion Model No. 1 (ADM1) with sulfate reduction for a very high strength and sulfate rich wastewater. *Water Research*, *71*, 42-54. DOI: 10.1016/J.WATRES.2014.12.026

Batstone, D. J., Puyol, D., Flores-Alsina, X., and Rodríguez, J. (2015). Mathematical modelling of anaerobic digestion processes: applications and future needs. *Reviews in Environmental Science and Bio/Technology*, *14*(4), 595-613. DOI: 10.1007/s11157-015-9376-4

Bhattacharyya, D., and Singh, K. S. (2010). Understanding the Mixing Pattern in an Anaerobic Expanded Granular Sludge

Bed Reactor: Effect of Liquid Recirculation. *Journal of Environmental Engineering, 136*(6), 576-584. DOI: 10.1061/(ASCE)EE.1943-7870.0000187

Danckwerts, P. V. (1953). Continuous flow systems: Distribution of residence times. *Chemical Engineering Science, 2*(1), 1-13. DOI: 10.1016/0009-2509(53)80001-1

De Nardi, I. R., Zaiat, M., and Foresti, E. (1999). Influence of the tracer characteristics on hydrodynamic models of packed-bed bioreactors. *Bioprocess Engineering, 21*(5), 469. DOI: 10.1007/s004490050704

Fuentes, M., Scenna, N. J., and Aguirre, P. A. (2011). A coupling model for EGSB bioreactors: Hydrodynamics and anaerobic digestion processes. *Chemical Engineering and Processing: Process Intensification, 503*, 316-324. DOI: 10.1016/J.CEP.2011.01.005

Hwu, C.-S., van Lier, J. B., and Lettinga, G. (1998). Physicochemical and biological performance of expanded granular sludge bed reactors treating long-chain fatty acids. *Process Biochemistry, 33*(1), 75-81. DOI: 10.1016/S0032-9592(97)00051-4

Karim, K., Thomas Klasson, K., Hoffmann, R., Drescher, S. R., De Paoli, D. W., and Al-Dahhan, M. H. (2005). Anaerobic digestion of animal waste: Effect of mixing. *Bioresource Technology, 96*(14), 1607-1612. DOI: 10.1016/J.BIORTECH.2004.12.021

Mao, C., Feng, Y., Wang, X., and Ren, G. (2015). Review on research achievements of biogas from anaerobic digestion. *Renewable and Sustainable Energy Reviews*, *45*, 540-555. DOI: 10.1016/j.rser.2015.02.032

Nicolella, C., van Loosdrecht, M.C.M., and Heijnen, J.J. (2000). Wastewater treatment with particulate biofilm reactors. *Journal of Biotechnology, 80*(1), 1-33. DOI: 10.1016/S0168-1656(00)00229-7

Odriozola, M., López, I., and Borzacconi, L. (2016). Modeling granule development and reactor performance on anaerobic granular sludge reactors. *Journal of Environmental Chemical Engineering, 4*(2), 1615-1628. DOI: 10.1016/J.JECE.2016.01.040

Pereda Reyes, I., Teixeira Correia, G., Pérez Pérez, T., Oliva Merencio, D., Zaiat, M., and Hong Kwong, W. (2014). Mathematical Modeling of the Hydrodynamics of an EGSB Reactor. *Journal of Chemistry and Chemical Engineering*, *8*, 602-610. Retrieved from http://www.davidpublisher.org/Public/uploads/Contribute/ 56d502fc07280.pdf

Pérez-Pérez, T., Pereda-Reyes, I., Pozzi, E., Oliva-Merencio, D., and Zaiat, M. (2018). Performance and stability of an expanded granular sludge bed reactor modified with zeolite addition subjected to step increases of organic loading rate (OLR) and to organic shock load (OSL). *Water Science and Technology, 77*(1), 39-50. DOI: 10.2166/wst.2017.516

Pérez-Pérez, T., Teixeira Correia, G., Hong Kwong, W., Pereda-Reyes, I., Oliva-Merencio, D., and Zaiat, M. (2017). Effects of the support material addition on the hydrodynamic behavior of an anaerobic expanded granular sludge bed reactor. *Journal of Environmental Sciences*, *54*, 224-230. DOI: 10.1016/j.jes.2016.02.011

Pérez, A., and Torres, P. (2008). Evaluation of hydrodynamic behavior as a tool to optimize anaerobic reactors of attached growth. *Revista Facultad de Ingeniería Universidad de Antioquia*, (45), 27-40. Retrieved from: http://aprendeenlinea.udea.edu.co/revistas/index.php/ingenieria/article/view/17963/15418

Taylor, G. (1953). Dispersion of Soluble Matter in Solvent Flowing Slowly through a Tube. *Proceedings of the Royal Society A: Mathematical, Physical and Engineering Sciences, 219*(1137), 186-203. DOI: 10.1098/rspa.1953.0139

Wang, J., Zhang, Z., Zhang, Z., Qaisar, M., and Zheng, P. (2007). Production and application of anaerobic granular sludge produced by landfill. *Journal of Environmental Sciences, 19*(12), 1454-1460. DOI: 10.1016/S1001-0742(07)60237-X

Ingeniería e Investigación vol. 39 No. 1, April - 2019 (15-23)

DOI: http://dx.doi.org/10.15446/ing.investig.v39n1.70080

Process simulation for xylitol production from brewer's spent grain in a Colombian biorefinery. Part 1: Xylose production from arabinoxilans extracted by the alkaline pretreatment of BSG

Simulación de proceso para la producción de xilitol a partir de bagazo de cebada en una biorrefinería en Colombia. Parte 1: producción de xilosa a partir de arabinoxilanos extraídos en el pretratamiento alcalino de BSG

Andrés A. Gil-Montenegro[1], Juan S. Arocha-Morales[2], Lilia C. Rojas-Pérez[3], and Paulo C. Narváez-Rincón[4]

ABSTRACT

This work presents the simulation in Aspen Plus® of a process to obtain arabinoxylans (AX) from Brewer's Spent Grain (BSG), which is the major byproduct of the brewing industry. The process is divided into two stages: alkaline pretreatment and enzymatic hydrolysis. These stages cover the extraction of proteins and AX from BSG using an alkaline pretreatment and enzymatic hydrolysis of the AX separated from the liquid stream to obtain xylose, i.e. the substrate required for the fermentation to xylitol. Simulation results show that xylose obtained corresponds to 8,5 % of the dry weight of the raw material, obtaining a yield of 58 %. Several streams of byproducts were obtained, such as proteins, polypeptides, amino acids, phenolic compounds and lignocellulosic residues that can be valorized in other processes. Simulation was performed in the context of a biorefinery in Colombia.

Keywords: Simulation, brewer's spent grain, xylitol, biorefinery.

RESUMEN

Este trabajo presenta la simulación en Aspen Plus® del proceso para obtener arabinoxilanos (AX) a partir de bagazo de cebada, principal subproducto de la industria cervecera. El proceso se divide en dos etapas: pretratamiento alcalino e hidrólisis enzimática. En la primera etapa, se logra la extracción de proteínas y AX de la cascarilla de cebada y en la segunda etapa, se hidrolizan enzimáticamente los AX separados de la corriente líquida hasta obtenerse xilosa, el sustrato requerido para el xilitol. Los resultados de la simulación mostraron que la xilosa obtenida corresponde al 8,5 % del peso de la materia prima, obteniéndose un rendimiento del 58 %. Adicionalmente se obtienen varias corrientes de subproductos como proteínas, polipéptidos, aminoácidos, compuestos fenólicos y residuos concentrados en lignina y celulosa, los cuales se pueden valorizar en otros procesos. La simulación del proceso se realizó en el contexto de una biorrefinería en Colombia.

Palabras clave: Simulación, cascarilla de cebada, xilitol, biorrefinería.

Received: January 30th, 2018
Accepted: February 11th, 2019

Introduction

Currently, global economy is based mainly on products derived from fossil resources. Most of the basic and intermediate chemical products are produced using crude oil and natural gas as feedstock. However, considering sustainability principles and objectives formulated by United Nations (UN), several countries have promulgated policies to reduce the negative effects of greenhouse gases emissions on global warming, simultaneously helping to mitigate the economic instability due to the volatility of crude oil price. Those policies have fostered research projects and industrial production that valorize non-fossil sources as raw material for food, feed, energy, chemicals and materials.

[1]Chemical Engineer, Universidad Nacional de Colombia Campus Bogotá, Colombia. E-mail: aagilm@unal.edu.co.
[2]Chemical Engineer, Universidad Nacional de Colombia Campus Bogotá, Colombia. E-mail: jsarocham@unal.edu.co.
[3] Chemical Engineer, M.Sc. and Ph.D. in Chemical Engineering, Universidad Nacional de Colombia Campus Bogotá, Colombia. E-mail: lcrojasp@unal.edu.co.
[4] Chemical Engineer, M.Sc. and Ph.D. in Chemical Engineering, Universidad Nacional de Colombia Campus Bogotá. Affiliation: Full-Professor, Universidad Nacional de Colombia, Colombia. E-mail: pcnarvaezr@unal.edu.co.

How to cite: Gil-Montenegro, A. A, Arocha Morales, J. S., Rojas-Pérez, L. C., and Narváez-Rincón, P. C. (2019). Process simulation for xylitol production from brewer's spent grain in a Colombian biorefinery. Part 1: Xylose production from arabinoxilans extracted by the alkaline pretreatment of BSG. *Ingeniería e Investigación, 39*(1), 15-23. DOI: 10.15446/ing.investig.v39n1.70080

Among the different effects of the development of biorefineries, the implementation of new production methods, as intensified technologies and bioprocesses, is noticeable (Hermann, Blok, and Patel, 2007). The increasing number of industries based on bioprocess has been the precursor of a new and more competitive market of bio-based products. Thus, the renewal of technologies based on fossil resources is imminent to promote the production of new products with characteristics different to those of the chemicals nowadays available. These new products should satisfy the new requirements of consumers who consider sustainability as a key factor in the decision-making process (Jong, Higson, Walsh, and Wellisch, 2011).

The industrial trend to implement sustainable processes, using renewable raw materials (biomass and residues) and producing bio-based products, has favored the development of the biorefinery concept. This concept intends to cover all the available technologies for the treatment of biomass, taking advantage of its wide range of possibilities for the generation of products with high added value (Cherubini, 2010). Although some bio-based products can be fabricated by simple processes, the same product can be obtained by integrated processes in biorefineries where energy, chemicals and materials can be produced simultaneously in a sustainable way (Jong *et al.*, 2011).

The main challenge of biorefineries is to find the biomass with the composition and characteristics required by its products and processes. This fact has led the bio-based chemical industry to seek allies in other manufacture sectors and find organic byproducts that can be used as raw material. In this context, brewery is one of the industries present worldwide and recognized for its large number of organic byproducts (Xiros and Christakopoulos, 2012).

Beer is an alcoholic beverage produced by the fermentation of sugars extracted from barley, whose aroma and flavor are given by hops. In Colombia, the brewing industry is one of the most important economic sectors, mainly due to the high demand of this product. In 2016, national production of beer reached 19,1 million hectoliters, which generated a high amount of organic solid byproducts corresponding to yeast, hops and, in greater proportion, to brewer's spent grain, commonly known as BSG. Usually, a brewery produces approximately 20 kilograms of wet BSG per hectoliter of beer, i.e. about 85 % of the total byproducts of the process (Reinold, 1997). Therefore, BSG is the most important residue in breweries.

Multiple research projects have investigated the use and valorization of BSG. Considering its properties and composition, a large number of potential products can be obtained. BSG has been assessed as feedstock for biotechnological processes, production of energy, supplementary food and feed, construction materials, coal production, fertilizers, among many others (Mussatto, Dragone and Roberto, 2006). The most advanced studies correspond to the use of BSG as a raw material in various chemical processes, e. g. phenolic antioxidant compounds, lactic acid, ethanol and xylitol (Meneses, Martins, Teixeira, and Mussatto, 2013; Mussatto and Roberto, 2008).

Xylitol is a five-carbon polyol, commonly employed in food and pharmaceutical industry as sweetener. It does not require insulin to be metabolized and it has low heat capacity (Ravella, Gallagher, Fish and Prakasham, 2012). For these properties, xylitol is generally used as sweetener agent in foods aimed at diabetic consumers. In consequence, its production and commercial use have greatly increased in the last decade. Currently, world xylitol production is about 160 000 t per year, equivalent to USD $ 670 million, and by 2020 it is expected that the production increases up to 242 000 t, equivalent to USD 1 billion (Ravella *et al.*, 2012).

Several studies have been published about the feasibility of biorefineries based on different processes for the production of xylitol from BSG as main raw material. Dávila, Rosenberg and Cardona (2016) reported a study of a biorefinery for the production of xylitol, ethanol and polyhydroxybutyrate from BSG. They established the feasibility for different process configurations with and without heat integration. Likewise, Mussatto, Moncada, Roberto and Cardona (2013) presented various researches using BSG for the production of xylitol. Results of these studies were applied in a techno-economic analysis for a BSG biorefinery located in Brazil, where the technological and environmental feasibility of the project was evaluated.

This work presents the simulation in Aspen Plus V9® of xylose production process from BSG. Xylose is the main sugar for xylitol production. The process for xylitol production includes three main stages: (1) alkaline pretreatment for AX extraction from BSG, (2) enzymatic hydrolysis of AX for xylose production and (3) xylose fermentation. This article presents the simulation of the first two stages. Process simulation was performed with the aim to carry out a feasibility study of a biorefinery in the Colombian context.

Process Description

As mentioned previously, the simulation presented in this work corresponds to the first part of a process designed to produce xylitol from BSG. This process pretreatment had as main objective the conditioning of raw material for the fermentation process, specifically xylose production, which is the main substrate for fermentation and production of xylitol. Figure 1 presents the simplified block flow diagram of this part of the process. Pretreatment process starts with conditioning of the raw material. BSG requires wet grinding to reduce its particle size, creating an interfacial area to facilitate the following operations. After grinding, BSG is preheated and fed to the alkaline treatment stage, where it is mixed with a 4M sodium hydroxide solution. Alkaline hydrolysis is performed to separate hemicellulose from cellulose and lignin, and produce and solubilize arabinoxylans (AX). BSG protein is extracted and alkaline hydrolysis takes place. The alkaline pretreatment implicates the saponification of intermolecular ester bonds cross-linking xylan hemicelluloses and other components, and the porosity of the lignocellulosic biomass

increases with the disintegration of the cross-links (Xu and Sun, 2016).

Then, to precipitate proteins and neutralize the NaOH in excess, both in the liquid fraction, a diluted sulfuric acid solution is added to reach pH 3. Protein fraction is separated from the liquid that contains the AX and the degraded lignin by centrifugation. Yield of the precipitation of protein is assumed 100 % for simulation. Then, azeotropic ethanol is added to the liquid fraction to precipitate AX, which are separated from the liquid by centrifugation. Despite its solubility, a fraction of the Na_2SO_4 produced in NaOH neutralization co-precipitates with AX. The degraded lignin remains in the liquid fraction as furan compounds. After washing the solid fraction with ethanol to dissolve the co-precipitated Na_2SO_4, AX are enzymatically hydrolyzed using six pure commercial enzymes simultaneously (endo-1,4-β-xylanases, α-L-arabinofuranidases, β-xylosidases and α-glucuronidases). The purpose is to obtain a mixture of xylose and arabinose that has to be concentrated for the fermentation stage.

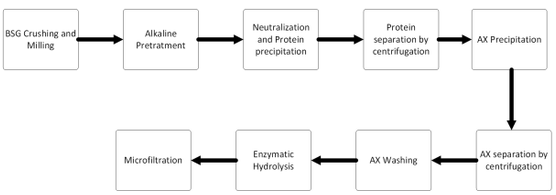

Figure 1. Simplified block diagram of the pretreatment process of BSG to produce xylose.
Source: Authors

Methods and materials

Components required for simulation

Simulation of the process previously described was performed in Aspen Plus V9®. The first step of the simulation was to select the compounds, in the simulator database, that adequately represent the substances involved in the process. BSG from Tocancipá (Colombia) Brewery was supplied by Bavaria S. A. It has ~80 % of moisture, and it is composed of the following five main fractions: hemicellulose (25,13 % dry basis [db]), glucans (18,63 % db), lignin (16,69 % db), protein (14,50 % db) and extractive compounds (22,58 % db) (Rojas-Pérez, 2018). As shown in Table 1, most of the compounds of BSG are not found in Aspen Plus V9® databases. Thus, it was necessary to define them manually, introducing physical and chemical properties available in the literature.

Parameters to define the properties required by the simulator for the different solid compounds were obtained from Wooley and Putsche (1996). Using this information, it was possible to define several solid compounds present in the process, such as cellulose, hemicellulose (kind of arabinoxylans) and lignin, as well as other solids present in the organic material. Additionally, water, ethanol, sodium hydroxide, xylose, arabinose and sodium sulfate were found in the simulator databases. Then, parameters for calculating its properties were taken directly from databases.

Selection of the calculation method

As the phase balance is not relevant for this part of the process, Gil, López, Zapata, Robayo, and Niño (2015) recommended the IDEAL method to perform the simulation. This method is also suitable for processes where unconventional solids are involved, because solid compounds and solubility values are specified by the user based on experimental data.

Then, in the simulation environment – Setup > Specifications section – the METBAR units system was selected. The type of stream selected was MIXCIPSD, because it corresponds to streams where unconventional solids are present and where, in some cases, it is necessary to specify the particle size distribution. This type of stream was chosen because the particle size is an important property for this simulation, considering that grinding and separations are made by the difference of particle size in BSG.

Process simulation specifications

Production capacity: Considering further economic feasibility to be performed according to the results of the simulation, it is necessary to evaluate the process at several production capacities. For this reason, three production capacities were selected regarding breweries located in Colombia:

- 40 000 hectoliters of beer per year that generate approximately 800 t of BSG per year, corresponding to Bogotá Beer Company Brewery – Tocancipá, Cundinamarca.
- 2,3 million hectoliters of beer per year that generate approximately 46 000 t of BSG per year, corresponding to Bavaria Boyacá Brewery – Tibasosa, Boyacá.
- 7,8 million hectoliters of beer per year that generate approximately 156 000 t of BSG per year, corresponding to Bavaria Tocancipá Brewery – Tocancipá, Cundinamarca.

Crushing: Figure 2 shows the crushing block and the streams associated. Grinding is the first stage of the process. The particle size of BSG at the brewery outlet does not facilitate the efficient removal of AX by hydrolysis. Thus, it is necessary to reduce its particle size. To simulate this stage, the input and output particle size distribution of the crushing block, streams 1 and 2 in Figure 2, have to be defined. The input size is specified in the solids sub-stream of the feed stream. An average size of 4mm (4 000 microns) was defined regarding the average size of the barley grain. According to the results of an experimental evaluation performed in this project, BSG must be ground to obtain a mean particle size of 501,2 µm (Rojas-Pérez, 2018).

Table 1. Description of the components used in the process simulation

Component ID	Type	Component name and source of properties	Alias
WATER	Conventional	WATER - Aspen Plus V9 Databases	H_2O
XYLOS-01	Conventional	XYLOSE - Aspen Plus V9 Databases	$C_5H_{10}O_5$-D2
ARABI-01	Conventional	ARABINOSE - Aspen Plus V9 Databases	$C_5H_{10}O_5$-D1
NAOH	Conventional	SODIUM-HYDROXIDE - Aspen Plus V9 Databases	NAOH
XYLAN	Solid	Xylan is considered as a solid throughout the process and never as solution. Additionally, xylan is a polymer, but its molecular weight formula will be taken only as the repeat unit. The other properties are determined on a weight basis and then converted to mole basis for the database, using the molecular weight of a repeat unit (Wooley and Putsche, 1996).	$C_5H_8O_4$
ARABINAN	Solid	Isomer of xylan. The same properties are specified	$C_5H_8O_4$
CELLULOS	Solid	Cellulose is considered as solid throughout the process and never as solution. Additionally, cellulose is a polymer, but its molecular weight formula will be taken only as the repeat unit. The other properties are determined on a weight basis and then converted to mole basis for the database, using the molecular weight of a repeat unit (Wooley and Putsche, 1996)	$C_6H_{10}O_5$
LIGNIN	Solid	Lignin is as solid throughout the process and never as solution (Wooley and Putsche, 1996)	–
ASH	Solid	Ashes contained in the barley are mainly calcium oxides (Mussatto and Roberto, 2005). The compound is defined by the properties of calcium oxide.	CAO
HEMICELU	Solid	Polymer of xylan - arabinan. Properties of xylan are specified.	$C_5H_8O_4$
SULFU-01	Conventional	SULFURIC-ACID - Aspen Plus V9 Databases	H_2SO_4
SODIU-02	Conventional	SODIUM-SULFATE - Aspen Plus V9 Databases	NA_2SO_4
ETHAN-01	Conventional	ETHANOL - Aspen Plus V9 Databases	C_2H_6O-2
PROT-SOL	Solid	Solid protein. Solid type compound. The composition of amino acids present in barley proteins are mainly glutamic acid and glutamine (Linko, Lapvetelainem, Laakso, and Kalio, 1989), thus the compound is defined with the properties of glutamic acid.	$C_5H_9NO_4$
PROTEIN	Conventional	Protein in solution, same properties of glutamic acid. L-GLUTAMIC-ACID	$C_5H_9NO_4$
ENZYME	Solid	The molecular structure, molecular weight, enthalpy of solid formation, heat capacity of solid and density of solid are specified. (Wooley and Putsche, 1996)	–
XYLAN-LQ	Conventional	Xylan in solution. Glutaric acid formation enthalpy is used because it is a compound with the same molecular composition of the xylan monomers (C5H8O4), calorific capacity and density of water, under the assumption that they behave like water because it is a compound that will be very diluted in the process.	$C_5H_8O_4$
ARABN-LQ	Conventional	Arabinan in solution. Same Xylan-LQ specifications.	$C_5H_8O_4$

Source: Authors

Alkaline pretreatment: Figure 3 presents the blocks associated with the alkaline pretreatment. It consists in the use of basic compounds to produce solvation of some polymeric chains present in biomass, increasing its surface area and porosity (Menon and Rao, 2012). The main advantage of this type of treatment is to avoid the formation of furan compounds with inhibitory action during the fermentation stage. Additionally, yield in hemicellulose degradation and pentose formation is high (Bhutto *et al.*, 2017).

The outlet stream of the mill (2 in Figure 2) contains BSG whose particle size has been reduced to facilitate the pretreatment steps. This stream is mixed with a stream of NaOH 4M at 1:14 mass ratio in dry basis of BSG. This relationship was selected according to the results of a previous experimental study performed to determine the effect of some variables on alkaline pretreatment. At that condition, approximately 76 % of the AX contained in the hemicellulose are extracted.

After mixing, the blend was fed to a stirred tank reactor operating at 40 °C. Since the kinetics of the hemicellulose alkaline hydrolysis to AX is unknown, the simulation is developed in a conversion reactor (B2 in Figure 3). Theoretically, in this kind of simulation block, the generation of shorter chains of AX in solution occurs and, likewise, the protein contained in the BSG is solubilized.

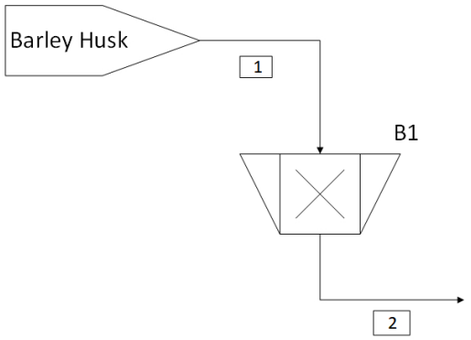

Figure 2. Schematic representation of the crushing block in the Aspen Plus Process Simulator V9® interface.
Source: Authors

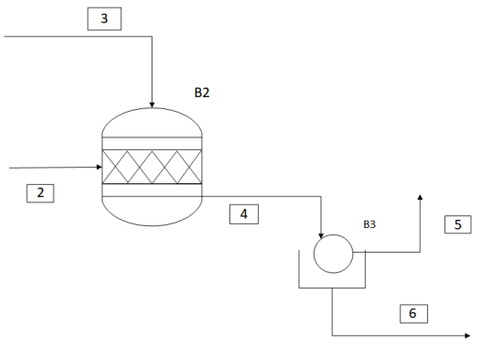

Figure 3. Schematic representation of an alkaline pretreatment section in Aspen Plus Process Simulator V9® interface.
Source: Authors

Knowing the composition of hemicellulose of BSG, ~70 % of this fraction corresponds to xylan and 30 % to arabinan. Thus, considering a yield of 76 %, the following reactions are specified in the reactor B2:

1) Generation of xylan in solution from hemicellulose (Conversion of 44,7 % of hemicellulose)

2) Generation of arabinan in solution from hemicellulose (Conversion of 20,3 % of hemicellulose)

3) Protein solid in solution (100 % of Solid Protein)

Finally, a tangential filtration is performed (B3 in Figure 3), where solids are separated from the liquid mixture. The solid stream contains mainly lignin and cellulose compounds and the liquid stream is an aqueous solution of AX and proteins.

Proteins Separation: Figure 3 presents the block associated with proteins separation stage. The liquid stream 6 from the filter B3 is treated in the tank B4 with sulfuric acid stream (7). It is added to neutralize the excess of the NaOH previously used in the alkaline hydrolysis and to bring the solution to the pH of the isoelectric point of the proteins, in order to precipitate them (Vieira *et al.*, 2014). Thus, the acid treatment produces a heterogeneous stream (8) fed to the centrifuge (B5 in Figure 4), where a solid stream (9) containing the protein and a liquid stream (10) containing the AX are obtained.

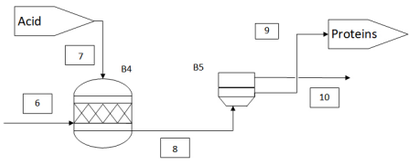

Figure 4. Schematic representation of the protein separation section in the Aspen Plus Process Simulator V9® interface.
Source: Authors

The specific reactions for reactor B4 are reported in Figure 5.

$$2NaOH + H_2SO_4 \Rightarrow 2H_2O + Na_2SO_4$$

$$Protein \Rightarrow ProtSol \qquad \text{Protein precipitation}$$

Figure 5. Reactions specified in the protein precipitation reactor B4.
Source: Authors

Arabinoxylans precipitation and washing: Precipitation of AX is carried out by the addition of ethanol, taking advantage of the low solubility of AX in this solvent. 100 % yield respect to AX precipitation was considered for simulation. Regarding the previous neutralization step, the aqueous stream 10, rich in AX, contains a considerable amount of dissolved Na_2SO_4. Although this salt is soluble in ethanol, a fraction co-precipitates with AX. For this reason, it is necessary to wash the solid AX with ethanol for solubilizing and thus entraining the salt present in the solid.

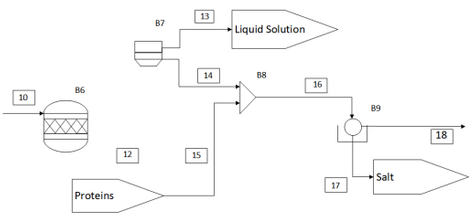

Figure 6. Schematic representation of AX precipitation and washing in the Aspen Plus Process Simulator V9® interface.
Source: Authors

For the simulation of this step, the AX rich liquid stream (10) is mixed with azeotropic ethanol (11) in a volume ratio 1:5 (Reis, Coelho, Coimbra, and Abu-Ghannam, 2015). This condition was selected from previous experimental evaluation. The mixture is sent to a conversion reactor (B6 in Figure 6), where precipitation of AX is specified. The solid-liquid mixture is fed to a centrifuge (B7 in Figure 6) where two phases are separated. Solids stream corresponds to concentrated AX (14). Then, this stream is mixed with azeotropic ethanol (15), to wash the solids and thus remove traces of Na_2SO_4. Finally, the liquid ethanol-salt mixture (stream 16) is separated from the solid AX using a filter (B9 in Figure 6).

Enzymatic Hydrolysis: Once the AX are obtained, enzymatic hydrolysis is carried out. This process is catalyzed by enzymes and the chains of AX are broken in xylose and arabinose.

For the simulation of this stage, two streams are fed to the reactor B10 in Figure 7: one of the streams corresponds to solid AX from filter B9 (18) and the other is the enzyme aqueous solution stream (19), which includes the water required to dilute the substrate to the required conditions. The conditions employed to simulate enzymatic hydrolysis were obtained from experimental tests developed in previous work of the research project (Rojas-Pérez, 2018). Enzymatic hydrolysis is performed at the following conditions: 40 °C, pH 5,5 and AX initial concentration 5 g/L. The reaction was specified in a conversion reactor (B10), where final concentration of xylose and arabinose are 1,31 g/L and 0,44 g/L, respectively. These values correspond to 65 % and 42 % yield, respectively.

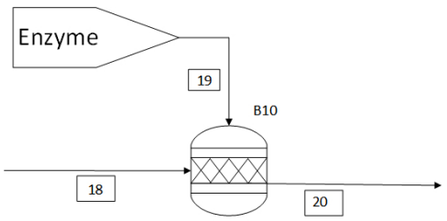

Figure 7. Schematic representation of the hydrolysis reactor in the Aspen Plus Process Simulator V9® interface.
Source: Authors

Results

Results of the simulation validate the process designed. Figure 8 presents the process flow diagram (PFD) and Table 4 shows the material balance for one of the three production capacities studied (156 000 t/year).

As the process for each of the three production cases evaluated was the same, PFD are similar and the differences in mass and energy balances are mainly due to the availability of AX to hydrolyze. Table 2 shows the xylose produced after the process. The final conversion of xylose is close to 8,5 % based on the initial dry weight of BSG, in all the cases. This conversion is mainly linked to yield of the enzymatic hydrolysis, because the conversion of AX into xylose and arabinose is incomplete. In addition to the stream containing xylose and arabinose in the feedstock fermentation section, three byproducts are generated: the solid residue rich in cellulose (stream 5), the protein extracted from BSG (stream 9) and the liquid rich in phenolic compounds, such as p-coumaric and ferulic acids (stream 13).

Table 2. Xylose produced as a function of the BSG production capacity

Brewery	Residual BSG (t/year)	Xylose produced (t/year)
Bavaria Tocancipá	156 000	2 657
Bavaria Tibasosa	46 000	783,5
BBC Tocancipá	800	13,6

Source: Authors

Table 3 shows the net heat duty for the main simulation blocks: Alkaline treatment tank (B2), neutralization and proteins precipitation tank (B4), ethanol mixing tank for AX precipitation (B6) and enzymatic hydrolysis reactor (B10). The only equipment that requires cooling services is the neutralization tank, mainly due to the sudden increase in temperature by the heat of reaction released during the formation of sodium sulfate.

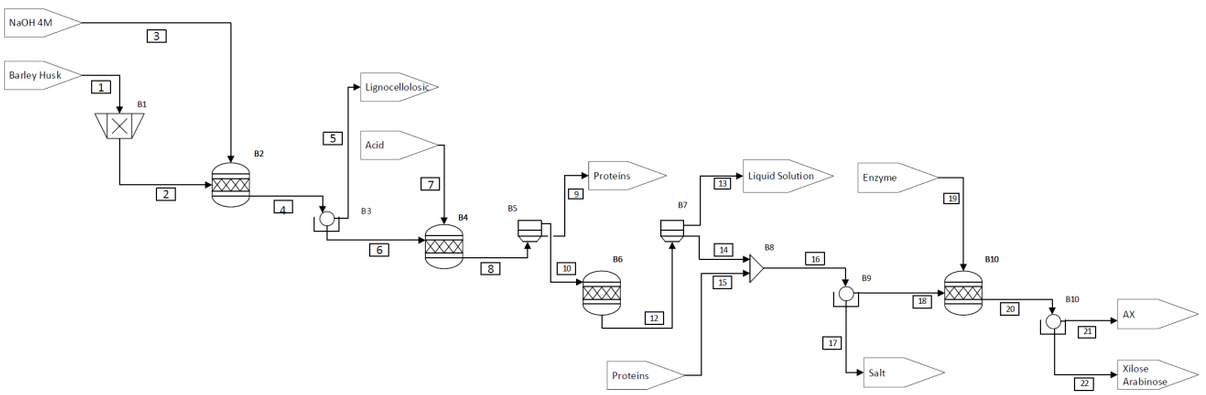

Figure 8. Process Flow Diagram for the simulated process. Residual wet BSG processed 156 000 t/year corresponding to Bavaria Tocancipá Brewery.
Source: Authors

Table 3. Energy consumption associated with the main equipment of the simulation

	B2	B4	B6	B10
Specified temperature (°C)	40	25	25	40
Treatment capacity of BSG (t/year)	**Net heat duty (kW)**			
156 000	902,2	-1 654,8	226,5	22,4
46 000	193,5	-4 879,4	66,8	6,6
800	3,4	-84,9	1,2	0,11

Source: Authors

In this section of the simulation, the detailed sizing of the pretreatment equipment is pending. Pretreatment and fermentation stages of the process are operated in batches, where the size of the equipment and its time of operation depends on the programming of the process and the required lot sizes. These factors will be established when performing the economic feasibility, as well as the detailed sizing.

Conclusions

The technical feasibility of the designed process for obtaining xylitol from BSG has been proved at different production rates through simulation in Aspen Plus. Simulation results show that xylose obtained corresponds to 8,5 % of the dry weight of the raw material, obtaining a yield of 58 %. Several streams of byproducts were obtained, such as proteins, polypeptides, amino acids, phenolics compounds and lignocellulosic residues that can be valorized in other processes. In the second part of this article, simulation for the three production capacities will be used to perform the economic feasibility assessment.

Acknowledgements

Authors greatly acknowledge the financial support provided by Universidad Nacional de Colombia-DIB (Researches Division-Campus Bogotá, project 35822). Additionally, Carolina Rojas is grateful with Colciencias for the funding granted through the program "Beca de doctorado nacional convocatoria 617 de 2014".

Table 4. Mass balance for the simulated process. Residual wet BSG processed 156 000 t/year corresponding to Bavaria Tocancipá Brewery (Units 1 to 11)

	Units	1	2	3	4	5	6	7	8	9	10	11
From			B1		B2	B3	B3		B4	B5	B5	
To		B1	B2	B2	B3		B4	B4	B5		B6	B6
Temperature	C	25	25	25	40	25	25	25	25	25	25	25
Pressure	atm	1	1	1	1	1	1	1	1	1	1	1
Mass Enthalpy	J/kg	-14 543 075	-14 543 074	-14 544 899	-14 501 577	-10 558 009	-14 670 137	-8 244 437	-14 540 127	-11 300 971	-14 597 035	-6 514 812
Mass Density	kg/ m^3	1 054	1 054	1 034	1 031	1 344	1 033	1 740	888	1 080	885	807
Volume Flow	m^3/year	140 359	140 359	498 337	643 715	14 070	623 781	55 330	834 349	1 1843	822 506	3 190 236
Mass Flows	t/year	147 982	147 982	515 424	663 406	18 907	644 498	96 255	74 0754	12 789	72 7964	2 575 454
WATER	t/year	124 800	124 800	438 547	563 347	5 633	557 714	1 925	593 919	5 939	587 980	128 496
XYLOS-01	t/year	0	0	0	0	0	0	0	0	0	0	0
ARABI-01	t/year	0	0	0	0	0	0	0	0	0	0	0
NAOH	t/year	0	0	76 877	76 877	769	76 108	0	0	0	0	0
XYLAN	t/year	0	0	0	0	0	0	0	0	0	0	0
ARABINAN	t/year	0	0	0	0	0	0	0	0	0	0	0
CELLULOS	t/year	4 961	4 961	0	4 961	4 961	0	0	0	0	0	0
LIGNIN	t/year	3 494	3 494	0	3 494	3 494	0	0	0	0	0	0
ASH	t/year	1 092	1 092	0	1 092	1 092	0	0	0	0	0	0
PROTEIN	t/year	0	0	0	5 491	55	5 436	0	0	0	0	0
HEMICELU	t/year	8 143	8 143	0	2 850	2 850	0	0	0	0	0	0
SULFU-01	t/year	0	0	0	0	0	0	94 330	1 016	10	1 006	0
SODIU-02	t/year	0	0	0	0	0	0	0	135 143	1 351	133 791	0
ETHAN-01	t/year	0	0	0	0	0	0	0	0	0	0	2 446 958
PROT-SOL	t/year	5491	5491	0	0	0	0	0	5436	5436	0	0
ENZYME	t/year	0	0	0	0	0	0	0	0	0	0	0
XYLAN-LQ	t/year	0	0	0	3 640	36	3 604	0	3 604	36	3 568	0
ARABN-LQ	t/year	0	0	0	1 653	17	1 636	0	1 636	16	1 620	0

Source: Authors

Table 5. Mass balance for the simulated process. Residual wet BSG processed 156 000 t/year corresponding to Bavaria Tocancipá Brewery (Units 12 to 22)

	Units	12	13	14	15	16	17	18	19	20	21	22
From		B6	B7	B7		B8	B9	B9		B10	B11	B11
To		B7		B8	B8	B9		B10	B10	B11		
Temperature	C	25	25	25	25	25	25	25	40	40	25	25
Pressure	atm	1	1	1	1	1	1	1	1	1	1	1
Mass Enthalpy	J/kg	-8 293 699	-8 297 667	-7 954 232	-6 514 812	-6 773 438	-6 798 536	-5 810 246	-15 802 087	-15 750 102	-9 029 946	-15 833 083
Mass Density	kg/ m^3	822	821	876	807	819	809	1479	979	981	1 303	995
Volume Flow	m^3/year	4 019 870	3 976 313	43 557	215 870	259 437	255 788	3 649	1 067 178	1 070 379	2 484	1 052 209
Mass Flows	t/year	3 303 418	3 265 248	38 170	174 270	212 440	207 045	5 395	1 064 274	1 069 669	3428	1 066 241
WATER	t/year	71 6476	709311	7 165	8 695	15 860	15 844	16	1 045 160	1 044 767	1 045	1 043 722
XYLOS-01	t/year	0	0	0	0	0	0	0	0	2 635	3	2 633
ARABI-01	t/year	0	0	0	0	0	0	0	0	773	1	772
NAOH	t/year	0	0	0	0	0	0	0	0	0	0	0
XYLAN	t/year	3 568	0	3 568	0	3 568	0	3 568	0	1 249	1 249	0
ARABINAN	t/year	1620	0	1620	0	1620	0	1620	0	940	940	0
CELLULOS	t/year	0	0	0	0	0	0	0	0	0	0	0
LIGNIN	t/year	0	0	0	0	0	0	0	0	0	0	0
ASH	t/year	0	0	0	0	0	0	0	0	0	0	0
PROTEIN	t/year	0	0	0	0	0	0	0	0	0	0	0
HEMICELU	t/year	0	0	0	0	0	0	0	0	0	0	0
SULFU-01	t/year	1 006	995	10	0	10	10	0	0	0	0	0
SODIU-02	t/year	133 791	132 453	1 338	0	1 338	1 337	1	0	1	0	1
ETHAN-01	t/year	2 446 958	2 422 488	24 470	165 575	190 045	189 855	190	0	190	0	190
PROT-SOL	t/year	0	0	0	0	0	0	0	0	0	0	0
ENZYME	t/year	0	0	0	0	0	0	0	19 113	19 113	191	18 922
XYLAN-LQ	t/year	0	0	0	0	0	0	0	0	0	0	0
ARABN-LQ	t/year	0	0	0	0	0	0	0	0	0	0	0

Source: Authors

References

Dávila, A. J., Rosenberg M., and Cardona, C. A., (2016). A biorefinery approach for the production of xylitol, ethanol and polyhydroxybutyrate from brewer's spent grain. *AIMS Agriculture and Food*, *1*(1), 52-66. DOI: 10.3934/agrfood.2016.1.52

Bhutto, A. W., Qureshi, K., Harijan, K., Abro, R., Abbas, T., Bazmi, A. A., . . . Yu, G. (2017). Insight into progress in pre-treatment of lignocellulosic biomass. *Energy*, *122*, 724-745. DOI: 10.1016/j.energy.2017.01.005

Cherubini, F. (2010). The biorefinery concept: Using biomass instead of oil for producing energy and chemicals. *Energy Conversion and Management*, *51* (7), 1412-1421. DOI: 10.1016/j.enconman.2010.01.015

Gil, I. D., López, J. R. G., Zapata, J. L. G., Robayo, A. L., and Niño, G. R. (2015). *Process Analysis and Simulation in Chemical Engineering*. Switzerland: Springer Publishing. DOI: 10.1007/978-3-319-14812-0

Hermann, B. G., Blok, K., and Patel, M. K. (2007). Producing bio-based bulk chemicals using industrial biotechnology saves energy and combats climate change. *Environmental Science and Technology*, *41* (22), 7915-7921. DOI: 10.1021/es062559q

Jong, E., Higson, A., Walsh, P., and Wellisch, M. (2011). *Bio-based Chemicals - Value Added Products from Biorefineries* (*Task 42: Biorefineries*). A Report Prepared for IEA Bioenergy. Retrieved from: https://www.ieabioenergy.com/wp-content/uploads/2013/10/Task-42-Biobased-Chemicals-value-added-products-from-biorefineries.pdf

Linko, R., Lapveteläinen, A., Laakso, P., and Kallio, H. (1989). Protein composition of a high-protein barley flour and barley grain. *Cereal Chem*, *66*, 478-482. Retrieved from: https://pdfs.semanticscholar.org/e782/b55d717ec48177bc8a28bd39f7f60dc08515.pdf

Meneses, N. G. T., Martins, S., Teixeira, J. A., and Mussatto, S. I. (2013). Influence of extraction solvents on the recovery of antioxidant phenolic compounds from brewer's spent grains. *Separation and Purification Technology, 108*, 152-158. DOI: 10.1016/j.seppur.2013.02.015

Menon, V., and Rao, M. (2012). Trends in bioconversion of lignocellulose: Biofuels, platform chemicals & biorefinery concept. *Progress in Energy and Combustion Science, 38* (4), 522-550. DOI: 10.1016/j.pecs.2012.02.002

Mussatto, S and Roberto, C. (2005). Acid hydrolysis and fermentation of brewer's spent grain to produce xylitol, *Journal of the Sicence of Food and Agriculture, 85*(14), 2453-2460. DOI: 10.1002/jsfa.2276

Mussatto, S. I., Dragone, G., and Roberto, I. C. (2006). Brewers' spent grain: generation, characteristics and potential applications. *Journal of Cereal Science, 43*(1), 1-14. DOI: 10.1016/j.jcs.2005.06.001

Mussatto, S. I., and Roberto, I. C., (2008). Establishment of the optimum initial xylose concentration and nutritional

supplementation of brewer's spent grain hydrolysate for xylitol production by Candida guilliermondii. *Process Biochemestry, 43* (5), 540-546. DOI: 10.1016/j.procbio.2008.01.013

Mussatto, S. I., Moncada, J., Roberto, I. C., and Cardona, C. A. (2013). Techno-economic analysis for brewer's spent grains use on a biorefinery concept: The Brazilian case. *Bioresource Technology, 148*, 302-310. DOI: 10.1016/j.biortech.2013.08.046

Ravella, S. R., Gallagher, J., Fish, S., and Prakasham, R. S. (2012). Overview on Commercial Production of Xylitol, Economic Analysis and Market Trends. In: da Silva S., Chandel A. (Eds.) *D-Xylitol*. Berlin, Alemania: Springer. DOI: 10.1007/978-3-642-31887-0_13

Reinold, M. R. (1997). *Manual Prático de Cervejaria*. Sao Paulo: ADEN Editora e Comunicações Ltda.

Reis, S. F., Coelho, E., Coimbra, M. A., and Abu-Ghannam, N. (2015). Influence of grain particle sizes on the structure of arabinoxylans from brewer's spent grain. *Carbohydrate Polymers, 130*, 222-226. DOI: 10.1016/j.carbpol.2015.05.031

Rojas-Pérez, L. C. (2018). Valorización de la cascarilla de cebada del proceso cervecero para la producción de xilitol. (Ph.D. Thesis, Universidad Nacional de Colombia-Campus Bogotá). Retrieved from: http://bdigital.unal.edu.co/69970/1/Tesis%20Doctorado%20Lilia%20Carolina%20Rojas%20P%C3%A9rez.pdf

Vieira, E., Rocha, M. A. M., Coelho, E., Pinho, O., Saraiva, J. A., Ferreira, I. M. P. L. V. O., and Coimbra, M. A. (2014a). Valuation of brewer's spent grain using a fully recyclable integrated process for extraction of proteins and arabinoxylans. *Industrial Crops and Products, 52*, 136-143. DOI: 10.1016/j.indcrop.2013.10.012

Wooley, R. J., and Putsche, V. (1996). *Development of an ASPEN PLUS Physical Property Database for Biofuels Components*. Golden, Colorado: National Renewable Energy Laboratory. Retrieved from: https://www.nrel.gov/docs/legosti/old/20685.pdf

Xiros, C., and Christakopoulos, P. (2012). Biotechnological potential of brewers spent grain and its recent applications. *Waste and Biomass Valorization, 3*(2), 213-232. DOI: 10.1007/s12649-012-9108-8

Xu, J.-K., and Sun, R.-C. (2016). Recent Advances in Alkaline Pretreatment of Lignocellulosic Biomass. In S. I. Mussatto. (Ed.), *Biomass Fractionation Technologies for a Lignocellulosic Feedstock Based Biorefinery* (pp. 431-459). Amsterdam, Holanda: Elsevier. DOI: 10.1016/B978-0-12-802323-5.00019-0

Ingeniería e Investigación vol. 39 No. 1, April - 2019 (24-35)

DOI: http://dx.doi.org/10.15446/ing.investig.v39n1.69703

Study of coagulating/flocculating characteristics of organic polymers extracted from biowaste for water treatment

Estudio de las características coagulantes/floculantes de polímeros orgánicos extraídos de residuos para el tratamiento de agua

B. Buenaño[1], E. Vera[2] and M. B. Aldás[3]

ABSTRACT

The aim of this research was to evaluate the coagulating/flocculating characteristics of three natural polymers: green plantain peel starch, orange peel pectin and tamarind seed extracts in three solutions (water, sodium chloride and ammonium acetate), for the purification of raw natural water with turbidity of 5,32 NTU. Natural polymers did not present coagulant activity due to the low turbidity of raw natural water. However, they showed flocculant activity in combination with aluminum sulfate. The optimal combinations of aluminum sulfate [mg/L] + natural polymer [mg/L] were: 50+0,2 for starch, 60+0,06 for pectin, 60+0,6 for tamarind extract in water, 60+0,5 for tamarind extract in sodium chloride and 60+0,2 for tamarind extract in ammonium acetate. Removal values of turbidity and color were about 87 % and 92 %, respectively. Residual sludge exceeded the maximum permissible limits for discharging to the sewer system. In addition, it showed a toxic effect on the mitotic activity of onion roots with an IC_{50} of 0,5 to 2 %.

Keywords: Coagulation/floculation, floculation aid, natural polymers, water purification.

RESUMEN

El objetivo de esta investigación fue evaluar las características coagulantes/floculantes de tres polímeros naturales: almidón de cáscara de plátano verde, pectina de cáscara de naranja y extracto de semilla de tamarindo en tres soluciones (agua, cloruro de sodio y acetato de amonio), para la purificación de agua natural cruda con turbidez de 5,32 NTU. Los polímeros naturales no presentaron actividad coagulante debido a la baja turbidez del agua natural cruda. Sin embargo, mostraron actividad floculante en combinación con sulfato de aluminio. Las combinaciones óptimas de sulfato de aluminio [mg/L] + polímero natural [mg/L] fueron: 50+0,2 para almidón, 60+0,06 para pectina, 60+0,6 para extracto de tamarindo en agua, 60+0,5 para extracto de tamarindo en cloruro de sodio y 60+0,2 para extracto de tamarindo en acetato de amonio. Los valores de eliminación de turbidez y color fueron aproximadamente 87 % y 92 %, respectivamente. El lodo residual excedió los límites máximos permisibles para la descarga al sistema de alcantarillado, además, mostró un efecto tóxico sobre la actividad mitótica de las raíces de cebolla a un CI_{50} de 0,5 a 2 %.

Palabras clave: Coagulación-floculación, ayudantes de floculación, polímeros naturales, potabilización.

Received: August 1st, 2018
Accepted: March 27th, 2019

Introduction

The study and use of natural coagulants/flocculants in water purification have had a growing interest due to their advantages over chemical coagulants/flocculants, such as low toxicity, biodegradability, low cost, abundant sources of production and mainly elimination of the toxic risk to the human being (Peruço, Lenz, Fiori and Bergamasco, 2013; Saritha, Srinivas, and Vuppala, 2017).

The conventional use of inorganic coagulants such as aluminum sulfate and ferric chloride, generate problems with their cost, undesirable large volumes of non-biodegradable sludge and effects on human body. For ferric salts, careful control in dosification is necessary because excessive residual iron could produce colored water (Choy, Prasad, Wu, Raghunandan, and Ramanan, 2014). For aluminum, the toxic risk is related to the presumed increase in the intake at 4 mg Al/day from aluminum sulfate (Suay and Ballester, 2002; World Health Organization, 2011). It also affects the liver, heart, brain, etc. and is related to Alzheimer's degeneration (Hayder and Rahim, 2015). In addition, the use of aluminum sulphate requires a good pH regulation, otherwise, clarification process is poor and solubilized aluminum can cause alterations in the effluent quality, due to the re-stabilization of charged particles in water (Cogollo, 2011).

[1]Environmental Engineer, Escuela Politécnica Nacional, Ecuador. Affiliation: Escuela Politécnica Nacional, Ecuador. E-mail: brenda.buenano@epn.edu.ec.
[2]Chemical Engineer, Escuela Politécnica Nacional, Ecuador. Ph.D. Process Engineer, Université de Montpellier II, France. Affiliation: Full-Professor, Escuela Politécnica Nacional, Ecuador. E-mail: edwin.vera@epn.edu.ec.
[3] Chemical Engineer, Escuela Politécnica Nacional, Ecuador. M.Sc. Environmental Engineer, Escuela Politécnica Nacional, Ecuador. Affiliation: Escuela Politécnica Nacional, Ecuador. E-mail: maria.aldas@epn.edu.ec.

How to cite: Buenaño, B., Vera, E., Aldás, M. B. (2019). Study of coagulating/flocculating characteristics of organic polymers extracted from biowaste for water treatment. *Ingeniería e Investigación*, *39*(1), 24-35. DOI: 10.15446/ing.investig.v39n1.69703

The total or partial substitution of the traditionally used coagulant, aluminum sulfate, with natural coagulants aims mainly to eliminate the toxic risks due to its biodegradation. But it also seeks to solve the problem of final disposal of the residual sludge and its incidence on plant communities, since these sludges have a poor dehydration capacity (90 % water) and 40 to 50 % unreacted aluminum (Peruço et al., 2013; Antov, Šćiban, Prodanović, Kukić, Vasić, Đorđević, and Milošević, 2018).

The coagulation and flocculation processes aim to remove particles and organic matter dissolved in natural water, in order to improve aesthetics and health aspects of water. The main mechanism of coagulation/flocculation of polymers is the sweeping action due to their high molecular weight and high number of segments in their chains (Mihelcic and Zimmerman, 2012; Silva, 2015).

Several polymers extracted from natural sources have been used as coagulants in natural water, such as Nirmali seed (80 % turbidity removal), *Cassia angustifolia* seed, mesquite bean, *Cactus latifaria*, chestnut and acorn. All of them have reached high turbidity removal from 70 % to 93 %. In contrast, *Cactus opuntia spp*. has reached only 50 % (Farhaoui and Derraz, 2016; Vijayaraghavan, Sivakumar and Kumar, 2011). Other studies assayed *Carica papaya* seeds (90 %), *Citrus sinensis* peel (85 %), *Feronia limonia* seeds (77 %) and *Tamarindus indica* seeds (80 %), as natural coagulants with relevant values of turbidity removal (Choy *et al*., 2014).

The most studied natural coagulant is *Moringa Oleífera* and presents a high removal efficiency for natural waters of high turbidity and even for waters of low turbidity (< 5 Nephelometric Turbidity Unit, NTU) with 6,5 abs/m color, 765 Colony forming unit (CFU)/100 mL and 605 CFU/100 mL *E. coli*, with a reduction of 41,4, 76,8 and 81,8 %, respectively, for a dose of 500 mg/L (Pritchard, Craven, Mkandawire, Edmondson and O'Neill, 2010). It must also be considered that the use of 5 % *Moringa oleifera* seeds does not affect measurements of hydrogen potential (pH), conductivity, alkalinity, cation and anion concentrations, but concentration of organic matter in the treated water can increase considerably, acting as precursor of trihalomethanes during desinfection with chlorine (Ndabigengesere and Narasiah, 1998). On the one hand, increasing the organic matter, nitrate and phosphate contents limits shelf life of coagulants and compromises its feasibility (Megersa, Beyene, Ambelu, and Triest, 2018). On the other hand, with the use of exudates gums from *Samanea saman*, a significant removal of fecal coliforms (99,7 %) and total coliforms (99,8 %) was achieved (González, Chávez, Mejías, Mas y Rubí, Fernández, and León de Pinto, 2006). This occurs because natural coagulants are not only water clarifying agents, but they also have antimicrobial properties in some cases (Saranya, Ramesh and Gandhimathi, 2014; Antov et al., 2018; Megersa *et al.*, 2018).

For all the above reasons, the use of natural coagulants/flocculants for purification has been widely studied in countries such as Spain, Serbia, Brazil, Iran, among others. However, in Ecuador there are few works carried out in this line of research, especially considering the reuse of organic food waste as a source of natural coagulants/flocculants (Bongiovani, Konradt-Moraes, Bergamasco, Lourenço, and Tavares, 2010).

In Ecuador, the generation of solid waste was 4,06 million metric tons in 2016, with a per capita generation of 0,74 kg/inhabitant/day and it was mainly constituted by organic solid waste (61 %) (Instituto Nacional de Estadísticas y Censos, INEC, 2016). The final disposal of solid waste is mainly in landfills (39 %), where there are several compounds of interest that can be extracted (INEC, 2016). With the use of biowaste, the useful life of sanitary landfills and the maintenance costs involved could be enhanced. Choy, Prasad, Wu, Raghunandan, and Ramanan (2015) identified at least 14 natural coagulants extracted from vegetables and legumes considered common. Likewise, it has been demonstrated that underutilized or untreated biomass (carboxycellulose nanofibers) can be used as an effective Cd (II), Pb (II) and other heavy metal ions removers for water purification (Sharma, Joshi, Sharma, and Hsiao, 2017; Sharma, Chattopadhyay, Sharma, Geng, Amiralian, Martin, and Hsiao, 2018a and Sharma, Chattopadhyay, Zhan, Sharma, Geng, and Hsiao, 2018b).

Consequently, it is proposed to conduct a study on the efficiency of the coagulant/flocculant activity of three natural polymers derived from organic solid food waste (plantain peel starch, orange peel pectin and tamarind seed extract) for the purification of water.

Materials and Methodology

The study was carried out in three experimental stages: 1) extraction and characterization of natural polymers, 2) evaluation of the coagulant and flocculant activity and 3) characterization of the residual sludges and their toxicological effect.

Extraction and characterization of natural polymers

Starch was extracted from the residues of plantain peel (*Musa paradisiaca L*). These residues also contained a small amount of unused plantain and rachis. The procedure was based on the methodology proposed by Hernández-Medina, Torruco-Uco, Chel-Guerrero and Betancur-Ancona (2008). Peels were selected, washed and milled in a Ramon cutter employing a ratio peel : 1 500 ppm sodium bisulfite solution (from Loba Chemie I.) of 1 : 0,5 (w/v) and pectinase at 0,2 mL/kg of peel. Then, the paste obtained was mixed in a Cripto Peerless EC-30 mixer with a ratio peel paste: 0,3 % citric acid solution of 1 : 0,5 (w/v). This last step was repeated three times. Then, the blend was allowed to stand for 12 hours and the supernatant was eliminated. The sedimented material was filtered through the No. 200 sieve using water (three washes) to eliminate fibers. The fraction that passed the sieve was decanted for 12 hours, and the lower white layer was separated and dried in a Blue M OV-500C-2 stove at 50 °C for 24 hours.

Pectin was extracted exclusively from albedo of orange peel (*Citrus sinensis*) based on the methodology proposed by Devia (2003). The following modifications were applied: acid hydrolysis at pH 1 with H_2SO_4 MERCK, filtration with cloth to remove insoluble solids, precipitation with ethanol 96 %, drying on a BLUE M OV-500C-2 stove at 35 °C for 12 hours, grinding in a Thomas 4275-Z10 mill and sieving through the No. 18 sieve.

Tamarind seed (*Tamarindus indica L*) extract was obtained from residues of wet pulping process, which also contained pulp and fiber residues; based on the methodologies proposed by García (2007) and Hernández, Mendoza, Salamanca, Fuentes, and Caldera (2013) with some modifications. Seeds were hydrated for 5 days to remove the skin; then, the almonds obtained were dryed in a Memmert UN55plus convection oven at 25-35 °C for 2 days. Dry almonds were grinded in a Thomas 4275-Z10 mill to obtain a fine white powder, which was put through the No. 18 sieve. Afterward, oil was extracted using a ratio powder: ethanol 96 % of 5 : 95 for 30 minutes. The solids were settled, separated and dried in the Memmert UN55 plus convection oven at 35 °C for 18 hours. Solutions of 5 %, 1 % and 0,1% (w/v) of defatted almond powder in 3 different solvents: distilled water, 0,5 M sodium chloride (from J. T. Baker) and 10 mM of ammonium acetate (from Loba Chemie) were prepared, heated to 65 °C and the supernatants were separated (tamarind seed extracts).

The extracted natural polymers were characterized by moisture, ethereal extract, protein, ash, crude fiber and total carbohydrates assays according to the Association of Official Agricultural Chemists (AOAC) methods: AOAC 925.10, AOAC 920.85, AOAC 2001.11, AOAC 923.03, International Cereal Chemists (ICC) # 13 and Food and Agriculture Organization (FAO), respectively (Association of Official Analytical Chemists and Horwitz, 2000).

Particle size and zeta potential were determined in a particle size analyzer Brookhaven model 90 Plus in 1% w/w aqueous solutions of each polymer.

IR spectra were obtained in a transmission cell of Perkin Elmer Model Spectrum One Fourier Transform Infrared Spectrometer. Pellets of dried samples were prepared employing potassium bromide FTIR grade (from Sigma-Aldrich). The spectrum of pectin and starch were compared with the spectrum of commercial food grade citric pectin and potato starch (from Loba Chemie).

Scanning electron microscopy (SEM) images were obtained by coating the dried samples with a thin layer of gold using a sputter coating apparatus Spi Module at 4 mBar for 10 s. The coated samples were examined in a Tescan Model Vega LMU scanning electron microscope operating at 15 kV or 20 kV in the secondary electron imaging mode.

Evaluation of the coagulant and flocculant activity

Natural water sampling: Raw water was obtained from a water purification plant. Sampling point was located before addition of chemical coagulant and aluminum sulfate. After undergoing a primary treatment of decantation, parameters measured in situ were temperature, pH and conductivity with a pH/Cond 340i WTW equipment.

Physicochemical and microbiological characterization of natural and clarified water: Raw and clarified water were characterized in their physico-chemical and microbiological properties by standardized assays of turbidity, color, solids (totals, settleable, suspended and dissolved), pH, alkalinity, Chemical Oxygen Demand (COD), Biochemical Oxygen Demand (BOD_5), hardness, aluminum and coliforms (APHA, 2005).

Coagulant and flocculant activity assays: Five chemical substances were used: starch, pectin, tamarind seed extract, aluminum sulfate (8,32 % Al_2O_3) and polyacrylamide (PAM). PAM was used as a reference for commercial polymer only in flocculant activity.

Primary coagulant activity assay: it was carried out with an adaptation of the methodologies used by García (2007) and Ghebremichael, Gunaratna, Henriksson, Brumer, and Dalhammar (2005), with the purpose of using a sample volume of 10 mL. It consisted in preparing synthetic turbid water with kaolin adjusted to 10 and 280 NTU (average value and highest value were found in the water purification plant). Then, 10 mL of turbid water were placed in a test tube, adding several doses from 50 to 200 μL of coagulant substances and distilled water (for the control). The sample was homogenized and initial absorbance was measured in a Hach DR 2700 spectrophotometer at 500 nm (Abs_{t_0}), The solution was left at rest for 1 hour and 3 mL of supernatant were extracted. Final absorbance ($Abs_{t_{60}}$) was measured and the percentage of coagulant activity was calculated by Equation (1).

$$\text{Coagulant activity } [\%] = \frac{Abs_{t_0} - Abs_{t_{60}}}{Abs_{t_0}} \times 100 \qquad (1)$$

Coagulating substances were aluminum sulfate, starch, pectin and the three solutions of the tamarind seed extract applied at 1 % and 5 % (w/v) for the two types of synthetic turbid water of 10 and 280 NTU, respectively.

Jars Test: For the evaluation of coagulant activity, coagulant substances used at 1 % (w/v) solution were: aluminum sulfate, starch and tamarind seed extract in water, sodium chloride and ammonium acetate. For the evaluation of flocculant activity, the coagulant substance was aluminum sulfate at 1 % (w/v) in combination with 6 flocculation aids substances: PAM, starch, tamarind seed extract in water, sodium chloride and ammonium acetate were used at 0,1 %, while pectin was applied at 0,01 %.

Jars test of 6 places equipment OVAN and 1 L beakers was used. The test was carried out using the raw water sampled, based on the American Society for Testing Materials ASTM D2035-13 standard (ASTM, 2013), with the following modifications: flash mix at 100 rpm for 1 minute, slow mix at 40 rpm for 20 minutes and sedimentation for 30 minutes. The floc was monitored using the Willcomb index and the Water Research Association (WRA) size comparator.

Parameters measured immediately were color in a Hach DR2700 spectrophotometer and turbidity in a Hach 2100P turbidimeter to calculate the percentage of removal according to Equation (2), where X is the value of the parameter measured before (initial) and after (final) test.

$$Removal\ [\%] = \frac{X_{initial} - X_{final}}{X_{initial}} \times 100 \qquad (2)$$

Willcomb index was: 0 (colloidal floc), 2 (floc visible, but very small), 4 (dispersed, well-formed floc, evenly distributed, but slow settling), 6 (floc clearly distinguishable, well formed, relatively large, but precipitates slowly), 8 (good floc, which precipitates easily) and 10 (excellent floc sediments completely, leaving the water crystal clear.). The WRA size comparator was: A (0,3-0,5 mm), B (0,5-0,75 mm), C (0,75-1,0 mm), D (1,0-1,5 mm). E (1,5-2,25 mm), F (2,25-3,0 mm) and G (3,0-4,5 mm) (Arboleda, 2000).

Characterization of residual sludge and their toxicological effect

Characterization of the residual sludge: Quantification of the residual sludge was carried out using the gravimetric method suggested by the American Public Health Association (APHA) 2540 F (APHA, 2005). Physico-chemical and microbiological characterization of sludge was carried out using the following standardized assays: moisture, conductivity, total, fixed, volatile, suspended and dissolved solids, density, pH, COD, aluminum and coliforms (APHA, 2005).

Acute toxicity tests with Allium cepa L and Lactuca sativa L: Mineral water were used as negative control. Their chemical analysis was: 80,06 mg/L Ca^{2+}, 144,85 mg/L Mg^{2+}, 135,23 mg/L Na^{+}, 9,31 K^{+}, 1,5 mg/L SO_4^{2-}, 174,7 mg/L Cl^{-} and 932 mg/L dissolved solids. A dilution factor of 0,3 was used (100, 30, 10, 3 and 1 % v/v).

Acute toxicity tests with *Allium cepa L* and *Lactuca sativa L* were carried out based on the procedure suggested by Romero and Cantú (2008) to calculate the percentage of growth inhibition and half maximal inhibitory concentration (IC_{50}) by the Probit method and the inhibition of elongation and germination, respectively.

Results

Coagulant substances and flocculation aids

Table 1 summarizes the main results obtained in extraction of each polymer.

Starch yield was 1,47 %, which is higher than the 0,69 % reported by Nasrin, Noomhorm, and Anal (2015). The reason is that the waste processed in this work did not only contain peels (92,11 %), but also unused plantain and pulp (7,89 %). Furthermore, another factor that could influence was the lower moisture value of the sample (88,53 %) compared with the average of 92,5 % reported by Ilori, Adebusoye, lawal, and Awotiwon (2007).

Table 1. Main results of polymer extraction process

Characteristics	Starch	Pectin	Tamarind powder
Color	White	Brown	White
Moisture of raw material [%]	88,53 (peels)	74,20 (peels)	41,81 (seeds)
Yield [%]	1,47(12,86 DM*)	3,44(13,34 DM)	43,00 (73,9 DM)

*DM= dry matter

Source: Authors

Pectin yield was 3,44 % (13,34 % DM), which is lower than the 9,83 % (15,92 % DM) reported by Devia (2003) and Aina, Barau, Mamman, Zakari, and Haruna (2012). Nevertheless, reported values in the literature correspond to flavedo plus albedo. This result could occur because processed albedo sample had a higher moisture of 74,2 % compared with the average of 63,7 % reported by Devia (2003), in addition to a possible loss of sample in filtratration with cloth or the influence of the degree of maturation of the orange.

Tamarind powder yield was 43 %, while moisture content was 41,81 %, which is a value higher than the 11,3 % reported by Bagula, Sonawane, and Arya (2015). The reason is that tamarind residues came from wet pulping process and the residues contained 89 % seeds and 11 % fibers and lint. 75,3 % of the seeds were completely covered (or their great majority) and 24,7 % were without peel (or partially covered).

From the chemical analysis performed to natural polymers extracted, the following results were obtained. The starch had a moisture of 17,83 % with a purity of 77,7 % on a wet basis (94,56 % DM). Although this percentage is high, it is lower than the 98,86 % (DM) reported by Nasrin et al. (2015). This is possibly due to a poor drying that resulted in a moisture of almost twice the average value of 9,12 % reported in the literature. Pectin powder had moisture of 14,56 %, constituted essentially by carbohydrates (73,13 %), ashes (7,46 %) and protein (4,82 %). Tamarind seed powder with a moisture of 8,07 % was lower than the 11,4 % reported by Bagula et al. (2015). It was constituted mainly by carbohydrates (71,54 %) and protein (16,35 %), which coincides with those reported of 72,2 % and 15 %, respectively.

Results of pH, Z potential and particle size of the natural polymers are presented in Table 2.

Table 2. pH, Z potential and particle size of natural polymers

Characteristics	Starch	Pectin	Tamarind powder
pH	4,75	2,82	5,59
Z potential [mV]	-46,91	-9,80	-14,57
Particle size [nm]	290,3	5 490,1	564,1

Source: Authors

Data in Table 2 evidence that aqueous solutions of polymers showed acid character. Pectin was the polymer with the lowest value (2,82), due to the presence of free carboxylic groups (Paredes, Hernández and Cañizares, 2015). Starch

solution presented a value of 4,75, which is within the range documented by Demiate, Dupuy, Huvenne, Cereda, and Wosiacki (2000) from 3,0 to 6,0. Tamarind powder presented an acid pH of 5,59. Agarwal, Bhuptawat, and Chaudhari (2006) determined that when the pH is below 6, the surface charge of the tamarind powder is positive and that above this value tamarind seed would have a net negative charge.

Natural water had shown negative charged particles with Z potential values of -14 to -30 mV (Vane and Zang, 1997). It can be observed that the main mechanism of action of the natural polymers is sweeping action and not charge destabilization, due to their negative values. This indicates that polymer chains are also negatively charged (Ndabigengesere and Narasiah, 1995; Li, Zhou, Zhang, Wang, and Zhu, 2008).

The particle size could have an influence on the efficiency of coagulation/flocculation since the main action of polymers is sweeping, however, no correlation was found.

Figure 1 presents the IR spectra of (a) starch/potato commercial starch, (b) pectin/commercial pectin and (c) tamarind powder.

Starch FTIR spectra shows a broad band at 3 443,82 cm^{-1} corresponding to the OH stretching. The peak at 2 926,55 cm^{-1} indicates the C–H stretching, while the bands at 1 648 and 1 458 cm^{-1} are related to the O–H bendings of water and CH_2, respectively. The bands from 764,98 to 1 174,18 cm^{-1} indicate the C–O bond stretching. The extracted sample shows same peaks in its FTIR spectra as the potato commercial starch (Xu, Kim, Hanna, and Nag, 2005; Bourtoom and Chinnan, 2008).

Pectin FTIR spectra shows a wide peak at 3 411,23 cm^{-1} due to O-H vibrations, demonstrating that pectin is a polysaccharide. The band in 2 926,63 cm^{-1} corresponds to the stretch of the C-H of CH_2 groups. The peaks between 2 000 and 2 300 cm^{-1} show uncharacteristic values, possibly indicating the presence of impurities. The bands that appear in 1 623,79 and 1 750,44 cm^{-1} indicate free carboxyl groups and carbonyls (C = O) of the ester and the acid. The peaks from 1 369,68 to 1 443,96 cm^{-1} correspond to the stretch vibration band of C–O–H. The peaks at 1 235,52 cm^{-1} show the asymmetric tension vibration band of the C–O–C and methoxy groups (–O–CH_3). Finally, the presence of the C–O group is in the band between 1 000 and 1 100 cm^{-1}. In addition, the spectrum of pectin appears to be similar to that of commercial pectin, showing the same peaks at a similar wavelength (Chasquibol-Silva, Arroyo-Benites, and Morales-Gomero, 2008; Barreto, Púa, De Alba, and Pión, 2017).

In tamarind powder FTIR spectra, a band in 3 600 cm^{-1} reveals the existence of hydroxyl groups. The broad band in 3 000 to 3 200 cm^{-1} corresponds to amino and carboxylic acid groups. The bands in 1 653 and 1 541 cm^{-1} appear due to primary amine and nitro compound. Additionally, the peak in 1 064 cm^{-1} indicates primary alcohol (C–O) stretching (Patel and Vashi, 2010; Kaur, Jain and Tiwary, 2009; Pal, Sen, Mishra, Dey, and Jha, 2008).

SEM micrographics of (a) starch, (b) pectin and (c) tamarind powder are presented in Figure 2.

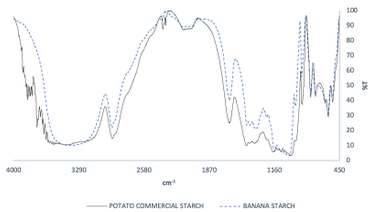

(a)

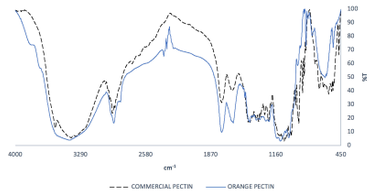

(b)

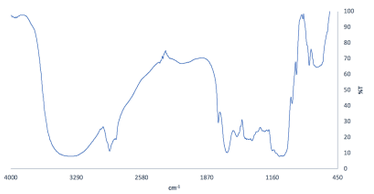

(c)

Figure 1. IR spectra: (a) starch/potato commercial starch, (b) pectin / commercial pectin and (c) tamarind powder.
Source: Authors

Starch granules appeared with oval shape and different size, similar to that of potato starch (Hernández-Medina *et al.*, 2008; Sujka and Jamroz, 2013). Pectine shows a porous, rough and irregular surface. Similar results have been presented by Mishra, Datt, and Banthia (2008) and Liu, Finkenstadt, Liu, Jin, Fishman, and Hicks (2007). Tamarind powder presents a porous surface, with irregular shape. This morphology have been reported in other studies (Patel and Vashi, 2010).

Evaluation of coagulant/flocculant activity

Narural water quality: Results of physico-chemical and microbiological analysis of natural water are summarized in Table 3. In general, raw water sampled quality for potabilization was good (color between 20-150 u Pt-Co, BOD_5 between 1,5-2,5 mg/L) to excellent (pH between 6-8,5, turbidity between 0-10 NTU, coliforms between 50-100 NMP/100 mL), according to Silva (2015).

Due to coliform and color values, a conventional treatment was required according to the *Texto Unificado de Legislación Secundaria de Medio Ambiente* - TULSMA (Libro VI Anexo 1) (2015), to comply with the maximum permissible limits (MPL) for turbidity (5 NTU), color (15 u Pt-Co) and coliforms (< 1,1 NMP/100 mL) of the *Norma Técnica Ecuatoriana* del

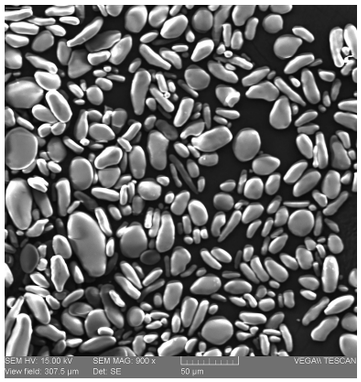

(a)

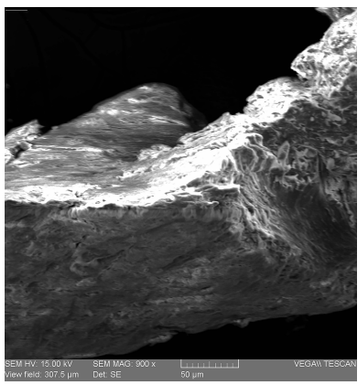

(b)

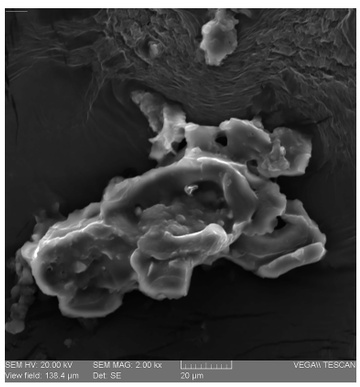

(c)

Figure 2. SEM micrographics of polymers: (a) starch, (b) pectin and (c) tamarind powder.
Source: Authors

Instituto Ecuatoriano de Normalización - NTE INEN 1 108 (INEN, 2014).

Natural water analysis identified the presence of non-sedimentary solids (settleable solids < 0,1 mg/L), which are difficult to settle on their own. Alkalinity was low and it was a soft water (< 75 mg/L $CaCO_3$) (Mihelcic and Zimmerman, 2012). Therefore, it could be concluded that coagulation/flocculation treatment was difficult in raw water

Table 3. Results of physicochemical and microbiological analysis of natural water

Parameter	Unit	Results
Temperature	°C	10,60 ± 0,30
Turbidity	NTU	5,30 ± 0,18
Apparent color	u Pt-Co	51 ± 2
Real color	u Pt-Co	40 ± 5
Conductivity	µS/cm	136 ± 5
Total solids	mg/L	150,5 ± 3,0
Settleable solids	mL/L	< 0,1
Suspended solids	mg/L	21,0 ± 12,0
Dissolved solids	mg/L	129,40 ± 12,90
pH	-	7,88 ± 0,08
Total alkalinity ($CaCO_3$)	mg/L	52,50 ± 2,50
COD	mg/L	< 10
BOD_5	mg/L	< 2
Total hardness ($CaCO_3$)	mg/L	72,50 ± 6,50
Aluminum (Al^{+3})	mg/L	0,10 ± 0,01
Coliforms	NMP/100mL	45 ± 13

Source: Authors

sampled, mainly due to its low turbidity (higher dose of coagulant and sweeping action), in addition to low alkalinity.

Primary coagulant activity: The result was that coagulant substances have deficient or no coagulant activity, for low (10 NTU) and high (280 NTU) turbidity assay of starch, pectin, tamarind extract and even aluminum sulfate. For this reason, it is concluded that the assay did not yield reliable results, possibly due to errors when adapting the methodology.

Efficiency of coagulant activity: Pectin was not used as coagulant because it is hydrophilic and it has the same negative charge of particles that are intended to destabilize (Sánchez and Untiveros, 2004; Vaclavik and Christian, 2014). That is why it is difficult to use it as a coagulant, unless sweeping action is desired, which in this case is not possible due to the low turbidity of the raw water (5,32 NTU). Consequently, only the flocculant activity of pectin was analyzed.

Natural polymers had a poor turbidity removal (less than 1 %), possibly due to the their coagulation mechanism, which is mainly sweeping action as a result of molecular weight and polymer chains, and not necessarily the destabilization of charges. However, as the turbidity of the water is low, there are not enough particles to create the sweeping action (Mihelcic and Zimmerman, 2012).

In comparison, aluminum sulfate obtained a high removal of 86,0 % turbidity and 88,7 % color, with an optimum dose of 65 mg/L. In addition, a final pH of 7,05 (15 °C) with a short floc formation time of 3 minutes indicate a rapid reaction rate. Floc was dispersed, well-formed and had slow sedimentation (Willcom index of 4) with a size between 0,5-0,75 mm (size WRA of B). The optimum pH for the dose of 65 mg/L of aluminum sulfate was between 7 and 8 units.

Although some natural polymers did not work appropriately as coagulants, they can be used as flocculation aids, as they showed turbidity and color removal up to 80 %. For example, *M. oleifera* seed extract is a polyelectrolyte, and it may be able to function as a flocculation aid, with an optimal dose of 10 mg/L in combination with 20 mg/L of alum (Bichi, 2013). *Tannis* has also been used as flocculation aid, achieving 96 % in turbidity removal when used with alum (Ozacar and Şengíl, 2002).

Therefore, it was evidenced that natural polymers starch, pectin and tamarind seed extract did not have coagulant activity to real conditions of raw water, because of its low turbidity. However, their flocculating activity was evaluated as flocculation aids, using aluminum sulfate as coagulant.

Efficiency of flocculant activity: Optimal combinations of aluminum sulfate + polymers obtained equal or greater removal percentages of turbidity and color than those obtained using only this coagulant, with an evident reduction in consumption of aluminum sulfate. Likewise, the natural polymers presented the same or better characteristics of flocculation aids than commercial synthetic polymer PAM.

Optimal combinations of **aluminum sulfate [mg/L] + polymer [mg/L]** were: **50 + 0,2** for starch, **60 + 0,06** for pectin, **60 + 0,6** for tamarind in water, **60 + 0,5** for tamarind in sodium chloride, **60 + 0,2** for tamarind in ammonium acetate and **50 + 0,2** for PAM, as can be seen in Figure 3.

Compared with the 65 mg/L of aluminum sulfate used as coagulant without the addition of polymers, the use of flocculation aids allowed a saving of aluminum sulfate of 15 mg/L when using starch and PAM and of 5 mg/L when using pectin and tamarind extract in water, sodium chloride and ammonium acetate.

In general, optimal combinations of aluminum sulfate + polymers obtained a turbidity and color removal of around 88 and 92 %, respectively. Final pH was maintained between 7,0-7,1 and the formation time of the first floc was short, between 2 and 3 minutes, indicating a rapid reaction rate, as shown in Table 4.

Table 4. Main characteristics of natural water treatment when using aluminum sulfate and optimal combinations of aluminum sulfate + polymers

Combination of coagulant + flocculant	Final pH	Removal [%]		Floc characteristics		
		Turbity	Color	Time [min]	W. I.	S. WRA
$Al_2(SO_4)_3$	7,05	86,0 ±1,3	88,7 ±1,7	3	4	B
$Al_2(SO_4)_3$ + PAM	7,17	86,9 ±1,7	88,9 ±1,0	2	4	D
$Al_2(SO_4)_3$ + Starch	7,23	87,4 ±1,8	98,0 ±1,2	2	4	C
$Al_2(SO_4)_3$ + Pectin	6,99	89,2 ±1,3	90,2 ±1,9	3	4	D
$Al_2(SO_4)_3$ + T_{WATER}	7,09	87,6 ±2,4	98,0 ±1,0	2	4	B
$Al_2(SO_4)_3$ + $T_{SODIUM\ CHLORIDE}$	7,12	87,5 ±1,9	92,2 ±2,1	3	4	B
$Al_2(SO_4)_3$ + $T_{AMMONIUM\ ACETATE}$	7,08	86,8 ±1,3	90,2 ±1,7	3	4	B

W.I.: Willcomb Index; S. WRA: Comparator size of WRA.
Source: Authors

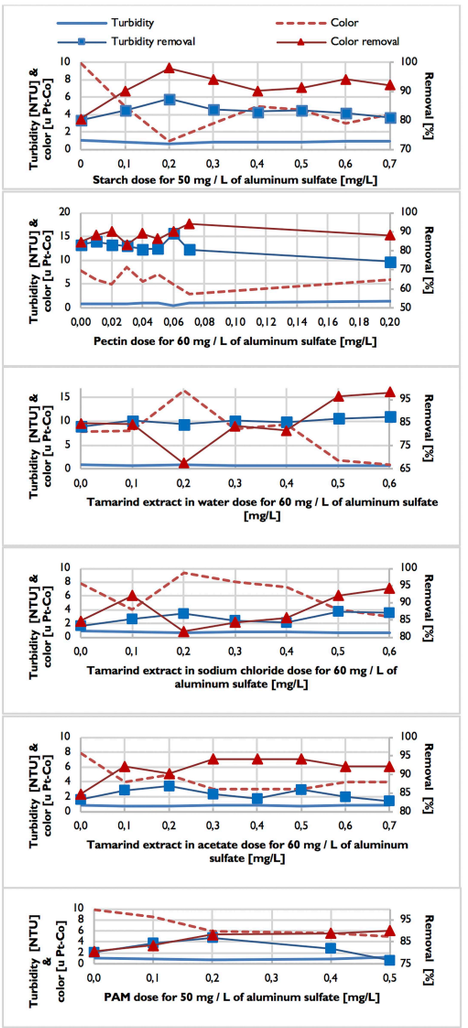

Figure 3. Optimal combinations of aluminum sulfate + polymers.
Source: Authors

There were differences in the size of the floc. The largest size obtained was 1,0-1,5 mm (T. WRA of D) when using pectin and PAM; followed by 0,75-1,0 mm (T. WRA of C) of starch; and, finally, a size of 0,5-0,75 mm (T. WRA of B) for the tamarind extract in water, sodium chloride and ammonium acetate. Among solutions in water, sodium chloride and ammonium acetate for the tamarind extract, there were no significant differences.

Feasibility of natural polymers used as flocculation aids. Combinations of aluminum sulfate + natural polymers obtained equal or higher removal percentages of turbidity and color than only using aluminum sulfate or aluminum sulfate + PAM, which showed the technical feasibility of their use. Social/environmental feasibility was observed, since the use of these polymers reduces consumption of aluminum sulfate, the possibility of generating residual aluminum and risks of adverse effects on humans health (Suay and

Ballester, 2002). In addition, natural polymers compared to commercial synthetic polymer PAM have low toxicity, are safe for consumption and responsible with environment, reduce chemical dependency and reusing organic solid waste, no surface is needed to plantation. However, biodegradability in water must be studied in detail, because it can be a rich substrate for microorganisms that have not been completely removed (Choy et al., 2014). Economic feasibility was not observed, due to high extraction costs linked to low yield (1,47, 3,44 and 43 %). Assuming a flow rate of 600 L/s for the same quality of raw water processed in this study during one day and considering exclusively the cost of the laboratory reagents, the most profitable options were the use of aluminum sulfate only or the combination of aluminum sulfate + PAM, with a saving of $ 115,11/day.

Clarified water quality: In general, clarified water presented a reduction in parameters of turbidity, color, conductivity, solids, pH, alkalinity, hardness and coliforms; while the settleable solids, COD and BOD_5 remained practically stable.

Figure 4 shows that parameters of turbidity, color and coliforms had a removal greater than 85 % and the rest of parameters obtained a reduction of less than 30 %. In the case of polymers, a lower reduction in alkalinity was obtained than when using only aluminum sulfate. Final pH also did not have a marked reduction (10 %) and remained around 7,1. In this way, clarified water complied with the physical characteristics of drinking water regulations, with values lower than 5 NTU and 15 u Pt-Co, but not with parameter of coliforms, which can be removed through complementary filtration and disinfection operations.

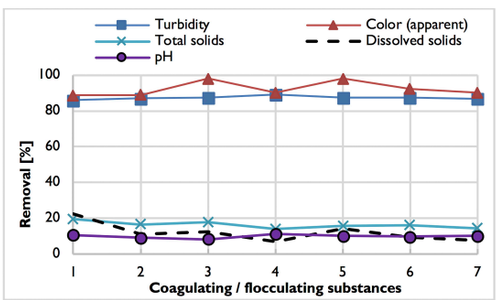

Coagulating/flocculating substances. 1: $Al_2(SO_4)_3$. **2**: $Al_2(SO_4)_3$+PAM. **3**: $Al_2(SO_4)_3$+Starch. **4**: $Al_2(SO_4)_3$+ Pectin. **5**: $Al_2(SO_4)_3$+ T. Water. **6**: $Al_2(SO_4)_3$+ T. NaCl. **7**: $Al_2(SO_4)_3$+ T. CH_3COONH_4

Figure 4. Removal percentage of physico-chemical and microbiological parameters of clarified water.
Source: Authors

Analysis of residual aluminum showed an increase with respect to the aluminum of raw water (0,1 mg/L). This increase was kept to margin of 0,2 mg/L normed by the Environmental Protection Agency (EPA) and the World Health Organization (WHO), except when only sulfate aluminum was used (0,21 mg/L) (Water Quality Association, 2013).

Toxicological evaluation of residual sludge

Quantification and characterization of sludges: Volume of residual sludge generated in each jar test was between 3 and 4 mL per liter of treated water, for both aluminum sulfate and combinations of aluminum sulfate + polymer.

Residual sludge moisture remained above 98 %, which corroborates its poor capacity of dehydration (90 % moisture), as mentioned by Joshi and Shrivastava (2011). Although the density of the sludge is close to that of water, it is enough to allow it to settle; while the pH remained around 7.

From total solids, around 26 % were volatile solids, thus the highest percentage is constituted by inorganic solids generated mainly by sediment flocs of aluminum sulfate. Likewise, values of COD (> 1 670 mg/L) and aluminum (> 275 mg/L) exceed values regulated by TULSMA (Libro VI Anexo 1) (2015) of 500 mg/L COD and 5 mg/L of aluminum and did not comply with the maximum permissible limits for the discharge to the sewer system.

Acute toxicity test with Allium cepa L: Acute toxicity test with *Allium cepa L* allowed to identify a toxic effect of residual sludge in cell division of radicular meristems by slowing mitotic activity and affecting normal elongation of onion root (Romero and Cantú, 2008). Average length of roots exposed to residual sludge was kept lower than 1,3 cm, which was lower than the length of 2,2 cm of roots exposed to negative control. This allows to state that the greater the dilution, the greater the length of the roots of each onion is. Inhibition percentage of roots length was between 40 and 86 %.

Calculation of IC_{50} was performed using Probit method and obtaining equations of the form Probit = a log (Concentration) + b. The values of R^2 were between 0,92 and 0,98 indicating a good linear correlation, as shown in Figure 5. From the obtained equations, Probit equal to 5 (50 % elongation inhibition) was calculated in order to obtain IC_{50}.

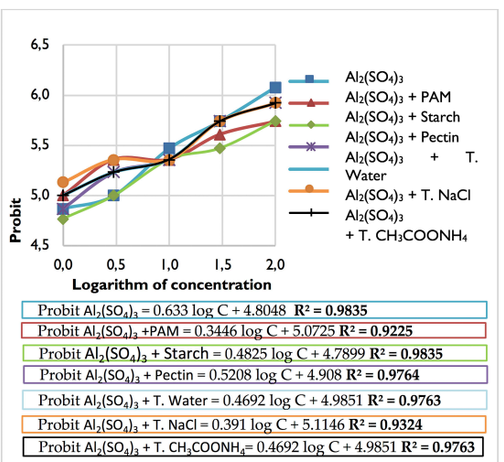

Figure 5. Probit Graphics.
Source: Authors

IC_{50} values were 2,03 % for aluminum sulfate, 2,73 % for aluminum sulfate + starch, 1,5 % for aluminum sulfate + pectin, 1,08 % for aluminum sulfate + tamarind in water, 0,51 % for aluminum sulfate + tamarind in sodium chloride, 1,08 % for aluminum sulfate + tamarind in ammonium acetate and 0,61 % for aluminum sulfate + PAM.

This study did not contemplate a microscopic analysis of the toxic effect shown in mitotic activity by means of nucleolar alteration, activity of antioxidant enzymes and content of soluble proteins. However, there are studies that prove that aluminum is responsible for negatively influencing these variables, as indicated by Qin, Jiao, Zhang, Jiang and Liu (2010).

In summary, residual sludge had a genotoxic effect on onions roots, reaching the inhibition in growth of 50 % onions roots at low concentrations between 0,5 to 2 %.

Acute toxicity test with Lactuca sativa L: Acute toxicity test with *Lactuca sativa L* did not allow to identify a toxic effect in the inhibition of germination or elongation (radicle + hypocotyl), due to the high variability of results and superior elongation of seedlings exposed to residual sludges with respect to control elongation.

Variability of results was possibly due to an improper homogenization of the sample, which affected differently germination and growth of seeds of lettuce. Otherwise, higher elongation could be due to the fact that not only aluminum is found in the sludge, but also essential micronutrients such as magnesium, zinc, cadmium, calcium, among others. These micronutrients promote growth, as mentioned by Pavón, Pacheco and Cárdenas (2005), and mask the toxicity, although seeds adsorb aluminum and accumulate it as indicated by Panizza-de-León, Aldama-Ojeda, Chacalo-Hilu, Va-ca-Mier, Grabinsky-Steider, Márquez-Herrera, and Durán-de-Bazúa, (2008).

Inhibition percentage of elongation was less than 25 %, except for combinations of aluminum sulfate + starch (28,95 %) and tamarind extract in sodium chloride (34,21 %). Inhibition percentage of elongation decreased when concentration of residual sludge decreased and it became zero for aluminum sulfate and combinations of aluminum sulfate + tamarind extract in water and ammonium acetate. Additionally, inhibition percentage in germination of seeds was on average low or none, as most of seeds germinated without problems; except for aluminum sulfate (1,67 to 11,67 % inhibition) and combinations of aluminum sulfate + tamarind extract in sodium chloride and ammonium acetate (0,67 to 5,00 % inhibition).

As no inhibition percentage in germination and elongation exceeded 12 and 35 %, half maximal lethal concentration (LC_{50}) or IC_{50} could not be determined. It was appreciated that the concentration at which no effect is observed (No Observed Effect Concentration, NOEC) and the lowest concentration at which the effect is observed (Lowest Observed Effect Concentration, LOEC) is around the concentrations of 1 and 3 % of residual sludge.

When natural coagulants are used alone in the coagulation process, sludges can be applied in agricultural soils. Feria-Díaz, Polo-Corrales, and Hernandez-Ramos (2016), studied the physico-chemical, nutritional and dangerous characteristics from a sludge obtained from coagulation of raw water with *M. oleifera* and found that the sludge appear as a soil improver, but not as a fertilizer, because of the deficiency of its macronutrients and fecal coliforms concentrations. Since the produced sludge cannot be disposed directly in the environment, some alternatives of treatment should be considered, e.g. the sludge could be used as partial substitute for clay in brick manufacturing. In the study carried out by Ramadan, Fouad, and Hassanain (2008), it was determined that 50 percent was the optimum sludge addition to produce brick from sludge-clay mixture. The sludge used in the study was from the clarification tanks where aluminum sulfate was used as coagulant. In addition, alum could be recovered from the sludge according to Boaventura, Duarte, and Almeida, (2000), who determined a recovery near 88 % through an alkaline extraction process applied to a primary coagulation sludge. Actually, recovered alum can be used again as coagulant for the domestic or industrial wastewaters treatment, reaching about 70 % of COD removal in sewage and surpassing even the commercial coagulant (Ishikawa, Ueda, Okumura, Iida, and Baba, 2007). In the study conducted by Chu (1999), alum sludge was recycled using a chemical precipitation process to remove lead metal in wastewater and reached up to 94 % of efficiency.

Sludge allowed germination of the lettuce seeds, either because the mud also contains essential micronutrients or because the sludge is organic. This opens the possibility of using it as an organic fertilizer with controlled release of the main macronutrients: nitrogen, potassium and phosphorus, taking care of the aluminum sulfate concentration (Qin et al., 2010; Ferrari, Genena, and Lenhard, 2016). Likewise, it should be considered that the use of natural polymers could increase the organic load of the mud.

Therefore, natural polymers can be used for natural water treatment, since they are safe and eco-friendly. They generate a smaller quantity of sludge with higher nutritional content. In addition, the raw material is available locally. Since natural polymers do not consume alkalinity as alum, the use of chemicals for pH adjustments is not necessary. Natural coagulants are also non-corrosive, that is why costs of using natural coagulants are always reduced, compared to those of the traditional ones (Choy et al., 2014). The use of natural polymers also allows the elimination of possible negative impacts of synthetic polymers on human health, avoiding the appearance of residual monomers from manufacturing process and byproducts (Saranya et al., 2014; Ramesh and Gandhimathi, 2013).

Conclusion

Natural polymers extracted from waste materials: starch from plantain peels, pectin from orange peels and tamarind seed extract did not have coagulant activity to real conditions of raw water tested, due to its low turbidity (5,32 NTU). However, they presented equal or better characteristics as flocculation aids than commercial polymer PAM, with an average removal of turbidity, color and coliforms of 87 %, 92 % and 96 %, respectively. In economic terms, natural polymers use was not viable. Additionally, residual sludge did not comply with the maximum permissible limits to discharge to sewage system and had a toxic effect on mitotic

activity of onion roots, reaching an IC_{50} at low concentrations between 0,5 and 2 %.

Acknowledgements

Authors are grateful for the funding granted by Escuela Politécnica Nacional for the realization of the research project "Semilla PIS 15-20 -Estudio de características coagulantes/floculantes de polímeros orgánicos extraídos de residuos para potabilización".

References

Aina, V., Barau, M., Mamman, O., Zakari, A., and Haruna, H. (2012). Extraction and Characterization of Pectin from Peels of Lemon (Citrus limon), Grape Fruit (Citrus paradisi) and Sweet Orange (Citrus sinensis). *British Journal of Pharmacology and Toxicology, 3*(6), 259-262.

Antov, M., Šćiban, M., Prodanović, J., Kukić, D., Vasić, V., Đorđević, T., and Milošević, M. (2018). Common oak (Quercus robur) acorn as a source of natural coagulants for water turbidity removal. *Industrial Crops and Products*, *117*, 340-346. DOI: 10.1016/j.indcrop.2018.03.022

American Public Health Association (APHA) (2005). *Standard Methods for Examination of Water and Wastewater* (21st ed.). Washington D.C.: APHA.

Association of Official Analytical Chemists, and Horwitz, W. (Eds.). (2000). *Food composition, additives, natural contaminants* (17th ed). Arlington, Va: AOAC International.

American Society for Testing Materials, ASTM. (2013). *D2035-13 Standard Practice for Coagulation-Flocculation Jar Test of Water*. West Conshohocken, PA: ASTM International. DOI: 10.1520/D2035-13

Arboleda, J. (2000). Teoría y práctica de la purificación del agua (3ra. ed.) Bogotá: McGraw Hill.

Agarwal, G., Bhuptawat, H., and Chaudhari, S. (2006). Biosorption of aqueous chromium(VI) by Tamarindus indica seeds. *Bioresource Technology, 97*(7), 949-956. DOI: 10.1016/j.biortech.2005.04.030

Bagula, M., Sonawane, S., and Arya, S. (2015). Tamarind seeds: chemistry, technology, applications and health benefits: *A review, Indian food Industry Magazine, 34*(3), 28-35.

Barreto, G., Púa, A., De Alba, D., and Pión, M. (2017). Extracción y caracterización de pectina de mango de azúcar (Mangifera indica L.), *Temas agrarios, 22*(1), 79-86. DOI: 10.21897/rta.v22i1.918

Bongiovani, M. C., Konradt-Moraes, L. C., Bergamasco, R., Lourenço, B. S. S., and Tavares, C. R. G. (2010). Os benefícios da utilização de coagulantes naturais para a obtenção de água potável. *Acta Scientiarum. Technology, 32*(2), 167-170. DOI: 10.4025/ actascitechnol.v32i2.8238

Bourtoom, T., and Chinnan, M. (2008). Preparation and properties of rice starch-chitosan blend biodegradable film. *LWT - Food Science and Technology, 41*(9), 1633-1641. DOI: 10.1016/j.lwt.2007.10.014

Bichi, M. (2013). A review of the applications of Moringa oleifera seeds extract in water treatment. *Civil and Environmental Research, 3*(8), 1-10.

Boaventura, R., Duarte, A., and Almeida, M. (2000). Aluminum recovery from water treatment sludges. Paper presented at the *IV International Conference on Water Supply and Water Quality*, Cracóvia.

Chasquibol-Silva, N., Arroyo-Benites, E., and Morales-Gomero, J. C. (2008). Extracción y caracterización de pectinas obtenidas a partir de frutos de la biodiversidad peruana. *Ingeniería Industrial*, (026), 175-199. DOI: 10.26439/ing.ind2008.n026.640

Choy, S. Y., Prasad, K. M. N., Wu, T. Y., Raghunandan, M. E., and Ramanan, R. N. (2014). Utilization of plant-based natural coagulants as future alternatives towards sustainable water clarification. *Journal of Environmental Sciences, 26*(11), 2178-2189. DOI: 10.1016/ j.jes.2014.09.024

Choy, S. Y., Prasad, K. M. N., Wu, T. Y., and Ramanan, R. N. (2015). A review on common vegetables and legumes as promising plant-based natural coagulants in water clarification. *International journal of environmental science and technology, 12*(1), 367-390. DOI: 10.1007/s13762-013-0446-2

Chu, W. (1999). Lead metal removal by recycled alum sludge. *Water Research, 33*(13), 3019-3025. DOI: 10.1016/ S0043-1354(99)00010-X

Cogollo, J. (2011). Clarificación de aguas usando coagulantes polimerizados: caso del hidroxicloruro de aluminio. *Dyna, 78*(165), 18-27.

Demiate, I. M., Dupuy, N., Huvenne, J. P., Cereda, M. P., and Wosiacki, G. (2000). Relationship between baking behavior of modified cassava starches and starch chemical structure determined by FTIR spectroscopy. *Carbohydrate Polymers, 42*(2), 149-158. DOI: 10.1016/s0144-8617(99)00152-6

Devia, J. (2003). Proceso para producir Pectinas Cítricas. Universidad EAFIT, 129, 21-29.

Farhaoui, M., and Derraz, M. (2016). Review on optimization of drinking water treatment process. *Journal of Water Resource and Protection, 8*(08), 777. DOI: 10.4236/jwarp.2016.88063

Feria-Díaz, J., Polo-Corrales, L., and Hernandez-Ramos, E. (2016). Evaluation of coagulation sludge from raw water treated with Moringa oleifera for agricultural use. *Ingeniería e Investigación, 36*(2), 14-20. DOI: 10.15446/ing.investig.v36n2.56986

Ferrari, C., Genena, A., and Lenhard, D. (2016). Use of natural coagulants in the treatment of food industry effluent replacing ferric chloride: a review. *Científica, 44*(3), 310-317. DOI: 10.15361/1984-5529.2016v44n3p310-317

García, B. (2007, diciembre 13). Metodología de extracción in situ de coagulantes naturales para la clarificación de agua superficial. Aplicación en países en vías de desarrollo (Master's Thesis, Universidad Politécnica de Valencia) Retrieved from: https://riunet.upv.es/bitstream/

handle/10251/12458/Tesi%20de%20Master_BEATRIZ%20GARCIA%20FAYOS.pdf?sequence=1

Ghebremichael, K., Gunaratna, K., Henriksson, H., Brumer, H., and Dalhammar, G. (2005). A simple purification and activity assay of the coagulant protein from Moringa oleifera seed. *Water Research, 39*(11), 2338-2344. DOI: 10.1016/j.watres.2005.04.012

González, G., Chávez, M., Mejías, D., Mas y Rubí, M., Fernández, N., and León de Pinto, G. (2006). Use of exudated gum produced by Samanea saman in the potabilization of the water. *Revista Técnica de la Facultad de Ingeniería Universidad del Zulia, 29*(1), 14-22.

Hayder, G., and Rahim, A. A. (2015). Effect of Mixing Natural Coagulant with Alum on Water Treatment. Paper presented at the 3rd National Graduate Conference, Kuala Lumpur, Universiti Teknologi Malaysia. Retrieved from: http://dspace.uniten.edu.my/jspui/handle/123456789/10229

Hernández, B., Mendoza, I., Salamanca, M., Fuentes, L., and Caldera, Y. (2013). Semillas de tamarindo (tamarindus indica) como coagulante en aguas con alta turbiedad. *REDIELUZ, 3* (1 y 2), 91-96.

Hernández-Medina, M., Torruco-Uco, J. G., Chel-Guerrero, L., and Betancur-Ancona, D. (2008). Caracterización fisicoquímica de almidones de tubérculos cultivados en Yucatán, México. *Ciencia E Tecnologia de Alimentos, 28*(3), 718-726. DOI: 10.1590/S0101-20612008000300031

Ilori, M., Adebusoye, S., Iawal, A., and Awotiwon, O. (2007). Production of Biogas from Banana and Plantain Peels. *American-Eurasian Network for Scientific Information, 1*(1), 33-38.

Instituto Nacional de Estadísticas y Censos (INEC) (2016). Información Ambiental en Hogares 2016. Quito: Grupo Técnico DEAGA. Retrieved from: http://www.ecuadorencifras.gob.ec/documentos/web-inec/Encuestas_Ambientales/Hogares/Hogares_2016/ Documento%20tecnico.pdf

Instituto Ecuatoriano de Normalización (INEN) (2014). NTE INEN 1108: Agua Potable. Requisitos. Quito: INEN. Retrieved from: http://normaspdf.inen.gob.ec/pdf/nte/1108-5.pdf

Ishikawa, S., Ueda, N., Okumura, Y., Iida, Y., and Baba, K. (2007). Recovery of coagulant from water supply plant sludge and its effect on clarification. *Journal of Material Cycles and Waste Management, 9*(2), 167-172. DOI: 10.1007/s10163-007-0173-1

Joshi, S., and Shrivastava, K. (2011). Recovery of Alum Coagulant from Water Treatment Plant Sludge: A Greener Approach for Water Purification. *International Journal of Advanced Computer Research, 2*(1), 101-103.

Kaur, G., Jain, S., and Tiwary, A. (2009). Chitosan-carboxymethyl tamarind kernel powder interpolymer complexation: investigations for colon drug delivery. *Scientia pharmaceutica, 78*(1), 57-78. DOI: 10.3797/scipharm.0908-10

Li, W., Zhou, W., Zhang, Y., Wang, J., and Zhu, X. (2008). Flocculation behavior and mechanism of an exopolysaccharide from the deep-sea psychrophilic bacterium Pseudoalteromonas sp. SM9913. *Bioresource technology, 99*(15), 6893-6899. DOI: 10.1016/ j.biortech.2008.01.050

Liu, L, Finkenstadt, V., Liu, C., Jin, T., Fishman, M, and Hicks, K. (2007). Preparation of poly(lactic acid) and pectin composite films intended for applications in antimicrobial packaging. *Journal of Applied Polymer Science, 106*(2), 801-810. DOI: 10.1002/app.26590

Megersa, M., Beyene, A., Ambelu, A., and Triest, L. (2018). Comparison of purified and crude extracted coagulants from plant species for turbidity removal. *International Journal of Environmental Science and Technology*, 1-10. DOI: 10.1007/s13762-018-1844-2

Mihelcic, J., and Zimmerman, J. (2012). *Ingeniería Ambiental: fundamentos, sustentabilidad, diseño* (1ra ed.). México: Alfaomega.

Mishra, R. K., Datt, M., and Banthia, A. K. (2008). Synthesis and characterization of pectin/PVP hydrogel membranes for drug delivery system. *Aaps Pharmscitech, 9*(2), 395-403. DOI: 10.1208/s12249-008-9048-6

Nasrin, T., Noomhorm, A., and Anal, A. (2015). Physico-Chemical Characterization of Culled Plantain Pulp Starch, Peel Starch, and Flour. *International Journal of Food Properties, 18*(1), 165-177. DOI: 10.1080/10942912.2013.828747

Ndabigengesere, A., and Narasiah, K. (1998). Quality of water treated by coagulation using Moringa oleifera seeds. *Water research, 32*(3), 781-791. DOI: 10.1016/s0043-1354(97)00295-9

Ozacar, M., and Şengíl, I. (2002). The use of tannins from turkish acorns (valonia) in water treatment as a coagulant and coagulant aid. *Turkish Journal of Engineering and Environmental Sciences, 26*(3), 255-264.

Pal, S., Sen, G., Mishra, S., Dey, R. and Jha, U. (2008). Carboxymethyl tamarind: Synthesis, characterization and its application as novel drug-delivery agent. *Journal of applied polymer science, 110*(1), 392-400. DOI: 10.1002/app.28455

Panizza-de-León, A., Aldama-Ojeda, A., Chacalo-Hilu, A., Vaca-Mier, M., Grabinsky-Steider, J., Márquez-Herrera, C., and Durán-de-Bazúa, C. (2008). Evaluación del compost elaborado a partir de lodos con alto contenido de sulfato de aluminio. *Revista Latinoamericana de Recursos Naturales, 4*(3), 342-348.

Paredes, J., Hernández, R., and Cañizares, A. (2015). Efecto del grado de madurez sobre las propiedades fisicoquímicas de pectinas extraídas de cascos de guayaba (Psidium guajava L.). *Idesia* (*Arica*), *33*(3), 35-41. DOI: 10.4067/S0718-34292015000300006

Patel, H., and Vashi, R. (2010). Adsorption of crystal violet dye onto tamarind seed powder. *Journal of Chemistry, 7*(3), 975-984. DOI: 10.1155/2010/143439

Pavón, T., Pacheco, V., and Cárdenas, L. (2005). Tratamiento de lodos de una planta potabilizadora para la recuperación de aluminio y hierro como coagulantes. *Ingeniería sanitaria y ambiental*, *78*, 60-64.

Peruço, J., Lenz, G., Fiori, R., and Bergamasco, R. (2013). Coagulants and Natural Polymers: Perspectives for the Treatment of Water. *Plastic and Polymer Technology, 2*(3), 55-62.

Pritchard, M., Craven, T., Mkandawire, T., Edmondson, A., and O'Neill, J. (2010). A comparison between Moringa oleifera and chemical coagulants in the purification of drinking water - An alternative sustainable solution for developing countries. *Physics and Chemistry of the Earth, Parts A/B/C, 35*(13-14), 798-805. DOI: 10.1016/j.pce.2010.07.014

Qin, R., Jiao, Y., Zhang, S., Jiang, W., and Liu, D. (2010). Effects of aluminum on nucleoli in root tip cells and selected physiological and biochemical characters in Allium cepa var. agrogarum L. *BMC Plant Biology*, *10*, 225. Retrieved from: http://www.biomedcentral.com/1471-2229/10/225

Ramadan, M., Fouad, H., and Hassanain, A. (2008). Reuse of water treatment plant sludge in brick manufacturing. *Journal of Applied Sciences Research, 4*(10), 1223-1229.

Romero, P., and Cantú, A. (2008). *Ensayos toxicológicos para la evaluación de sustancias químicas en agua y suelo: la experiencia en México*. México D.F.: Instituto Nacional de Ecología.

Sánchez, S., and Untiveros, G. (2004). Determinación de la actividad floculante de la pectina en soluciones de Hierro III y Cromo III. *Revista de la Sociedad Química del Perú, 70*(4), 201-208.

Saranya, P., Ramesh, S., and Gandhimathi, R. (2014). Effectiveness of natural coagulants from non-plant-based sources for water and wastewater treatment–A review. *Desalination and Water Treatment, 52*(31-33), 6030-6039. DOI: 10.1080/19443994.2013.812993

Saritha, V., Srinivas, N., and Vuppala, N. (2017). Analysis and optimization of coagulation and flocculation process. *Applied Water Science, 7*(1), 451-460. DOI: 10.1007/s13201-014-0262-y

Sharma, P., Joshi, R., Sharma, S., and Hsiao, B. (2017). A simple approach to prepare carboxycellulose nanofibers from untreated biomass. *Biomacromolecules, 18*(8), 2333-2342. DOI: 10.1021/acs.biomac.7b00544

Sharma, P., Chattopadhyay, A., Sharma, S., Geng, L., Amiralian, N., Martin, D., and Hsiao, B. (2018). Nanocellulose from Spinifex as an Effective Adsorbent to Remove Cadmium (II) from Water. *ACS Sustainable Chemistry & Engineering, 6*(3), 3279-3290. DOI: 10.1021/acssuschemeng.7b03473

Sharma, P., Chattopadhyay, A., Zhan, C., Sharma, S., Geng, L., and Hsiao, B. (2018). Lead removal from water using carboxycellulose nanofibers prepared by nitro-oxidation method. *Cellulose, 25*(3), 1961-1973. DOI: 10.1007/s10570-018-1659-9

Silva, M. (2015). *Potabilización. Procesos y Diseños de Plantas* (1ra.). Quito, Ecuador: Edicumbre.

Suay, L., and Ballester, F. (2002). Revisión de los estudios sobre exposición al aluminio y enfermedad de Alzheimer. *Revista Española de Salud Pública, 76*(6), 645-658. DOI: 10.1590/S1135-57272002000600002

Sujka, M., and Jamroz, J. (2013). Ultrasound-treated starch: SEM and TEM imaging, and functional behaviour. *Food Hydrocolloids, 31*(2), 413-419. DOI: 10.1016/j.foodhyd.2012.11.027

TULSMA. (2015) NORMA DE CALIDAD AMBIENTAL Y DE DESCARGA DE EFLUENTES?: RECURSO AGUA (Libro VI Anexo 1). Quito: Presidencia de la República. Retrieved from: http://extwprlegs1.fao.org/docs/pdf/ecu112180.pdf

Vaclavik, V., and Christian, E. (2014). Essentials of Food Science. New York, NY: Springer New York. Retrieved from: http://link.springer.com/10.1007/978-1-4614-9138-5

Vane, L., and Zang, G. (1997). Effect of aqueous phase properties on clay particle zeta potential and electro-osmotic permeability: Implications for electro-kinetic soil remediation processes. *Journal of Hazardous Materials, 55*(1-3), 1-22. DOI: 10.1016/S0304-3894(97)00010-1

Vijayaraghavan, G., Sivakumar, T., and Kumar, A. (2011). Application of plant based coagulants for waste water treatment. *International Journal of Advanced Engineering Research and Studies, 1*(1), 88-92.

Water Quality Association. (2013). Aluminium Fact Sheet. Lisle, Illinois: Water Quality Association, National Headquarters and Laboratory. Retrieved from: https://www.wqa.org/Portals/0/Technical/Technical%20Fact%20Sheets/2014_Aluminum.pdf

World Health Organization (WHO) (2011). Guidelines for Drinking-water Quality. Malta: WHO. Recuperado de http://apps.who.int/iris/bitstream/10665/44584/1/9789241548151_eng.pdf

Xu, Y., Kim, K., Hanna, M., and Nag, D. (2005). Chitosan-starch composite film: preparation and characterization. *Industrial crops and Products, 21*(2), 185-192. DOI: 10.1016/s0926-6690(4)00048-2

Ingeniería e Investigación vol. 39 No. 1, April - 2019 (36-42)

DOI: http://dx.doi.org/10.15446/ing.investig.v39n1.71670

Assessment of groundwater level variations using multivariate statistical methods

Evaluación de cambios en el nivel freático mediante métodos estadísticos multivariados

Fausto Molina-Gómez[1], Lenin A. Bulla-Cruz[2], Luis Á. Moreno-Anselmi[3], Juan C. Ruge[4], and Carol Arévalo-Daza[5]

ABSTRACT

Fluctuation of groundwater level induces changes in pore-water pressure of soil. However, this variation is not considered for underground constructions. This article explores the application of a statistical method to evaluate the groundwater level variation in geotechnical designs. The methodology included: (i) data collection, (ii) statistic formulation, and (iii) statistic data analysis. We collected information from the technical studies of the project "Metro de Bogotá", and selected four boreholes spanning 160 m, approximately, where the 1° de Mayo metro station will be built, in the south of the city. We used groundwater level readings reported by different piezometers for 30 days and data variance was assessed using a multivariate statistical method: analysis of repeated measures profiles. Results present a procedure to estimate the groundwater level fluctuation during a short monitoring period. We concluded that the analysis of repeated measures profiles allows estimating the groundwater level variation under a significance level 1-α.

Keywords: Analysis of repeated measures profiles, boreholes, infrastructure projects, Metro of Bogotá city.

RESUMEN

La fluctuación del nivel freático induce cambios en la presión de poros del suelo. Sin embargo, esta variación no se contempla en construcciones subterráneas. Este documento explora la aplicación de un método estadístico para evaluar la variación del nivel freático en diseños geotécnicos. La metodología incluyó: (i) recolección de datos, (ii) formulación estadística y (iii) análisis estadístico de datos. Se recopiló información de los estudios técnicos del proyecto "Metro de Bogotá". Se seleccionaron cuatro sondeos que abarcan 160 m, aproximadamente, donde se construirá la estación 1° de Mayo, al sur de la ciudad. Se utilizaron lecturas de nivel freático reportadas por varios piezómetros, durante 30 días y la variabilidad de los datos se evaluó utilizando el método estadístico multivariado: análisis de perfiles de medidas repetidas. Los resultados presentan un procedimiento para estimar la fluctuación del nivel freático durante un período corto de monitoreo. Se concluyó que el análisis de perfiles de medidas repetidas permite estimar la variación del nivel freático bajo un nivel de significancia 1-α.

Palabras clave: Análisis de perfiles de medidas repetidas, Metro de la ciudad de Bogotá, proyectos de infraestructura, sondeos.

Received: April 12th, 2018
Accepted: February 28th, 2019

Introduction

Geotechnical explorations often require to register the position of the water along the soil profile. This registration is a parameter known as groundwater level. The identification of groundwater level allows calculating the effective stress. Likewise, such reference point is used to establish the possible drainage conditions of the soil in the structure design. Moreover, groundwater level depends on the hydro-geological conditions of the ground (Gonzalez de Vallejo and Ferrer, 2011) and its variation is conditioned by the weather and the hydraulic properties of soil in the hydraulic parameters of the soil layers (Ruge, Da Cunha, Colmenares, and Mendoza, 2017).

However, in many cases, the variability of this state is not contemplated as part of the design process. Osterberg (2004) states that better exploration and sample practices are necessary to improve the building quality. Hence, in order to avoid extra laboratory tests, the groundwater

[1]Civil Engineer, Universidad Militar Nueva Granada, Colombia. M.Sc., Universidad de los Andes, Colombia. Affiliation: Universidad Militar Nueva Granada, Colombia. E-mail: fausto.molina@unimilitar.edu.co
[2]Civil Engineer, Universidad Militar Nueva Granada, Colombia. M.Sc., Universidad Nacional de Colombia, Colombia. Affiliation: Universidad Nacional de Colombia, Colombia. E-mail: labullac@unal.edu.co
[3] Civil Engineer, Universidad Francisco de Paula Santander, Colombia. M.Sc., Universidad de los Andes, Colombia. Affiliation: Universidad Militar Nueva Granada, Colombia. E-mail: luis.moreno@unimilitar.edu.co
[4] Civil Engineer, Universidad Francisco de Paula Santander, Colombia. Ph.D., Universidade de Brasilia, Brasil. Affiliation: Universidad Militar Nueva Granada, Colombia. E-mail: juan.ruge@unimilitar.edu.co
[5] Civil Engineer, Universidad Francisco de Paula Santander, Colombia. M.Sc., Universidad de los Andes, Colombia. Affiliation: Universidad Militar Nueva Granada, Colombia. E-mail: carol.arevalo@unimilitar.edu.co.

How to cite: Molina-Gómez, F., Bulla-Cruz, L. A., Moreno-Anselmi, L. A., Ruge, J. C., and Arévalo-Daza, C. (2019). Assessment of groundwater level variations using multivariate statistical methods. *Ingeniería e Investigación*, *39*(1), 36-42. DOI: 10.15446/ing.investig.v39n1.71670

level variation must be included in the designs of underground constructions (Tristá, Sotolongo, Cristía, and Fernández, 2016).

The variation of water content affects the stiffness of the material and increases its strains during reload stages (Molina-Gómez, Camacho-Tauta, and Reyes-Ortiz, 2016). In addition, fluctuations in the groundwater level induce variations in the lateral pressure, and those changes can be considered in the design of retaining wall construction (Ruge, 2014). Ausilio and Conte (2005) affirm that the groundwater level position is an issue when computing the bearing capacity of shallow foundations. Therefore, the groundwater level may affect the stability of geotechnical structures, such as tunnels.

Nevertheless, the study of the effect of the groundwater level variation has acquired relevance, especially, in the slope stability analysis. Reddi and Wu (1991) and Cascini, Calvello, and Grimaldi (2010) proposed a model to derive the time-dependent shear strength along the main slip surfaces. Conte and Troncone (2011) developed a method, based on a simple sliding-block model, to estimate the probability of failure in slopes, induced by the increment of pore water pressure during the rising of groundwater level. During seismic events, water under the surface controls the saturation degree, which can affect the soil strength due to the liquefaction phenomena (Soares and Viana da Fonseca, 2016).

The fluctuation of the groundwater level can be assessed, mainly, by statistical methods. Zhao, Li, Zhang, and Wang (2016) used a regression model to calculate the position of the water table. They validated the results using field measurements and found that the equation can predict the water level variations, with good precision. Han et al. (2016) implemented a groundwater level modelling framework through the coupling of two spatial and temporal clustering techniques. In addition, their procedure used self-organizing map technique to identify spatially homogeneous clusters of groundwater level piezometers. Yoon et al. (2016) predicted the long-term groundwater level fluctuation using a time series model and artificial neural network to evaluate the effect of rainfall on the soil.

In this study, we applied the analysis of repeated measures profiles to the estimation of the groundwater fluctuation. The remainder of this paper has four sections. The first section corresponds to the compilation of theoretical background and the description of the statistical method. The second section shows the data source and describes the soil composition of the study case. The third section refers to the validation of the null hypothesis of the technique. Finally, the fourth section presents the analysis and conclusions of this research.

Repeated measures profiles

Multivariate analysis allows to solve problems based on analytical criteria, which include all the variables involved (Gatingon, 2013). Hence, those methods can help to interpret better any type of information (Johnson and Wichern, 2007). Statistics methods do not only analyze numerical information, but they can also interpret graphical data with a quantitative approach. One of those methods is the repeated measures profiles, which analyzes graphical results.

Through a repeated measures profiles design, it is possible to estimate the variation of a response variable subjected to different treatments. As stated by Tabachnick and Fidell (2013), the data set may come from a dependent variable measured several times under the same pattern, i.e. the same independent variable is considered. This technique is an application of multivariate analysis of variance (MANOVA), where all samples (n) are measured within a fixed or constant variable. It focuses mainly on the comparison of variances, hence, the mean vectors of an specific treatment measured at the same level are compared (Friendly, 2010).

We evaluate three null hypotheses, according to Davis (2002). Those hypotheses are parallelism, flatness and coincidence. Harrar and Kong (2016) affirm that the technique seeks to respond the following questions: (*i*) whether there is interaction effect between-subjects and within subject factors, (*ii*) whether there is a between-subject factor effect, and (*iii*) whether there is a within-subject factor effect. Figure 1 presents a graphical representation of the null hypothesis.

Figure 1. Null hypotheses: (a) parallelism; (b) flatness; (c) coincidence.
Source: Authors

Mathematically, the profiles of repeated measures analyze the variance or covariance of the data (Johnson and Wichern, 2007). Therefore, the method compares the matrix of the slope parameters. Timm (2004) suggested Equations (1-3) to describe the null hypotheses (H_0).

$$H_{0_1}: \begin{bmatrix} \mu_{1,1}-\mu_{2,1} \\ \mu_{2,1}-\mu_{3,1} \\ \vdots \\ \mu_{p-1,1}-\mu_{p,1} \end{bmatrix} = \begin{bmatrix} \mu_{1,2}-\mu_{2,2} \\ \mu_{2,2}-\mu_{3,2} \\ \vdots \\ \mu_{p-1,2}-\mu_{p,2} \end{bmatrix} = \begin{bmatrix} \mu_{1,3}-\mu_{2,3} \\ \mu_{2,3}-\mu_{3,3} \\ \vdots \\ \mu_{p-1,3}-\mu_{p,3} \end{bmatrix} \quad (1)$$

$$H_{0_2} : \mu_{slope} = \begin{bmatrix} \mu_1 - \mu_2 \\ \mu_2 - \mu_3 \\ \vdots \\ \mu_{p-1} - \mu_p \end{bmatrix} \quad (2)$$

$$H_{0_3} : \mu_{1,1} + \mu_{2,1} + \cdots + \mu_{p,1} \neq \mu_{1,2} + \mu_{2,2} + \cdots + \mu_{p,2} = 0 \quad (3)$$

where μ represents the media of the measurement in each repetition; p the number of the measurement and i the number of the profile.

Moreover, all the hypotheses validation has been programmed in several statistical software, due to the amount of information collected. Through those routines, it is possible to calculate the variance and significance level between data. Those criteria can be estimated via p-value, which is a parameter used to reject or not reject the null hypothesis in any statistical model (Habiger, 2015). In addition, the p-value provides results with a confidence level $1 - \alpha$. Therefore, if the p-value is lower than α, the null hypothesis is rejected (Wackerly, Mendenhall, and Scheaffer, 2008). However, it is important to establish previously if the hypothesis must be rejected or not. Bulut and Desjardins (2017) stated that the repeated measures profiles are parallel, flatness and coincident when the p-value $< \alpha$.

Data collecting

Information comes from the geotechnical exploration of the site designated as 1° de Mayo metro station. Such station is part of the most important infrastructure project in the city: the metro of Bogotá. For this project, an exhaustive ground identification, which included 15 months of geological-geotechnical exploration was performed. The Institute for Urban Development of the city affirms that they hired the drilling of 563 boreholes in the 27 km of the metro line (IDU, 2015a). Each perforation had 50 m depth and were approximately 100 meters from each other. Likewise, the studies identified the physical, mechanical and dynamical properties of the subsoil, through more than 2000 laboratory tests. The data used in this article comes from the records reported in the geotechnical study for the metro of Bogotá (IDU, 2015b) for the boreholes SE1-25, SE1-26, SE1-27 and SE1-28. Figure 2 presents the localization of the boreholes.

According to the information provided in the Decree 523 of 2010, "Microzonificación Sísmica de Bogotá", the soil of the area in Figure 2 corresponds to an alluvial material (Secretaría General de la Alcaldía Mayor de Bogotá D. C., 2010). Molina-Gómez, Moreno-Anselmi, and Arévalo-Daza (2016) explain that this type of soil has medium to high load-carrying capacity, low compressibility, medium liquefaction susceptibility and could be unstable in open excavations. In addition, Caicedo, Mendoza, López, and Lizcano, (2018) indicate that these deposits are located in plain areas composed of loose to compacted clayey sands. Table 1 shows the soil lithology of the zone based on the classification proposed by the Unified System of Soils Classification (USCS).

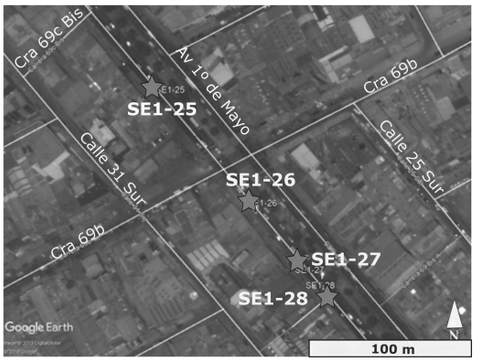

Figure 2. Location of the boreholes of the 1° de Mayo Station.
Source: Authors adapted from Google Earth®

Table 1. Soil classification and its physical properties

Depth (m)	SE1-25	SE1-26	SE1-27	SE1-27
2,4-3,0	ML	SM	SC	SM
6,0-6,6	SM	CL	SC	SM
9,0-9,6	CL	CL	CL	CL
11,4-12,0	MH	CL	CL	CL
20,0-20,6	SM-SC	SC	SM	CL-ML
24,0-24,6	CL	SM	CL	SC
29,4-30,0	SM	CL	CL	CL

Source: Authors adapted from IDU (2015b)

The zone for the 1° de Mayo metro station is located in the area of Tunjuelo River, which is a basin in the locality of Kennedy. The underground water flow of such river moves in southwest to northeast direction along 73 km distance. In addition, the slope of this aquifer changes 15 to 3, with an average slope of 5 at the south of Bogotá. According to geological-geotechnical reports for the first line of metro (Oteo-Mazo, 2015), the piezometric level of the aquifer is between 2560 and 2540 masl. Figure 3 presents the hydrogeological profile of the 1° de Mayo Station.

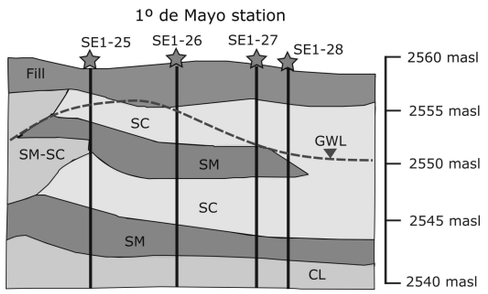

Figure 3. Hydrogeological profile of the 1° de Mayo Station.
Source: Authors

In the area for the 1° de Mayo Station construction, piezometers were positioned after drilling at the four research points for the future metro station (Figure 4). Piezometric readings were registered daily. For this research, readings at the same specific time were selected, in order to ensure repeated measures in the entire exploration site.

Figure 4. Piezometric space for groundwater level reading into borehole SE1-26.
Source: IDU (2015b)

Results and analysis

We used ***RStudio*** to process the data, which is a free statistical software based on an object-oriented algorithm. This software allows data plotting and information modelling by several techniques. In addition, ***RStudio*** has different packages to estimate the data variance using different multivariate techniques.

In this research, we used *profile*R package, which was proposed by Bulut, Davison, and Rodriguez (2017). Computation procedure covers an experiment design, including calculation of variance through sums squares matrix and vector products of the Equations (1-3). This tool provides a set of multivariate methods and data visualization options to implement profile analysis and cross-validation techniques described by Bulut (2013) and Davison and Davenport (2002). Likewise, it includes routines to perform criterion-related profile analysis, profile analysis via multidimensional scaling, moderated profile analysis, profile analysis by group, and a within-person factor model to derive score profiles. In addition, it allows to compare simultaneously the effect of treatments by univariate techniques as the Hotelling's T^2 test.

Furthermore, we used four different techniques to assess the parallelism of groundwater level along the boreholes. Those statistics were Pillai trace, Wilks' Lambda, Hotelling-Lawley trace and Roy's largest root. The aforementioned statistical models were described by Molina-Gómez et al., (2016). We validated the null hypothesis using the application of the procedure proposed by Bulut and Desjardins (2017), which evaluates the profiles of repeated measures with the *profile*R package.

Based on the exploration records, we selected thirty different measures of groundwater level during thirty different days. The measures started on March, 2014 and finished on April, 2014. During the monitoring period, there are no values of groundwater level at the surface. Topographic records indicate that all the research points and piezometers are at the elevation position, 2558 masl. Figure 5 shows the descriptive exploration of the groundwater level readings in the research points.

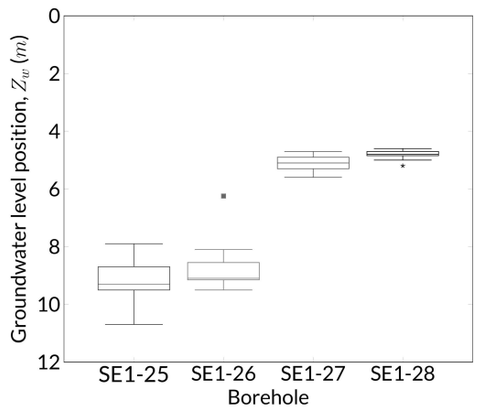

Figure 5. Box plot of the measures.
Source: Authors

Results revealed an interaction of information between the boreholes SE1-25 with SE1-26 and SE1-27 with SE1-28. We found similar inter-quartile distribution in all measures. However, we identified an outlier in SE1-26 and SE1-28, which is the first measure in SE1-26, and a change during monitoring in SE1-28.

In order to satisfy the homogeneity of variances assumption, using the median, we performed the Levene's test before executing the analysis of repeated measures profiles. The null hypothesis of this test assesses if all the populations' variances are equal and the alternative hypothesis considers that at least two of them differ. Results showed that the groundwater variances of the profiles are homogenous, under a confidence level of 99 (α = 0,01). If data satisfy the homogeneity condition, it is valid to apply the analysis of repeated measures profiles technique. Table 2 presents the Levene's model outcomes.

Table 2. Results of the homogeneity of variance evaluation

Source	DF	*F*-test	*p*-value
Boreholes	3	3,6153	$1{,}53 \times 10^{-2}$
Residuals	116		

Source: Authors

Figure 6 presents the repeated measures profiles of the groundwater measurements. From a qualitative viewpoint, we observed that all the profiles remain constant along the readings. Nevertheless, we confirmed the outlier of Figure 6 and a decreasing groundwater level during day

23, as well as a lower fluctuation in SE1-28. Possible reasons for the variation are the soil permeability and the material heterogeneity. According to the soil classification presented in Table 1 and the contrast with the typical values of permeability coefficient presented in the literature by Warrick (2003), it is possible to affirm that the soil has intermediate hydraulic conductivity and could experience fluctuations during short periods of time.

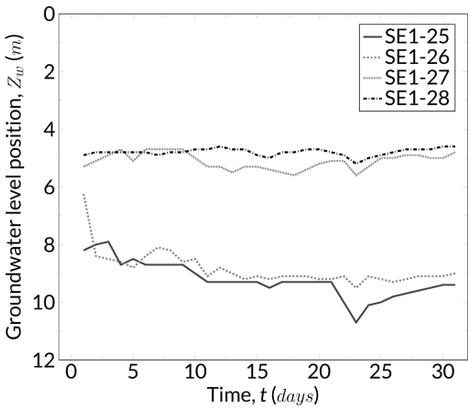

Figure 6. Groundwater level profiles.
Source: Authors

Table 3 presents the analysis of the repeated measures results. We assessed the three null hypotheses of the method, under a confidence level of 99 (α = 0,01). The value of α selected is based on the experiments design in the literature by Kuehl (2000) and Ramachandran and Tsokos (2009). Since the p-value obtained is less than α, there is statistical evidence to reject all the hypotheses (Habiger, 2015; Wackerly et al., 2008) under a confidence level of 99. Therefore, results suggest that the profiles of groundwater level are flat (horizontal), but not parallel and neither coincident.

Statistical results showed that the groundwater level of the aquifer remains constant during the period of study. In addition, under the area for the station construction, the water flows through stratified zones where the piezometric readings change from a research point to the other due to the effect of the equivalent hydraulic conductivity of the layered soil (Dulcey-Leal, Molina-Gómez, and Bulla-Cruz, 2018). However, for underground constructions, like the metro, it is necessary to ensure a constant groundwater level using a set of monitoring/control procedures, in order to avoid additional pore-water pressures that can increase soil lateral stresses. In this context, flatness hypothesis (horizontality) is the most important null hypothesis, H_{02}, since it establishes the uniformity of groundwater level during the monitoring period.

Table 3. Validation results of null hypotheses and variance

Hypothesis Tested:	Multivariate Test	*F*-test	*p*-value
H_{01}: Profiles are parallel	Wilks' Lambda	54 767,19	$1{,}22 \times 10^{-51}$
	Pillai trace	230,55	$3{,}96 \times 10^{-28}$
	Hotelling-Lawley trace	819 581	$3{,}14 \times 10^{-55}$
	Roy's largest root	313 737	$4{,}76 \times 10^{-31}$
H_{02}: Profiles are flat (horizontal)	–	56,44	$2{,}03 \times 10^{-2}$
H_{03}: Profiles are coincidental	–	1 449 329	$2{,}17 \times 10^{-16}$

Source: Authors

Conclusions

This article addressed a statistical assessment of groundwater variations for underground constructions. Results present a quantitative procedure to estimate the uniformity of the groundwater level position. We analyzed four different research points using data collected for the design of the infrastructure project "Metro de Bogotá". The points are continuous and cover a distance of 160 m. From results, the following conclusions were drawn:

1. We obtained a profile of repeated measures. We analyzed data that came from the geotechnical studies of the "Metro de Bogotá" project, including thirty different measures of groundwater level position. By visual inspection, not all the boreholes presented variations in the groundwater level position, except in day 23. However, we identified that the plot does not indicate the degree or quantitative value of the variation of such level.

2. We implemented a multivariate graphical statistical method, the analysis of repeated measures profiles, and assessed the variation of groundwater level for underground constructions. We evaluated the null hypotheses of the repeated measures analysis. Outcomes showed that the profiles are flat (horizontal), but are not parallel and not coincident under a confidence level of 99 (α = 0,01). Thus, we found no variations of groundwater level in a period of 30 days, which indicates no probable pore-water pressure build-up and no increments in the lateral stress of the soil during the station construction.

3. Analysis of repeated measures profiles showed that, when assessing groundwater variations, the most important null hypothesis is H_{02}, which determines the horizontality of the profiles. Hence, the measurements of the four boreholes have a between-subject factor effect. In this way, we found that there are no variations of the groundwater level. Therefore, we can affirm that the groundwater level is statistically uniform, even if we observed some variations graphically.

Acknowledgements

This work is part of the Research Project INV-DIS-2068 supported by the Vicerrectoría de Investigaciones of the Universidad Militar Nueva Granada.

References

Ausilio, E., and Conte, E. (2005). Influence of groundwater on the bearing capacity of shallow foundations. *Canadian Geotechnical Journal, 42*(2), 663-672. DOI: 10.1139/T04-084

Bulut, O. (2013). *Between-person and Within-person Subscore Reliability: Comparison of Unidimensional and Multidimensional IRT Models*. (Ph.D. thesis, University of Minnesota). Retrieved from: http://citeseerx.ist.psu.edu/viewdoc/download?doi=10.1.1.816.4794&rep=rep1&type=pdf

Bulut, O., Davison, M. L., and Rodriguez, M. C. (2017). Estimating Between-Person and Within-Person Subscore Reliability with Profile Analysis. *Multivariate Behavioral Research, 52*(1), 86-104. DOI: 10.1080/00273171.2016.1253452

Bulut, O., and Desjardins, C. D. (2017). *Profile Analysis of Multivariate Data in R. R Library* [R Package version 0.3-5]. Retrieved from https://cran.r-project.org/web/packages/profileR/profileR.pdf

Caicedo, B., Mendoza, C., López, F., and Lizcano, A. (2018). Behavior of diatomaceous soil in lacustrine deposits of Bogotá, Colombia. *Journal of Rock Mechanics and Geotechnical Engineering, 10*(2), 367-379. DOI: 10.1016/J.JRMGE.2017.10.005

Cascini, L., Calvello, M., and Grimaldi, G. M. (2010). Groundwater Modeling for the Analysis of Active Slow-Moving Landslides. *Journal of Geotechnical and Geoenvironmental Engineering, 136*(9), 1220-1230. DOI: 10.1061/(ASCE)GT.1943-5606.0000323

Conte, E., and Troncone, A. (2011). Analytical Method for Predicting the Mobility of Slow-Moving Landslides owing to Groundwater Fluctuations. *Journal of Geotechnical and Geoenvironmental Engineering, 137*(8), 777-784. DOI: 10.1061/(ASCE)GT.1943-5606.0000486

Davis, C. S. (2002). *Statistical methods for the analysis of repeated measurements* (2nd ed.). New York: Springer.

Davison, M. L., and Davenport, E. C. (2002). Identifying criterion-related patterns of predictor scores using multiple regression. *Psychological Methods, 7*(4), 468-484. Retrieved from http://www.ncbi.nlm.nih.gov/pubmed/12530704

Dulcey-Leal, E., Molina-Gómez, F. A., and Bulla-Cruz, L. A. (2018). Hydraulic conductivity in layered saturated soils assessed through a novel physical model. *DYNA, 85*(205), 119-124. DOI: 10.15446/dyna.v85n205.64473

Friendly, M. (2010). HE Plots for Repeated Measures Designs. *Journal of Statistical Software, 37*(4), 1-40. DOI: 10.18637/jss.v037.i04

Gatingon, H. (2013). *Statistical Analysis of Management Data* (3rd ed.). New York: Springer Science & Business Media.

González de Vallejo, L. I., and Ferrer, M. (2011). *Geological Engineering*. London: CRC Press/Balkema. DOI: 10.1201/b11745

Habiger, J. D. (2015). Multiple test functions and adjusted p-values for test statistics with discrete distributions. *Journal of Statistical Planning and Inference, 167*, 1-13. DOI: 10.1016/j.jspi.2015.06.003

Han, J.-C., Huang, Y., Li, Z., Zhao, C., Cheng, G., and Huang, P. (2016). Groundwater level prediction using a SOM-aided stepwise cluster inference model. *Journal of Environmental Management*, 182, 308-321. DOI: 10.1016/j.jenvman.2016.07.069

Harrar, S. W., and Kong, X. (2016). High-dimensional multivariate repeated measures analysis with unequal covariance matrices. *Journal of Multivariate Analysis*, *145*, 1-21. DOI: 10.1016/j.jmva.2015.11.012

Instituto de Desarrollo Urbano - IDU. (2015a). *Estudios geológicos y geotécnicos*. Unpublished raw data.

Instituto de Desarrollo Urbano - IDU. (2015b). *Información Geotécnica PLMB Tramo I*. Unpublished raw data.

Johnson, R. A., and Wichern, D. W. (2007). *Applied Multivariate Statistical Analysis* (6th ed.). New Yersey: Pearson Education International.

Kuehl, R. (2000). *Design of experiments: statistical principles of research design and analysis* (2nd ed.). Pacific Grove (Calif.): Duxbury/Thomson Learning.

Molina-Gómez, F. A., Moreno-Anselmi, L. Á., and Arévalo-Daza, C. E. (2016). *Aplicación del análisis de perfiles de medidas repetidas en exploraciones geotécnicas*, Paper presented at the XV Congreso Colombiano de Geotecnia (p. 7). Cartagena, Sociedad Colombiana de Geotecnia.

Molina-Gómez, F. A., Camacho-Tauta, J. F., and Reyes-Ortiz, O. J. (2016). Stiffness of a granular base under optimum and saturated water contents. *Revista Tecnura, 20*(49), 75-85. DOI: 10.14483/udistrital.jour.tecnura.2016.3.a05

Osterberg, J. O. (2004). Geotechnical Engineers, Wake-up—The Soil Exploration Process Needs Drastic Change. In J.P. Turner, and P.W. Mayne (Eds.), *GeoSupport 2004: Drilled Shafts, Micropiling, Deep Mixing, Remedial Methods, and Specialty Foundation Systems* (pp. 450-459). Reston, VA: American Society of Civil Engineers. DOI: 10.1061/40713(2004)38

Oteo-Mazo, C. (2015). *Condiciones geotécnicas del Proyecto de la Línea 1*. Bogotá. Unpublished raw data.

Ramachandran, K. M., and Tsokos, C. P. (2009). *Mathematical statistics with applications*. San Diego, CA: Elsevier/Academic Press.

Reddi, L. N., and Wu, T. H. (1991). Probabilistic Analysis of Ground Water Levels in Hillside Slopes. *Journal of Geotechnical Engineering, 117*(6), 872-890. DOI: 10.1061/(ASCE)0733-9410(1991)117:6(872)

Ruge, J. C. (2014). *Análise do comportamento de cortina de estacas executada em solo poroso metaestável mediante o uso de um modelo constitutivo hipoplástico considerando a resposta não saturada*. (Ph.D. thesis, Universidade de Brasília). Retrieved from: http://repositorio.unb.br/handle/10482/17558?mode=full

Ruge, J. C., Da Cunha, R., Colmenares, J. E., and Mendoza, C. C. (2017). Class A prediction of a retaining structure made by a pile curtain wall executed on a tropical soil. *DYNA, 84*(202), 278-288. DOI: 10.15446/dyna.v84n202.63965

Secretaría General de la Alcaldía Mayor de Bogotá D. C. (September 16, 2010). Por el cual se adopta la Microzonificación Sísmica de Bogotá D. C. [Decreto 523 de 2010]. Retrieved from http://www.alcaldiabogota.gov.co/sisjur/normas/Norma1.jsp?i=40984

Soares, M., and Viana da Fonseca, A. (2016). Factors Affecting Steady State Locus in Triaxial Tests. *Geotechnical Testing Journal, 39*(6), 20150228. DOI: 10.1520/ GTJ20150228

Tabachnick, B. G., and Fidell, L. S. (2013). *Using multivariate statistics* (6th ed.). Boston: Pearson Education.

Timm, N. H. (2004). *Applied Multivariate Analysis*. New York, NY: Springer New York. DOI: 10.1007/b98963

Tristá, J. G., Sotolongo, G. Q., Cristía, W. C., and Fernández, C. G. (2016). Simulation of the soil-water characteristic curve using laboratory tests and empirical models for Cubans unsaturated soils. *Revista de la Construcción, 15*(1), 22-31.Retrieved from: http://revistadelaconstruccion.uc.cl/index.php/rdlc/article/view/494/127

Wackerly, D. D., Mendenhall, W., and Scheaffer, R. L. (2008). *Mathematical statistics with applications*. Belmont, CA: Thomson Brooks/Cole.

Warrick, A. W. (2003). *Soil Water Dynamics* (1st ed.). New York: Oxford University Press.

Yoon, H., Hyun, Y., Ha, K., Lee, K.-K., and Kim, G.-B. (2016). A method to improve the stability and accuracy of ANN- and SVM-based time series models for long-term groundwater level predictions. *Computers & Geosciences*, *90*, 144-155. DOI: 10.1016/j.cageo.2016.03.002

Zhao, Y., Li, Y., Zhang, L., and Wang, Q. (2016). Groundwater level prediction of landslide based on classification and regression tree. *Geodesy and Geodynamics, 7*(5), 348-355. DOI: 10.1016/j.geog.2016.07.005

Ingeniería e Investigación vol. 39 No. 1, April - 2019 (43-52)

DOI: http://dx.doi.org/10.15446/ing.investig.v39n1.71346

Support for incident management in optical networks through critical points identification

Soporte de gestión de incidentes de redes ópticas a través de la identificación de puntos críticos

Aminadabe B. Sousa[1], Alberto S. Lima[2], Neuman de Souza[3], and J. A. B. Moura[4]

ABSTRACT

In incident management for optical networks, when a fault or event occurs, a network element will often send a notification, in the form of an "alarm", to operators and managers. Alarms contain valuable information to support the fault management process at the operating level, because it is a persistent indication of a fault. Alarms usually clear only with the triggering of the solution for its cause. To mitigate business risks related to faults in optical networks, service managers need to estimate the impact of a network fault in relation to business needs. In optical networks, identifying redundancy points of high-impact on the network is still a challenge for managers. They often rely on their own experience to prioritize points that possibly need to have redundancy in those networks. This work presents a simulation model capable of locating suitable points for the application of asset redundancy to reduce optical network disruptions, based on business risk. The model is implemented in a software tool and then used in a case study of two reference networks, whose elements may fail according to a realistic failure scenario. Results of the study allow face validity with preliminary evidence that the model is useful to support incident management in optical networks.

Keywords: Fault Management, Optical Networks, Service Management, Risk Management, Business-driven IT Management.

RESUMEN

En la gestión de incidentes de redes ópticas, cuando ocurre una falla o evento, generalmente un componente de la red envía una notificación a los operadores y gerentes. Las alarmas contienen información importante para respaldar el proceso de gestión de fallas a nivel operativo, porque es una indicación persistente de una falla que se borra solo con la solución de condición de disparo. Para mitigar los riesgos comerciales relacionados con las fallas en las redes ópticas, los administradores de servicios deben estimar el impacto de una falla de red en relación con las necesidades del negocio. En las redes ópticas, la identificación de puntos de redundancia de alto impacto de red todavía es un desafío para los gerentes. Usualmente, estos gerentes confían en su propia experiencia para priorizar puntos que posiblemente deban tener redundancia en esas redes. En este trabajo, presentamos una evaluación de un modelo de simulación, capaz de localizar puntos adecuados para la aplicación de redundancia de activos y así reducir las interrupciones de la red óptica, en función del riesgo comercial. El modelo se implementó en una herramienta de software y se procedió a un estudio de caso que incluye dos escenarios de simulación de redes de referencia, con resultados prometedores.

Palabras clave: Gestión de fallas, Redes ópticas, Administración de servicios, Gestión de riesgos, Gestión de TI impulsada por los negocios.

Received: March 30th, 2018
Accepted: April 1st, 2019

Introduction

When working in incident management activities, managers need to understand the actions to take and the life cycle of the incident, which includes detection and recording, user support, investigation and diagnosis, resolution and recovery of service, incident ownership, monitoring, and communication (OGC, 2007). According to Lu *et al.* (2016), service level agreements (SLAs) have been proposed as contracts used to record the rights and obligations of service providers and their customers, including the fault-tolerance concerns and strategies. Hanemann, Sailer and Schmitz (2004) state that to avoid SLA violations, managers should identify the root cause of a fault in a very short time or even act proactively.

[1]Electrical Engineer, Federal University of Ceará, Brazil. Ph.D. Teleinformatics Engineering, Federal University of Ceará, Brazil. Affiliation: Teleinformatics Engineering, Federal University of Ceará, Brazil. E-mail: aminadabebs@gmail.com.
[2]Computer Science, State University of Ceará, Brazil. Ph.D. Teleinformatics Engineering, Federal University of Ceará, Brazil. Affiliation: Adjunt Professsor, Federal University of Ceará, Brazil. E-mail: albertosampaioi@ufc.br.
[3]Civil Engineer, Federal University of Ceará, Brazil. Ph.D. Computer Science, University of Paris VI, France. Affiliation: Full Professor, Federal University of Ceará, Brazil. E-mail: neuman@ufc.br.
[4]Electrical Engineer, Federal University of Paraiba, Brazil. Ph.D. Electrical Engineering, University of Waterloo, Canada. Affiliation: Full Professor, Federal University of Campina Grande, Brazil. E-mail: antao@dsc.ufcg.edu.br.

How to cite: Sousa, A. B., Lima, A. S., De Souza J. N., Moura J. A. B. (2019) Support for incident management in optical networks through critical points identification. *Ingeniería e Investigación*, *39*(1), 43-52.
DOI: 10.15446/ing.investig.v39n1.71346

Service and network managers monitor events and perform actions based on fault management information and management recommendations and standards, such as ITU-T (1995). The process of fault management tries to identify events and take corrective actions or activate notifications that allow a proper intervention. The study of the business risk involved in network management has been highlighted as one of the ways to find a more effective link among the levels of strategic, tactical and operational management.

The decision about network points that need interventions, including the creation of redundancy measures, has always been a topic of discussion among network and service managers (Stein, 1999). The need to consider business aspects in this activity has considerably increased the complexity of this challenge for service managers.

This paper proposes an incident management supporting model, implemented in a software tool, for identifying and signaling critical points that can be redundant in an optical network (Ramaswami, and Sivarajan, 2001), based on the risk to the business. When defining critical network redundancy points, managers can use model outputs to make better decisions and improve the fault management process. A case study was carried out in a real company, using two simulation scenarios of reference networks.

The remainder of this article is organized as follows. Section 2 includes theoretical foundation for the research and discusses related work. Section 3 shows the detailed design and implementation of the model. Sections 4 and 5 show the case study and result analysis, respectively. Finally, the conclusions and future work are described in Section 6.

Related work

IT services can be provided using other services called subservices and resources (e.g., network links, network components, etc.). Organizations need to be aware of and manage the risks related to their vital assets. Managers need to plan and to be aware of both the probable and improbable events (Gómez, Mora, Gewald, Nebel and O'Connor, 2017). Risk management addresses situations that can be classified as opportunities or threats. The need to develop and maintain control over the interdependencies among network infrastructures was presented in Bloomfield, Popov, Salako, Stankovic, and Wright (2017).

The process of incident management seeks to restore a normal service operation as quickly as possible and minimize the impact on business operations (OGC, 2007). A problem record should be created when multiple occurrences of related incidents are observed. The main goal of *problem management* differs from *incident management*, because the latter focuses on the detection of the underlying causes of an incident and the best resolution and prevention. An incident can appear again if the problem resolution is not found. An incident is where a failure or an error occurs. Incidents are usually more visible and its impact on business is more immediate. The result of network diagnostics, revealing that some systems are not operating is considered a problem (OGC, 2007). According to Hanemann *et al*. (2004), a fault does not lead to the total failure of a service, but its quality of service (*QoS*) parameters, i.e. service levels agreement (SLA), might not be met.

According to Specialski (2018), failures are not the same as errors. A failure is an abnormal condition whose recovery requires management action and is usually caused by incorrect operations or an excessive number of errors. A failure is a persistent abnormal condition that requires an immediate repair action (e.g. interrupt a communication link). Meanwhile, an error is an occasional abnormal condition (e.g. bit error or sync failure on a communication link). Fault management includes resource monitoring, verifying the network point and predicting when a failure or an error can occur. Managers need to isolate the failure point, seek alternative solutions until problem resolution, in order to reduce the impact on the whole system (and its consequent business impact), and to repair the fault. Hanemann *et al*. (2004) state that a single fault can cause a burst of failure events. There is a high cost for repairing and restoring a network. Mas, Krauß and Casier (2011) affirm that fault management is one of the most expensive operational processes.

Fen Yanqin and Li (2016) argue that many unsurpassable problems have appeared in traditional transmission networks, which motivates the development of smarter optical networks. Due to the usually high data traffic in optical networks, the number of alarms sent from a fault is often very large, making human work quite complicated and slow (Meira and Nogueira, 2000). In order to facilitate this task execution, solutions called *fault localization algorithms* were proposed (Mas, Thiran and Le Boudec, , 1999; Mas,Tomkos and Tomguz, 2005; Mas and Thiran, 2000; Lehr, Dassow, Zeffler, Gladisch and Hanik, 1998).

Alarms received by the network management system (NMS) or the contact of the customer service line can initiate the fault management process (Mas *et al*., 2011). Configuration or physical failures can trigger different subprocesses. Time interval between the first symptom that a service does not perform properly, and the verified fault repair needs to be minimized, especially with respect to SLAs, as such agreements often contain guarantees like a mean time to repair (Hanemann *et al*., 2004).

Organizations need to be aware of and manage the risks associated with their vital assets. Managers need to plan and prepare for probable and improbable events (Gómez *et al*., 2017). According to Benhcine, Elbiaze and Idoudi (2013), network resiliency has become one of the major requirements of the service provider to deploy real-time applications and meet the customer's quality of service (QoS) needs. The loss time and the convergence time after link failure were evaluated in different scenarios. *Fast Reroute* protection efficiency has been affected by the network size. Loss time increases as network topology size does.

Sterbenz *et al*. (2010) proposed a systematic framework architecture that unifies resilience disciplines, strategies, principles and analyses. The rule was to defend, detect,

correct, recover + diagnose and refine. The *ResiliNets* strategy leads to a set of design principles that guide the analysis and design of resilient networks. In Smith *et al*. (2011), a systematic approach to network resilience is described. The aspects of this work represent a longer-term view of resilience and require more radical changes in the way network operators currently think about resilience.

Da Silva and Fagotto (2014) state that the literature efforts focus on maximizing network and services availability , as well as providing a rapid reestablishment of the network in case of failures. A Fault Localizing Algorithm (AFA-FLA) was recommended in Mas and Thiran (2000) and Mas *et al*. (2005). In Sousa, Delfino, De Sousa and Everardo (2005), an algorithm for fault localization was presented, whose main advantage over other algorithms was the small amount of information needed to locate the faults. However, their proposed solution did not address the inherent business risks of the identified failures. They use the alarm domain as a conceptual basis for the development of the proposed model (Sousa *et al*., 2005).

Homma and Shinomiya (2016) presented a failure recovery method, using ring structures called tie-sets and proposing an algorithm that searches for a group of tie sets that generate a shorter deviation path in the case of a link failure. The authors idealized tie-sets based on graph theory, dividing a mesh network into logical loops, managing faults with them.

Rodríguez-García, Ramírez-López and Travieso-Torres (2015) state that while, transport networks supported the increased load, routing generated much delay compared to switching, causing transport networks to evolve towards fiber optics. This technology, in turn, evolved into WDM (Wavelength Division Multiplexing) networks. The authors also presented the simulation of *Snake One*, a heuristic algorithm, and a comparison between three heuristic algorithms: Genetic Algorithms, Simulated Annealing, and Tabu Search, using blocking probability and network utilization as standard indicators.

According to Mas *et al*. (2011), optical networks need to use more fiber infrastructure and longer transmission distances with less operational effort. These networks also allow new opportunities, for example, new cuttings of access areas with larger sizes and fewer network locations. The design of an intelligent optical metro network was presented and compared to some traditional approaches in Fen *et al*. (2016).

According to Li-xia and Yue-Jin (2014), connection-oriented ethernet passive optical networks (EPONs) include fault management in their functional architecture, and the creation of a network of automatic protection mechanisms to test the function of simulation tests and the protection of their original programs. The application of this method can provide automatic and rapid protection to meet the requirements of the transmission network survival capability.

The work in Maltz *et al*. (2015) relates to the one herein because it shows a technology that considers network impact, and automatically mitigates datacenter failures, instead of relying on human intervention. Our proposed model (*ASP - Asset Redundancy Points Locator algorithm*) is similar to the one used by Oliveira, Brito and Brasileiro (2003) for working with a fault detector that has knowledge about which components may have failed. The work presented by Fabre, Benveniste, Haar, Jard and Aghasaryan (2004) relates to the one here, since it predicts failure situations in an optical link. They simulate the physical layer with transmitter, receiver and optic fiber.

Identification of redundancy points in optical networks

Downtime in a computer network can affect a company in many ways, generating primarily financial impacts. In order to estimate the cost that a network failure could generate for a company, it is necessary to obtain statistics that involve the actors of the process. These actors that use the network dependent services must be in relation to the occurrence of network failures and the current financial information.

Network downtime can also cause a loss in the company's reputation and customer loyalty. For example, the fact that a customer is waiting to make a payment in a commercially-held company, while their systems are stationary can cause loss of loyalty in the short term. The same situation in a new company may cause some customers not to return.

Any investment in redundancy should generate some return for the company. While investments with returns above capital cost increase the value of company; investments with lower returns than capital cost, will reduce it.

Model description

The following optical and optoelectronic devices ("elements") are considered in the proposed model. **Optical fiber** is a passive device that sends no type of alarm. Every time the **Transmitter (TX)** passes from one work regimen to another, an alarm is sent. For security reasons, if the transmitter starts to work in a not permitted regime, it is automatically turned off and an alarm is sent to management. The **Receiver (RX)** sends an alarm to the management control dashboard when the incoming optical power is below a specified value. **Add/Drop Filters (ADF)** are responsible for the insertion (derivation) of one wavelength in (from) a signal composed of several wavelengths. Each filter sends an alarm when it is not working properly. In the **3R Amplifier**, an alarm is sent when it is not possible to recover the synchronism of the input signal. When the signal chosen as reference wavelength has not enough optical power, the **Protection Switch (PS)** will choose another input signal with acceptable optical power and an alarm is sent to control dashboard. When the **Switch (SW)** shows bad functioning, it sends an alarm to control dashboard. The **Multiplexer/Demultiplexer** is a passive device and sends no type of alarm.

On the one hand, the elements of the model that are not able to send alarms are named passive elements (P). On the other hand, during the occurrence of some abnormal functioning

condition, elements that can send alarms are microprocessor-based and they are called alarming elements (A). Alarming elements are grouped herein into three categories: Self-Alarmed (Category A1 or A3), Out-Alarmed (Category A2) and Failure-Masking (Category A3) (Sousa *et al*., 2005).

Another model (and network) entity, is the node. A node utilizes an alternate wavelength and a physical association between two nodes that has two fibers, one for every communication direction. An information activity routed to a given node can achieve it through no less than two distinct paths and a protection switch will decide which of them will be used according to their optical power level. The nodes are classified as central or local. Each network element has a unique identification, in order to identify which network element is damaged and which node it belongs to when a fault occurs. This identification is composed of a string of four fields (A,B,C,D), which has a meaning for a local node (Sousa *et al*., 2005). In this paper, the notation (A,B,C,D) means network element (A B) between nodes C and D.

The connection between elements that can send an alarm or not is considered in the model. The *ASP algorithm* has the ability to find damaged passive elements, needing only the identification of the elements that are sending alarms. The employed correlation of alarms reduces the amount of suspect network elements. That amount varies with the number of channels that use the damaged element(s).

The proposed *ASP* model was automated in a software tool named *ASP* software, that can simulate optical network scenarios by using *ASP* model process. This is a useful tool to support decisions on incident management, related to fault management process. The *ASP* software was developed in a research project at the Federal University of Ceará, Brazil. Its advantages over traditional network simulators include the consistent analysis of the number of alarms generated by a failure, along with risk in business scenario simulations. It has been used in projects that seek the assessment of business scenarios for optical network providers. More than 700 scenario simulations were performed with the software. The disadvantage of *ASP* is that its scope is limited to redundancy points identification in optical networks. The *ASP* project is a work in progress in final phase, and its applications will be available to research community when it is totally finalized.

As shown in Figure 1, managers must perform the following steps to use the *ASP* model:

STEP 1 - Modeling the optical network topology in *ASP*. The information about the topology, channels and elements of the optical network scenario are informed through the *ASP* software input interface.

STEP 2 - Definition of business evaluation parameters in the model. The following parameters are reported as input to the proposed model:

Model Coverage Degree: for simulations execution, the model allows the selection of scope for risk calculation, where the impact estimation can be performed by network elements category or by each network element.

Business Impact of a network element: The Business Impact Analysis (B.I.A.) for network failures is a very complex process because there is a huge dependence on other services that are supported on the network service. The proposed model is simple and flexible, allowing the definition and use of several formulas (proposals) to calculate the business impact of a network element.

STEP 3 - Setting Model Calibration Parameters. The *ASP* model uses a consensus-based approach among managers to estimate the parameters for their use. The strategy is based on the *Delphi method* (Rowe and Wright, 1997), counting two rounds of evaluation, as well as on the use of questionnaires as a tool for collecting the information from the managers. The activity description of the two rounds of evaluation is done sequentially.

1. First round: managers estimate the following parameters, through specific questionnaires. For each answer, managers must present their motivation (justification).

For the optical network:

- Number of IT services that are dependent on the evaluated optical network (number).

- Manager's perception of the importance of high network availability for the business.

  - Very high (5) - High (4) - Medium (3) - Low (2) - Very low (1).

- Perception of the importance to the business of maintaining a high quality of services

  - Very high (5) - High (4) - Medium (3) - Low (2) - Very low (1).

For each element category of the optical network (topology) or for each network element of the evaluated topology:

- Probability of failure - percentage (0 - 100%)

- Relevance of the network element for the business

  - Very high (5) - High (4) - Medium (3) - Low (2) - Very low (1).

- The empirical criteria to be considered by managers, when estimating relevance of a network element for the business are:

  - Number of IT services dependent on optical networks
  - Importance of the optical network availability for the business
  - Importance of the optical network service quality for the business
  - Importance of the network element importance in topology

- Existing redundancies in topology.

The justifications of the answers may be based on empirical or statistical business data.

2. Second round: The results of the first round are presented, as well as a list of evaluators' answers and their justifications. In the choice phase, managers can change their answers if they are convinced by any of presented justifications. In this way, a consensus is sought among the group.

STEP 4 - Scenario simulation execution. The simulation environment is configured to generate the physical route domain of the library, topology, channels and alarms (input data). When executing *ASP* software (see Figure 2), in the physical route domain, all the network components that comprise any channel are numbered and associated with each of these components and their respective alarms. The next action is to check for alarms from components A1 and A3. The respective components are potential suspects if there are alarms and are then added to the list of suspect components. When checking the alarms coming from the A2 components of each channel, the algorithm takes only the first alarmed component of each channel, if any. This strategy eliminates redundant alarms. The channel is analyzed in reverse way, until it reaches the first transmitter, to consider the rest of the A2 components. This process must be performed on all channels. Next, a list of all the alarmed components A2 and the first transmitter is generated. The generated list is used to form sets, in order to check all the listed components one by one, making sure they are able to produce the alarms observed in the management function in case of failure. This is done by comparing the alarm domain of each component with the physical route domain. The components that passed the test form different sets.

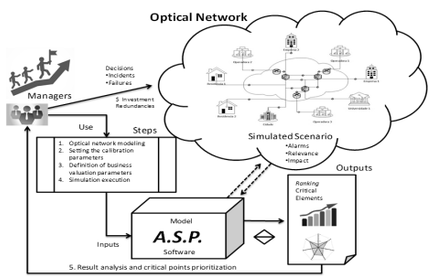

Figure 1. *ASP* model use view.
Source: Authors

When no component passes the test, it is performed again using component pairs, and so on. The formed sets are added to the suspect components list. Next, *ASP* model estimates the expected risk value (ERV) for all network elements that presented alarms in simulation. The risk estimate of a network element in the model is done through the formula: *Expected Risk Value* (ERV_e) = *Probability of failure* (P_e) *X Impact* (i_e).

The *ASP* model is effective in identifying the most critical elements of the optical network. Each network element that is considered a critical point in a management view, is related to a high-risk value. For ERV_e calculation, one assumes the risk of an element (e) to be given by multiplying its probability of occurrence (P_e) with its impact degree (i_e) on business (equation 1).

$$ERV_e = P_e \times i_e \tag{1}$$

Managers can choose different equations to estimate the network element impact (i_e), because the *ASP* model is flexible. For future work, the plan is to build a "library of possible equations" to estimate network element impact. In this paper, the focus was to simplify the impact estimative, to illustrate the model use and collect possible evidence that it works and is useful. Business relevance is estimated by managers for each optical network element using a consensus-based approach, based on *Delphi method* (Rowe and Wright, 1997). The network element impact is estimated (as shown in equation 2) by the total number of the element alarms (Ag_e) multiplied by its business relevance (R_e– a relative weight or percentage), divided into the sum of all the generated alarms multiplied by their respective relevance (weights):

$$i_e = \frac{(Ag_e \times R_s)}{\sum_{1}^{e}(Ag_e \times R_s)} \tag{2}$$

where:

i_e – Impact of element e in the network

Ag_e – Number of alarms generated when element e fails

R_e – Relevance of the element for the business (*Very High - 5; High - 4; Medium - 3; Low - 2; Very* Low - *1*)

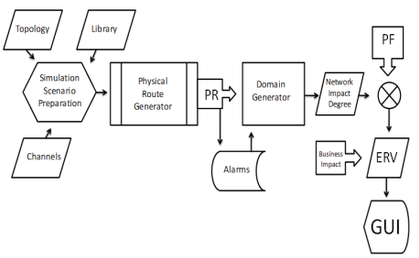

Figure 2. *ASP* model process view.
Source: Authors

To reduce analysis efforts by model users, business relevance of an optical network element in the *ASP* model may be aggregately defined for a category of elements (e.g. switches) or for each network element node, according to its location in the optical network topology. In this work, *Alpha* company managers decided to estimate the business relevance in the simulated scenarios by network element category. Note that equation 2 implicitly assumes that the impact of an element (or its category) is directly proportional to the number of alarms it may generate and its business relevance. In situations where this may be a rather simplistic or unrealistic assumption, users (managers) may compensate the result by pondering R_e more carefully.

Model results can be used i) to support decision-making (Sergio, De Souza and Gonçalves, 2017) in proactive user information, ii) to reduce the number of inquiries by users and

distribute information about optical network critical points (as incident management reports), iii) to supply possible incident-related information to other service management processes, and iv) to ensure that improvement potentials are derived from possible incidents.

Case study and result analysis

Case study

We proceeded to a case study (Yin, 2018), for analysis and validation of the proposed model, with the simulation of two reference networks. Simulation planning and results were presented, discussed and analyzed in a face validity exercise (Runerson and Host, 2009), by service and network managers of a real Brazilian telecommunications company - herein identified as the *Alpha company*.

ASP software tool was used with the focus on incident management related activities (fault management), to support decision on which network points need interventions - including the creation of redundancy measures.

The first scenario considers a USnation-type network (Figure 3). Its composition includes 24 nodes (*n01 – n24*), where 17 of them are local and the other 7 are central nodes. There are 43 links and 133 network elements.

As shown in Figure 3, the channels pass through 17 local nodes, 7 central nodes and 28 links.

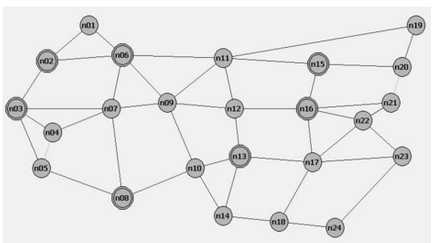

Figure 3. USnation - Network topology.
Source: Authors

The USnation network has the following parameters: 28 fibers, which generate 96 alarms; 7 LAP, which do not generate alarms; 7 demultiplexers, which generate 24 alarms; 7 multiplexers, which generate 27 alarms; 19 Add Drop Filters, which generate 103 alarms; 13 transmitters, which generate 52 alarms; 13 receivers, which generate 18 alarms; 7 switches, which generate 7 alarms; 13 Protection Switches, which generate 16 alarms and 13 3R amplifiers, which generate 5 alarms. There is a total of 127 used network components and 348 generated alarms. The values of the estimated failure probabilities for the network elements in the case study are shown in Figure 4. In *ASP* model, the probability of failure of each element is estimated by managers. As previously shown, these values are used in the model to estimate the network elements risks, in relation to their business impacts. In case of variations of these probabilities or due to different impacts to the business on different network channels, the risk values of the network elements may vary.

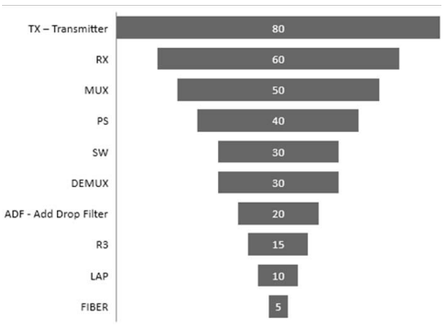

Figure 4. Failure probabilities for network elements in case study.
Source: Authors

ASP software generates statistical validation data for each simulation. Results of the USnation *scenario* statistical validation are presented in Figure 5.

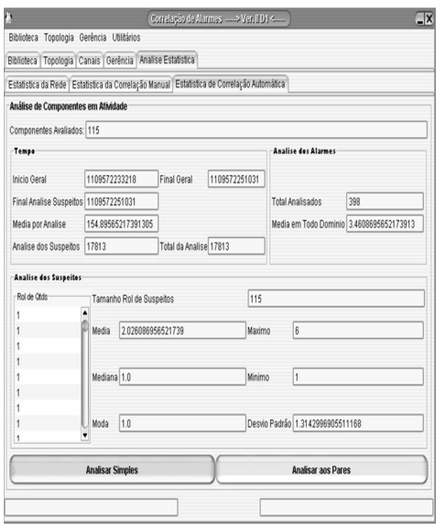

Figure 5. Statistical validation of the USnation network simulation.
Source: Authors

Managers can verify assertiveness and consistency of the performed simulation, through evaluation of standard deviation, mean, mode, median, minimum value and maximum value.

The second simulation scenario considers a network of type *ER_NET* (Figure 6). Its composition includes 37 nodes, where 24 of them are local and the other 13 are central nodes. There are 65 links and 128 network elements. The channels pass through 24 local nodes, 13 central nodes, and 65 links.

The network topologies in Figures 4, 5, 6 and 7 are formed by local and central nodes. The local nodes are composed of ADF, RX, TX, PS, SW, 3R and LAP, while the central nodes are composed of MUX, DEMUX, RX, TX, PS, SW, 3R and LAP. The nodes are interconnected by the optical fibers. The channels determine the active elements that will be analyzed.

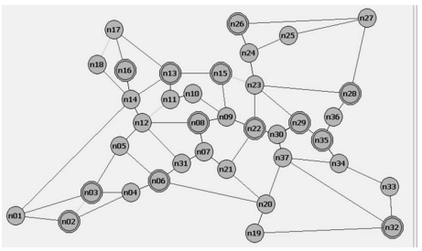

Figure 6. *ER_NET* - Network topology.
Source: Authors

Results and discussion

First Simulation Scenario

We proceeded to the *US Nation* scenario simulation using the *ASP* software tool (Figure 7).

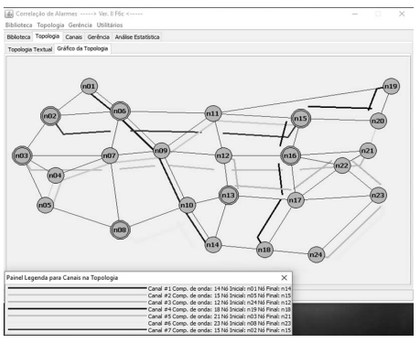

Figure 7. USnation simulation in ASP software tool.
Source: Authors

ASP model generates a risk ranking table that includes all the optical network elements in scenario. Table 1 shows the risks of the first 24 network elements. Figure 8 shows USnation network elements risk zone. A Multiplexer is the element with the highest estimated risk. Managers can analyze risk intervals and proceed to a drill-down analysis, using this useful information to decide on redundancy points choice. *Alpha* managers affirm that this support improves the quality of decision-making quality. Results of the *ASP* model simulation for *US Nation network* indicated that Regenerator 3R (3R amplifiers) were the elements with the lowest risk values.

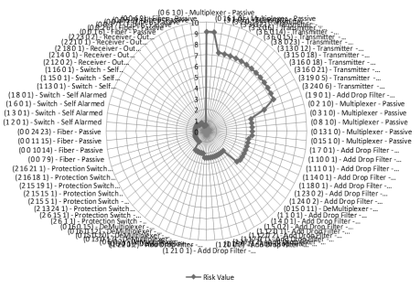

Figure 8. *US Nation* - Risks of optical network elements.
Source: Authors

Table 1 shows the risk ranking generated by the *ASP* model. The *ERVs* estimated by the *ASP* model are influenced by network topology, channels and business impact. It can be observed that the risk related to Multiplexers, Transmitters and Add Drop Filters are in different ranking positions, due to possible differences in topology position, channels and business relevance.

Table 1. Network elements risk ranking - First scenario

Network Element	Risk Value
(0 6 1 0) - Multiplexer - Passive	9,10
(0 16 1 0) - Multiplexer - Passive	9,10
(3 1 0 5) - Transmitter - Failure Masking	7,28
(3 2 0 15) - Transmitter - Failure Mask-ing	7,28
(3 3 0 21) - Transmitter - Failure Mask-ing	7,28
(3 5 0 6) - Transmitter - Failure Masking	7,28
(3 6 0 14) - Transmitter - Failure Mask-ing	7,28
(3 6 0 15) - Transmitter - Failure Mask-ing	7,28
(3 8 0 23) - Transmitter - Failure Mask-ing	7,28
(3 13 0 12) - Transmitter - Failure Masking	7,28
(3 15 0 18) - Transmitter - Failure Masking	7,28
(3 16 0 18) - Transmitter - Failure Masking	7,28
(3 16 0 21) - Transmitter - Failure Masking	7,28
(3 19 0 5) - Transmitter - Failure Mask-ing	7,28
(3 24 0 6) - Transmitter - Failure Mask-ing	7,28
(1 9 0 1) - Add Drop Filter - Self Alarmed	6,07
(0 2 1 0) - Multiplexer - Passive	4,55
(0 3 1 0) - Multiplexer - Passive	4,55
(0 8 1 0) - Multiplexer - Passive	4,55
(0 13 1 0) - Multiplexer - Passive	4,55
(0 15 1 0) - Multiplexer - Passive	4,55
(1 7 0 1) - Add Drop Filter - Self Alarmed	4,25
(1 10 0 1) - Add Drop Filter - Self Alarmed	4,25
(1 11 0 1) - Add Drop Filter - Self Alarmed	4,25

Source: Authors

In Figure 9, ERV for each network element was estimated in a risk zone between 4,5 and 9,1. The Multiplexer located in topology notation (0 6 1 0) has the highest risk value and probably will receive redundancy. All the priority levels of the elements are shown and the decision on redundancy is supported by the *ASP* model.

Figure 10 shows the risk related to ADF network element category in USnation scenario. Simulation results indicated that *ASP* model identified ADFs with different risk values in the network topology. Managers can evaluate topology, channels and nodes distribution to identify possible alarms sources, that could have influenced each element risk estimative. Observation of ADF risk zone (interval between 2,4 and 6) can show 11 ADFs with risk value 2,4 and 8 ADFs with a higher risk value. Managers can analyze this information and ADF nodes location to support decision-making process. Other useful information that can be generated by the *ASP* model for managers is the risk value related to each element category, as a complementary support for decision-making.

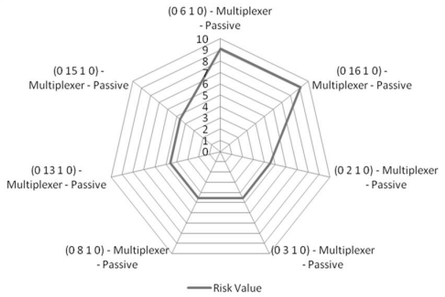

Figure 9. Risks related to the Multiplexer category - Usnation scenario
Source: Authors

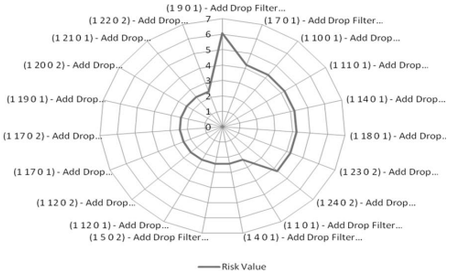

Figure 10. Risks related to ADF element category.
Source: Authors

Second Simulation Scenario

In *ER_NET* scenario, the *ERV* for each network element was estimated in a risk zone between 0,5 and 10,2 (Figure 11). The *Multiplexer* located in topology notation (0 22 1 0) has the highest risk value and is likely to receive redundancy. All the priority levels of the element are shown, and redundancy decision is supported by the *ASP* model. The network elements with the lowest identified risk belong to *Regenerators* and *Receivers* categories. At any time, managers can access the complete ranking list if they need to evaluate each element location, for possible decision making.

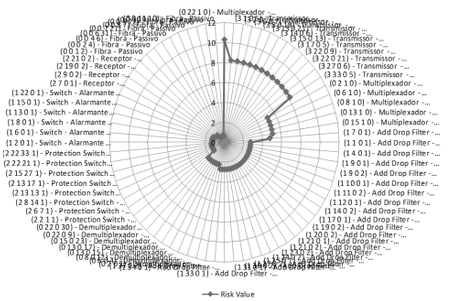

Figure 11. *ER_NET* scenario risk zone.
Source: Authors

Table 2 shows the first 24 elements in risk ranking. As previously stated, *ERVs* for network elements are estimated by the *ASP* model, influenced by network topology, channels and business impact. The risk related to Multiplexers, Transmitters and ADFs is distributed in different positions of the ranking, probably due to differences in their location in topology, number of channels that pass through it, and their degree of business relevance.

Table 2. Network elements risk ranking - second scenario

Network Element	Risk Value
(0 22 1 0) - Multiplexer – Passive	10,28
(3 1 0 5) - Transmitter - Failure Masking	8,23
(3 2 0 7) - Transmitter - Failure Masking	8,23
(3 6 0 7) - Transmitter - Failure Masking	8,23
(3 8 0 19) - Transmitter - Failure Masking	8,23
(3 13 0 21) - Transmitter - Failure Masking	8,23
(3 14 0 6) - Transmitter - Failure Masking	8,23
(3 15 0 13) - Transmitter - Failure Masking	8,23
(3 17 0 5) - Transmitter - Failure Masking	8,23
(3 22 0 9) - Transmitter - Failure Masking	8,23
(3 22 0 21) - Transmitter - Failure Masking	8,23
(3 27 0 6) - Transmitter - Failure Masking	8,23
(3 33 0 5) - Transmitter - Failure Masking	8,23
(0 2 1 0) - Multiplexer – Passive	5,14
(0 6 1 0) - Multiplexer – Passive	5,14
(0 8 1 0) - Multiplexer – Passive	5,14
(0 13 1 0) - Multiplexer – Passive	5,14
(0 15 1 0) - Multiplexer – Passive	5,14
(1 7 0 1) - Add Drop Filter - Self Alarmed	4,80
(1 1 0 1) - Add Drop Filter - Self Alarmed	2,74
(1 4 0 1) - Add Drop Filter - Self Alarmed	2,74
(1 9 0 1) - Add Drop Filter - Self Alarmed	2,74
(1 9 0 2) - Add Drop Filter - Self Alarmed	2,74
(1 10 0 1) - Add Drop Filter - Self Alarmed	2,74

Source: Authors

Multiplexer of node 22 has the highest risk value in relation to other multiplexers in the topology, due to the greater number of channels passing through it, which can concatenate a larger alarms number, in case of failure (Figure 12).

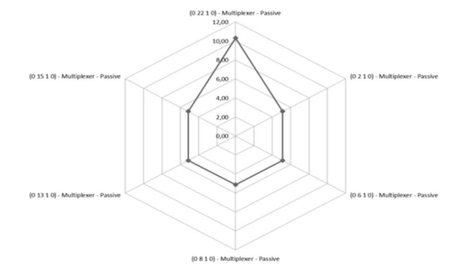

Figure 12. Risks related to Multiplexer category - ER_NET scenario.
Source: Authors

Conclusion and future work

This paper presented a model to assist managers in the process of identifying critical points in optical networks.

This model is different from competing models, because managers can use a business view to identify optical networks redundancy points. It aims to aid in the decision-making process in fault management activities, considering the risk impact. It is not intrusive and can be used in addition to *incident management* and *fault management* supporting tools. The contribution of this work lies in the model itself, which can mitigate risks in optical network incident management, facilitating the managers' work in fault management activities.

Based on the outputs generated by the model, managers obtain a risk ranking, where they can quickly and assertively identify the critical points that can be applied to establish redundancy in an optical network.

Results of the case study indicated that the identification of critical points, in an optical network from a risk perspective, allows managers to define more effective redundancy points in the network, as well as to justify the adoption of actions that can mitigate risks, thus contributing to a more effective service management process.

A face validity exercise (Runerson and Host, 2009) was conducted and results indicated that the model is useful, preferable, complete and effective. In order to elicit managers' opinions about *ASP* model and the associated tool, the model usage was evaluated by 6 network managers and 11 IT managers, who were asked to answer a questionnaire. The model was presented to them, as well as the results of the simulations. Four hypotheses regarding the utility, preference, completeness and efficiency of the proposed model were analyzed. Additional insights were gathered, through talks with managers. The negative hypotheses were refuted in a face validity exercise (Runerson and Host, 2009). A binomial statistical test (Casella and Berger, 2002) with 5% significance was used to produce the results shown in Table 3**.** We can claim face validity of the model. However, full validation is an activity that requires many years and several repetitions.

Table 3. Hypotheses to test face validity

Hypotheses	% who believe	Is there sufficient statistical evidence to support the hypothesis?
Preference: managers preferred the presented model in relation to the current form of identification of redundant points in optical networks.	94	Yes
Utility: Managers considered the model useful.	100	Yes
Completeness: Managers considered the model complete in relation to its objectives.	88	Yes
Efficiency: Managers considered the model effective for the management of optical networks.	94	Yes

Source: Authors

As a threat to validity, the single case study and the short periods of observation imply deficiency in statistical significance of conclusions. On the other hand, the hypotheses that were tested used data from 17 managers and were reported with a 95% confidence level and the scenarios simulations were statistically validated by *ASP* software. There is no threat here. There is always doubt that inputs metrics are well understood by the managers (in relation to construct validity) and this subjectivity leads to a threat: one may not be obtaining the outputs that match reality.

As a future work, we intend to customize the proposed model to simulate next generation optical networks and their business scenarios, with the use of financial values in the estimation of impact and proceed a comparative study with this work results. To consider sensitivity of results on business impact estimative is another research thread.

References

Benhcine, T., Elbiaze, H. and Idoudi, K. (2013). *Fast Reroute-based network resiliency experimental investigations*. Paper presented at the 15th International Conference on Transparent Optical Networks (ICTON), Cartagena SP, IEEE, Universidad Politécnica de Cartagena. DOI: 10.1109/ICTON.2013.6603065

Bloomfield, R. E., Popov, P., Salako, K., Stankovic, V. and Wright, D. (2017). Preliminary Interdependency Analysis: An Approach to Support Critical-Infrastructure Risk-Assessment. *Reliability Engineering and System Safety*, *167*, 198-217. DOI: 10.1016/j.ress.2017.05.030

Casella, G. and Berger, R. L. (2002). *Statistical Inference* (2nd Ed.). California: Duxbury Advanced Series.

Da Silva, C. and Fagotto, E. A. M. (2014). *Diagnóstico e tratamento de incidentes na rede de computadores*. Paper presented at the 11th International Conference on Information Systems and Technology Management, Shangai, CONTECSI.

Fabre, E., Benveniste, A., Haar, S., Jard, C. and Aghasaryan, A. (2004). *Algorithms for Distributed Fault Management in Telecommunications Networks*. Paper presented at the 11th International Conference on Telecommunicatons (ICT'2004), Fortaleza, BR, IEEE. DOI: 10.1007/978-3-540-27824-5_108

Fen, Z., Yanqin, Z. and Li, C. (2016). *Research on Metro Intelligent Optical Network Planning and Optimization*. Paper presented at the15th International Conference on Optical Communications and Networks (ICOCN), Hangzhou, IEEE Photonics Society. DOI: 10.1109/ICOCN.2016.7875735

Gómez, J. M., Mora, M., Gewald, H., Nebel, W. and O'Connor, R. V. (2017). *Engineering and Management of Data Centers: An IT Service Management Approach*. New York: Springer International Publishing AG. DOI: 10.1007/978-3-319-65082-1

Hanemann, A., Sailer, M. and Schmitz, D. (2004). *Assured Service Quality by Improved Fault Management*, Paper presented at the 2nd international conference on Service oriented computing - ICSOC'04, New York, ACM

SIGSOFT, ACM SIGWEB, and University of Trento. DOI: 10.1145/ 1035167.1035194

Homma, M. and Shinomiya, N. (2016). Finding Tie-sets with the Minimal Number of Total Elements for Effective Failure Recovery. Paper presented at the 7th International Conference on Computing Communication and Networking Technologies, Dallas TX, IEEE. DOI: 10.1145/2967878.2967888

ITU-T. (1995). Rec. M3100. Generic Network Information Model. Geneva: International Telecommunication Union, Telecommunication Standardization Sector. Retrieved from: https://www.itu.int/rec/dologin.asp?lang=e&id=T-REC-M.Imp3100-200008-S!!MSW-E&type=items

Lehr, G., Dassow, H., Zeffler, P., Gladisch, A. and Hanik, N. (1998). Management of All-Optical WDM Networks: First results of European research project MOON. Paper presented at the NOMS 98 -1998 IEEE Network Operations and Management Symposium, New Orleans, LA, IEEE. DOI: 10.1109/NOMS.1998.655229

Li-Xia, L. and Yue-Jin, Z. (2014). *Design of a New EPON Connection Automatic Protection System*, Paper presented at Ninth International Conference on P2P, Parallel, Grid, Cloud and Internet Computing, Guangdong, China, IEEE. DOI: 10.1109/3PGCIC.2014.121

Lu, K., Yahyapoura, R., Wieder, P., Yaquba, E., Abdullah, M., Schloer, B. and Kotsokalis, C. (2016). Fault-tolerant Service Level Agreement lifecycle management in clouds using actor system, *Future Generation Computer Systems 54*, 247-259. DOI: 10.1016/j.future.2015.03.016

Maltz, A., Yuan, L., Zhang, M., Wu, X., Turner, D. J. and Chen, C. (2015). *Automated datacenter network failure mitigation*, U.S. Patent No. 9,025,434. Washington, D C.: U.S. Patent and Trademark Office.

Mas, C. and Thiran, P. (2000). An Efficient Algorithm for Locating Soft and Hard Failures in WDM Networks. *IEEE Journal on Selected Areas in Communications*, *18*(10), 1900-1911. DOI: 10.1109/49.887911

Mas, C., Krauß, S. and Casier, K. (2011). *Fault Management and Service Provisioning Process Model of Next Generation Access Networks*. Paper presented at the 7th International Conference on Network and Service Management (CNSM), Paris, IEEE

Mas, C., Thiran, P. and Le Boudec, J. Y. (1999). Fault location at the WDM Layer. *Photonic Network Communication, 1*(3), 235-255. DOI: 10.1023/A:1010063713383

Mas., C., Tomkos, I. and Tomguz, O. K. (2005). Failure location algorithm for transparent optical networks. *IEEE Journal on Selected Areas in Communications*, *23*(8), 1508-1519. DOI: 10.1109/JSAC.2005.852182

Meira, M. and Nogueira, J. M. S. (2000). *A Recursive Approach for Alarm Correlation in Telecommunication Networks*. Paper presented at the IFIP/IEEE Network Operations and Management Symposium (NOMS 2000), Honolulu, IEEE. DOI: 10.1109/NOMS.2000.830469

OGC-Office of Government Commerce. (2007). ITIL v3 (Information Technology Infrastructure Library). London: TSO.

Oliveira, E. W., Brito, A. E. M. and Brasileiro, F. V. (2003). Projeto e Implementação de um Serviço de Detecção de Falhas Perfeito. Paper presented at the XXI Simpósio Brasileiro de Redes de Computadores, Natal, RN, Sociedade Brasileira de Computação and Laboratório Nacional de Redes de Computadores. Retrieved from: http://ce-resd.facom.ufms.br/sbrc/2003/044.pdf

Ramaswami, R and Sivarajan, K. N. (2001). Optical Networks – A Practical Perspective (2nd Ed.). San Francisco CA: Morgan Kaufmann.

Rodríguez-García, A., Ramírez-López, L. and Travieso-Torres, J. C. (2015). New heuristic algorithm for dynamic traffic in WDM optical networks. *Ingeniería e Investigación*, *35*(3), 100-106. DOI: 10.15446/ing.investig.v35n3.51676

Rowe, G. and Wright, G. (1997). The Delphi technique as a forecasting tool: issues and analysis, International Journal of Forecasting, *15*(4), 353-375. DOI: 10.1016/S0169-2070(99)00018-7

Runerson, P. and Host, M. (2009). Guidelines for conducting and reporting case study research in software engineering. *Empirical Software Engineering, 14*, 131-164. DOI: 10.1007/s10664-008-9102-8

Sergio, M. C., De Souza, J. A. and Gonçalves, A.L. (2017). Idea Identification Model to Support Decision Making. *IEEE Latin America Transactions*, *15*(5), 968-973. DOI: 10.1109/TLA.2017.7912594

Smith, P., Hutchison, D., Sterbenz, J. P. G., Scholler, M., Fessi, A., Karaliopoulos, M., Lac, C., Plattner, B. (2011). Network resilience: a systematic approach. *IEEE Communications Magazine, 49*(7), 88-97. DOI: 10.1109/MCOM.2011.5936160

Sousa, B., Delfino, C., De Sousa, JN. and Everardo J. (2005). *An Algorithm for Fault Location, in SDH/WDM Networks*. Paper presented at the 12th International Conference on Telecommunicatons (ICT'2005), Institute of Electrical and Electronics Engineers

Specialski, S. (2018). Gerencia de Redes de Computadores e de Telecomunicações, white paper. Florianópolis: Universidade de Santa Catarina. Retrieved from: http://cassio.orgfree.com/disciplinas/gredes/ApostilaGerenciamento.pdf.

Stein, K. U. (1999). Redundancy-optimized communication network for the transmission of communication signals, U.S. Patent No. 5, 946, 294. Washington, D C.: U.S. Patent and Trademark Office

Sterbenz, J. P. G., Hutchison, D., Çetinkaya, E. K., Jabbar, A., Rohrer, J. P., Schöller, M., Smith, P. (2010). Resilience and survivability in communication networks: Strategies, principles, and survey of disciplines. *Computer Networks 54*(8), 1245-1265. DOI: 10.1016/j.comnet.2010.03.005

Yin, R. K. (2018). Case Sudy Research and Applications. Design and Methods (6th Ed.). Los Angeles CA: SAGE Publications.

Ingeniería e Investigación vol. 39 No. 1, April - 2019 (53-62)

DOI: http://dx.doi.org/10.15446/ing.investig.v39n1.72402

Procedure for the continuous improvement of human resource management

Procedimiento para la mejora continua de la gestión de recursos humanos

Germán Gemar[1], Ana M. Negrón-González[2], Carlos J. Lozano-Piedrahita[3], Vanesa F. Guzmán-Parra[4], and Norberto Rosado[5]

ABSTRACT

The hotel sector in the historic center of Havana reveals deficiencies in customer satisfaction regarding human resource. This research is aimed at analyzing the results of the implementation of a continuous improvement of human resource management that allows the enhancement of services quality, assuming the Cuban norm. The main results show that 55 % of the items identified with the application of the SERVQUAL model show quality deficit associated with processes of human resource management, such as work competences and work organization. The main dysfunctions identified were unproductive times due to organizational and technical issues and labor fluctuation. Subsequently, hidden costs due to deficiencies were calculated, which amount to a value of 13 249,89 MU/year. To monitor these problems, objectives and indicators are proposed through the Integral Command Table, as well as a plan of corrective and preventive actions.

Keywords: Hidden cost, Process, Dysfunctions, Indicators.

RESUMEN

El sector hotelero en el centro histórico de La Habana revela deficiencias de satisfacción del cliente en relación con los recursos humanos. Esta investigación tiene como objetivo analizar los resultados de la implementación de una mejora continua de la gestión de los recursos humanos que permite mejorar la calidad de los servicios, asumiendo la norma cubana. Los principales resultados muestran que el 55 % de los ítems identificados con la aplicación del modelo SERVQUAL reflejan un déficit de calidad asociado a los procesos de gestión de recursos humanos, como las competencias laborales y la organización del trabajo. Las principales deficiencias encontradas son los tiempos improductivos debido a problemas técnicos y organizacionales y la fluctuación laboral. Posteriormente, se calcularon los costos ocultos generados por los disfuncionamientos existentes, los cuáles ascienden a un valor de 13 249,89 MU/año. Para monitorear estos problemas, los objetivos e indicadores se proponen a través de la Tabla de Comando Integral, así como un plan de acciones correctivas y preventivas.

Palabras clave: Costo oculto, Proceso, Disfunciones, Indicadores.

Received: June 1st, 2018
Accepted: April 2nd, 2019

Introduction

Management encompasses several functions: planning, organizing, conducting or directing, and controlling an organization (Agrawal, 2011). This element is essential, and it is precisely where the competitive advantage of companies in the management of human resource (HR) lies. That is why, man is related as the main asset and strategic advantage of an organization and terms, such as human capital, are introduced.

In many modern companies, human resource are the most valuable assets, as they provide necessary knowledge to transform raw materials into finished products (García-Alcaraz, Adarme-Jaimes, and Blanco-Fernández, 2016). Employee flexibility is a success factor for current organizations that contributes to improve both operational results (e.g. work productivity, customer satisfaction, etc.) and financial performance of companies (Beltrán Martín, Escrig Tena, Bou Llusar, and Roca Puig, 2013).

[1]Ph.D. in Economics and Business Administration, Universidad de Málaga, España. Affiliation: Professsor of Economics and Business Administration, Universidad de Málaga, España. E-mail: ggemar@uma.es.
[2]M.Sc. in Human Resource Management, Universidad Tecnológica de La Habana "José Antonio Echevarría", Cuba. Affiliation: Ph.D. Student. Ph.D. Program in Economics and Business, Universidad de Málaga, España. E-mail: anamarianegrong@uma.es/gmail.com.
[3]M.Sc. in Health and Safety at Work, Universidad Nacional de Colombia-Campus Bogotá. Affiliation: Professor. Universidad Nacional de Colombia-Campus Bogotá. M.Sc. in Integrated Management Systems. Universidad Internacional de la Rioja, España E-mail: cjlozanop@unal.edu.co/gmail.com.
[4]Ph.D. in Economics and Business, Universidad de Málaga, España. Affiliation: Professsor of Economics and Business Science, Universidad de Málaga, España. E-mail: vgp@uma.es.
[5]M.Sc. in Human Resource Management, Universidad Tecnológica de La Habana "José Antonio Echevarría", Cuba. Affiliation: Specialist in Human Resource Management, CITMATEL, La Habana, Cuba, E-mail: norberosado@nauta.cu.

How to cite: Gemar, G., Negrón-González, A. M., Lozano-Piedrahita, C. J., Guzmán-Parra, V. F., and Rosado, N. (2019). Procedure for the continuous improvement of human resource management. *Ingeniería e Investigación*, *39*(1), 53-62 DOI: 10.15446/ing.investig.v39n1.72402

Human Capital Management responds to the needs of the business through the integration system of recruitment, learning, performance and succession planning. Most organizations manually managed human capital through competencies, models, specific curricula, multi-evaluators, and prescriptive approaches that led human resource to be increasingly strategic (Boon, Eckardt, Lepak, and Boselie, 2018; Nieves and Quintana, 2016).

Although there is no universal agreement regarding the definitions of Human Resource Development (HRD) and Human Resource Management (HRM), it is generally accepted that HRM often emphasizes policy, staffing, HR-related information technology, compensation, and other policy-related issues. HRD is usually described as development, learning, and performance focused at individual, group, organization, and larger system levels (Blackman, Moscardo, and Gray, 2016).

In Cuba, Human Resource Management has been extensively researched. Thus, since 2005 an integrated model of human resource and knowledge, which in turn integrated the organizational strategy, with a technology for its practical application, encompassing, among other things, the Strategic Control (Cuesta, 2012). Subsequently, the Cuban Model Management of Human Capital (MMHC) emerged, designed by Alfredo Morales, where self-control as a control process is envisaged towards the continuous improvement of human resource management. The process of designing and implementing this system, contextualized to each Cuban organization, has required the application of technologies that contribute to increase its effectiveness (Hernández, Fleitas, and Salazar, 2010; Negrón González et al., 2018).

The tourism sector in Cuba has a great impact because of its relevance in economic and social development due to the accelerated pace in the growth of hotel management systems. The process of self-control is able to establish the improvement in the management of its human capital in a systematic way, as well as to develop the evaluation and control of its functioning (González-Alvarez, Torres-Estévez, Pérez-DeArmas, and Varela-Izquierdo, 2012).

The main objective of the hotel sector in the historic center of Havana is to contribute to the restoration of the historical area and the welfare of the community. The application of this research includes three hotels of that company. Interviews to staffs and executives, and direct observation at job stations were conducted, as well as the analysis of documents related to human resource management and economic management, such as financial accounting records and economic balances of the last 5 years. As a result, the following has been identified:

- Existence of expenses associated with the management of human resource that are not considered in the accounting records. This entails the falsification of the information, and infringes its veracity and the maximum use of the reserves of productivity.
- 70% of the survey respondents stated that all costs associated with human resource are not taken into account on the economic balance. They only focus on salary expenses and on safety and work health management.
- Unproductive times of inactivity are not quantified, which leads to a decrease in work productivity.

Based on this situation, the research problem has been stated as follows: the lack of a systematic evaluation of the human resource management in the hotels limits the outreach of better results in the personnel performance, which directly affects the quality of the service and, consequently, customer satisfaction.

In order to solve the problem, the following objective is proposed: to analyze the results of the implementation of a procedure for the continuous improvement of human resource management that allows an upgrading in the quality of services.

The scientific novelty is given by the evaluation based on a procedure for the continuous improvement of human resource management with the integration of social and economic elements, as well as the way of identifying the dysfunctions associated to them and the quantification of the hidden costs from the existing ones.

Literature Review

The traditional management of personnel aims to understand the human component as a key element in organizational success. In this way, the traditional conception of the function begins to undergo important changes, where the interest is concentrated on the strategic value of the human resource and its management systems. Thus, a more proactive role is given to the function, planning and deciding in the long term. This implies a change in both the vision of the management teams and the functions performed by the human resource managers (García Carbonell, Martín Alcázar, and Sánchez Gardey, 2014).

Human capital is one of the interest groups that companies must support, promoting their professional and personal development, since they are the basis of business growth and market positioning. Besides, employees are the best publicists of the organization (López Salazar, Ojeda Hidalgo, and Ríos Manríquez, 2017).

The Human Resource (HR) function in the organizations has had a long history, which has evolved through a series of different stages. From a mere record-keeping function to one of strategic importance and its impact has ranged from reputation of human resource to its effectiveness (Ferris et al., 2007). This is important for organizational or HR leaders driving the incorporation of analytical methods to consider the purpose behind these efforts (King, 2016).

The reality is that the context of Human Resource Development exists in the interplay of individuals, organizations, and national forces in all countries (Alagaraja and Githens, 2016), particularly linked to human resource management in the enterprise. Contemporary scientific literature highlights

the achievement of a high sense of employee commitment to the organization, considering both the humanist component, as the person gets socially involved to the community, and the economic component, as it is associated with the increase in labor productivity or high performance (Cuesta, 2015). However, it is also recognized that employees become more responsible, more careful and work better when they feel appreciated, thereby increasing productivity (Blaga and Jozsef, 2014).

In studies conducted, for example, in Romania, human resource is highlighted as a determinant factor of sustainable development and how it impacts on their quality, taking into account the deprofessionalization of human resource due to its excessive turnover, among others (Chitescu and Lixandru, 2016).

The uniform vision to approach the management of HR, and more specifically high-performance practices, can be hiding a reality that suggests that different HR practices may coexist. Thus, various authors warn about the necessity of considering this fact, in order to avoid falling in a too simplistic vision of HRM (Melián González and Verano Tacoronte, 2008).

In Cuba, the Labor and Social Security Ministry developed a research that covered from 2003 to 2005 and analyzed more than 3 000 organizations. This research states that only 13 % of the organizations had strategic orientation when measuring the level of strategic integration of the human resource management in the company. As a result of this research, a model was designed and taken as reference to make the proposal of the Cuban model for the design and implementation of Management of Human Capital, proposed by the Cuban Norm of the 3 000 group (Hernández et al., 2010).

One of the essential processes in this model is self-monitoring, which is aimed at monitoring, verifying, evaluating and influencing the results of the most related key organizational indicators to the use of Human Capital and Human Capital Management Processes on time. Self-monitoring takes advantage of improvement opportunities and acts on the problems and deviations detected.

In the analysis of the research conducted in 2016 on Human Capital Measurement Models, the internal audit of the human resource management system is only oriented at selection processes, work organization, and evaluation and education processes (Sotolongo, 2005).

After the establishment of the Cuban Norms (CN) 3000-3002 (2007), Nieves and Quintana (2016) state that self-control is the monitoring and regulator component of internal control and they limited their research only to the processes of selection, evaluation, stimulation and labor competencies. Meanwhile Comas (2013) shows the management control from the strategic alignment and conceives the process of human capital management as the one responsible for ensuring, controlling and evaluating human resource.

Additionally, there are socioeconomic researches that propose how to improve the performance associated with the management of the human resource in a company from the strategic point of view and not only with the control. Purposely, they incorporate the hidden costs that come from dysfunctions.

The hidden costs associated with the existing malfunctions are defined as the difference between the desired operation and the actual operation, which are not identified in the company's information systems (budget, general and analytical accounting, driving board) (Savall, 2011). Moreover, their identification has also been limited to six fields, such as: working conditions, work organization, communication, coordination, time management, integrated training and on-going strategic implementation (Pereda and Berrocal, 2005).

Bampoky (2012) states that indicators for grouping hidden costs that are based on absenteeism, work accidents, staff turnover, non-quality and lack of productivity will allow to improve the internal processes of the company, taking into account that it is important to know not only the total cost of a product or service, but also other elements that have a negative impact on the value chain and escape from the traditional methods and tools of management control.

The effectiveness of human resource management is certainly associated with the human capital investment and also with the strategic cost minimization. Vardarlier (2016) indicated that there are also researches on the use of technology to facilitate human resource processes. This typically improves efficiency, and lowers the costs associated with human resource transactions (Stone and Deadrick, 2015). It also analyzes the relationship of the employees' perceptions of the human resource management system and how this affects organizational outcomes through motivation and attitude (García Carbonell et al., 2014).

An essential tool used in this research to relate the results of its application to the existing malfunctions in human resource management is the SERVQUAL model, which is leaded by Parasuraman, Berry and Zeithaml (1985, 1988). Its main influence has been in practice. From its representative, the SERVQUAL, main contribution of this school, defines the quality of the service as the difference between the actual clients' perceptions of the service and their previous expectations about it. In this sense, a client values negatively / positively the quality of a service in which the perceptions that he/she have obtained are lower / higher than the expectations he/she had. Therefore, service companies where one of their objectives is the differentiation through a qualitative service must pay special attention to exceed the expectations of their customers (Matsumoto Nishizawa, 2014; Pan, 2013).

Each of these factors or dimensions, as they are called in the SERVQUAL model, is subdivided into other sub-dimensions that will affect the customer's perception. These subdivisions originate the 22 questions of the SERVQUAL questionnaire, which refer to the most important aspects of each dimension that define the quality of service of the quality provider.

Methodology

This research is based on the implementation of a procedure for the continuous improvement of human resource management that allows an upgrading in the quality of service. This procedure provides the new processes of the Cuban Human Capital Management Model. It also shows the steps to identify the dysfunctions and quantify the hidden costs associated with these processes, as well as indicators to monitor them. This procedure is shown in Figure 1.

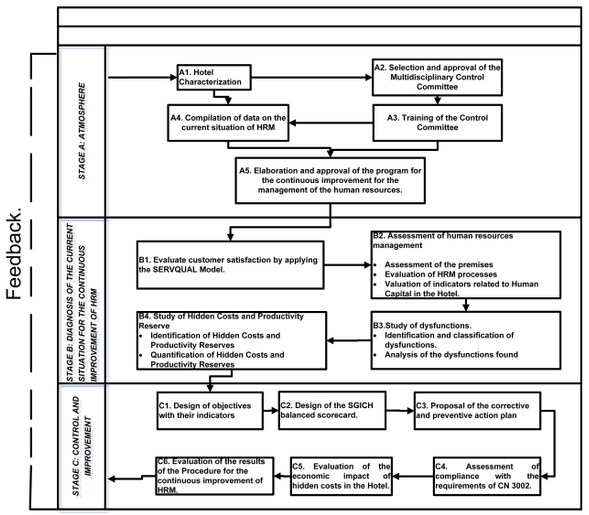

Figure 1. Procedure for continuous improvement of human resource management.
Source: Authors

The procedure consists of the following stages: i) atmosphere, ii) diagnosis of the current situation for the continuous improvement of HRM and iii) control and improvement. Each of them is integrated by diverse activities that allow the feedback between the distinct stages.

The objective of the procedure is:

To achieve continuous improvement of HRM processes to raise organizational performance and produce goods and services that meet customers' needs through a higher job performance and an increase in work productivity.

Results

This procedure was applied in the three hotels of that company. This article presents the results obtained in one of them.

Stage A. Atmosphere: The Hotel Management of the company is in charge of developing the strategy to be followed by the administration of the hotels for tourism, which are located in the historic center.

A1. Characterization of the Hotel: In this first phase, a brief characterization of the Hotel is carried out. The general objectives of the company and of the Hotel, both tactical and strategic, are enunciated. It reflects the mission, vision, processes and services provided by the Hotel areas, the main customers and suppliers that the facility has, It also includes the analysis of the SWOT matrix.

A2. Selection and approval of the Multidisciplinary Control Committee (CCM): The work team in charge of implementing the process of continuous improvement for human resource management is composed of managers of the different areas of the Hotel, i.e. the General Manager, Public Relations, Commercial Manager, Manager of technical services and the management in charge of Human Resource.

A3. Training of the Multidisciplinary Control Committee for the continuous improvement of the human resource management: For the training of the Committee of Multidisciplinary Control (CCM), a diagnosis of the level of knowledge is made to its 10 members, through a survey designed for expert skills. A total of 7 experts in the subject are selected, categorized as High experts for having a competence coefficient superior to 0,8 ($0{,}8 \leq K \leq 1$). The average competence coefficient of the selected experts was of 0,79.

For the staff who resulted to be not experts in the subject, it is proposed to carry out a training on business development, socio-economic management, and HRM. This training is planned using Microsoft Project, which lists all the activities of training, with a total duration of 26 days.

A4. Compilation of information about the state of HRM at the Hotel: It includes labor legislation in force, procedures and records of human resource management existing in the organization and human resource accounting statements, in order to carry out the collection of the information. The Documentary Analysis Guide for the compilation of information is used.

A5. Elaboration and approval of the program for the continuous improvement for the human resource management. In the current phase, the improvement program is made. The following aspects are taken into account for the implementation: name of the stage, objectives, and tools used, start date and completion date, as well as the name of the center, object of the self-control, the period to be evaluated and the organization to which it belongs.

Stage B: Diagnosis of the current situation for the realization of the continuous improvement of HRM.

B1. Evaluate customer satisfaction by applying the SERVQUAL model: In this phase, the customer satisfaction level is analyzed through the application of the SERVQUAL model. The quality evaluation of the services offered by the hotel is obtained according to the expectations and perception of the client. In addition, it is known which items related to human resource management influence directly and negatively external customer satisfaction. It can be seen in Figure 2.

When obtaining the overall assessment of service quality and the evaluation of the five dimensions analyzed, the following is concluded.

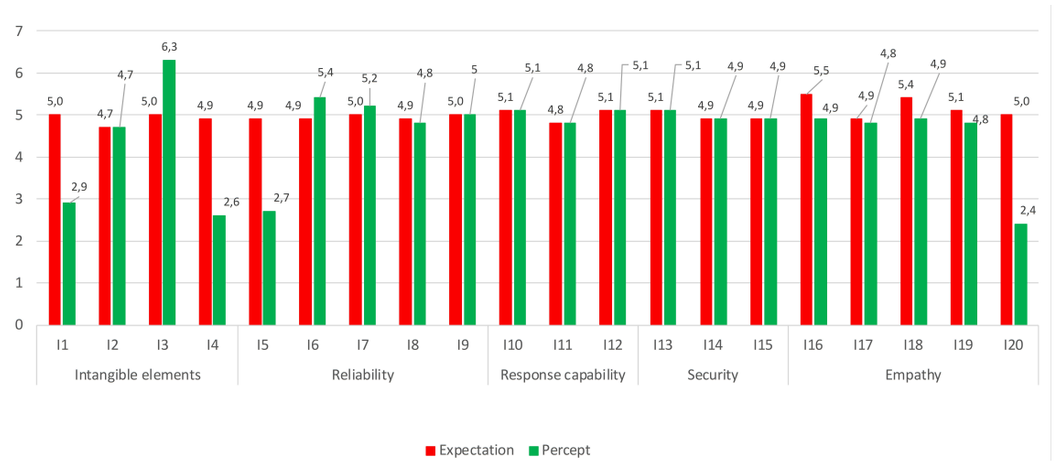

Figure 2. Comparison between expectation and perception.
Source: Authors

There is a quality deficit in the following items:

- Item 1: The service company has equipment of modern appearance (Tangible Elements).
- Item 4: Material elements (brochures, statements, etc.) are visually attractive (Tangible Elements).
- Item 5: When the service company promises to do something in a timeframe, it does it (Reliability).
- Item 17: Employees have sufficient knowledge to answer customer questions. (Security), Item 22: The service company understands the specific needs of its customers (Empathy).

The items assessed by clients as deficient are directly related to the human resource management. Those correspond to: "When the service company promises to do something in a certain time, it does it"; "Employees have sufficient knowledge to respond to Customer questions"; and "The service company understands the specific needs of its customers". These statements are specifically associated with labor competencies, as there are deficiencies in the training and evaluation of the performance of Hotel staff as well as in the organization of the work, which has a direct impact on the quality of service and, therefore, on customer satisfaction.

Evaluation of HRM.

In this phase, assessment of the state of strategic integration that exists in the organization towards human resource management is made. For this effect, three essential points are analyzed: Premises evaluation, evaluation of HRM processes and evaluation of the related indicators to human capital in the Hotel.

B2. Assessment of human resource management

Evaluation of premises: For the implementation of the evaluation of premises, the checklist is applied, showing compliance in 81,8 % of the dissimilar elements that compose it. This proves the lack of a design of HRM in the Hotel. In addition, as the center has established a process map where strategic, key and support processes are defined, the Quality System reflects a process approach. Quality management is done through the evaluation of the ISO 9001 NC and positive results were obtained in the audits carried out to the hotel.

This analysis allows to know the starting point for the realization of continuous improvement.

Evaluation of human resource management processes: After applying the diagnostic and support technologies, the company continues the process of implementation of the Cuban Model for Human Capital Management, by the incorporation of the following modules: Work Competences (WC), Work Organization (WO), Selection and Integration of Human Resource (SIHR), Training and Development (TD), Moral and Material Stimulation (MMS), Occupational Health and Safety Management (OHSM), Working Performance Assessment (WPA), Organizational Communication (OC) and Self-Control.

The previous modules allow to identify the gaps in the management processes. One of the essential techniques used for the human resource audit is the checklist, which facilitates to determine the degree of compliance with the requirements of Cuban Norms 3000: 3002, 2007, focused on human capital. Results can be observed in Figure 3.

Valuation of indicators related to Human Capital in the Hotel: In the present phase, the existing indicators in each specific hotel are analyzed, as well as the hotel's income, correlation of average wage-productivity, labor productivity, implementation of control measures and staff training are evaluated. These indicators are not consistent with the objectives outlined by the Hotel Management for the year 2015.

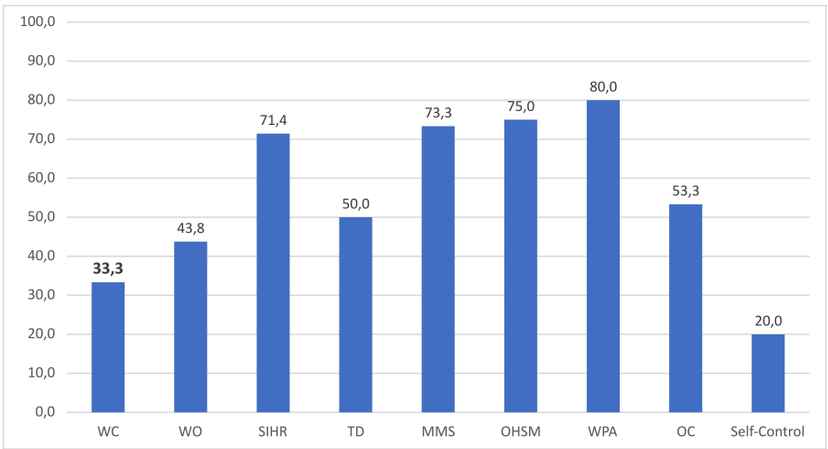

Figure 3. Percentage of Compliance with the requirements of Cuban Norms 3002, 2007.
Source: Authors

B3. Study of dysfunctions.

For the identification of the malfunctions, the checklist is applied. The percentage of the existing malfunctions was obtained by Microsoft Excel, after evaluating the checklist through the requirements established by the CN 3000: 3002, 2007.

Analysis of the dysfunctions found: In Figure 4, the processes with the highest percentage of dysfunctions are those corresponding to Work Competences and Self-Control.

B4. Study of Hidden Costs and Reserve of Productivity.

All the dysfunctions are present, failing to meet numerous requirements such as: The existence of unsuitable workers to occupy their positions, training is not performed focused on the corresponding DNA, incorrect identification of competencies, staff with irrelevant competencies for the position they occupy, the expected results are not achieved by HRM and there is no feedback on the Human Resource Management functioning.

For various problems, such as lack of data, no-documentation of information generated at the Hotel and other causes, it is not possible to quantify most of the malfunctions detected. As a result, the dysfunctions able to be quantified were related to Unproductive times due to technical-organizational problems, underutilization of the results of work studies, poor time management, demotivation and labor fluctuation. This is shown in Table 1 and Table 2.

Stage C. Control and Improvement

C1. Design of objectives and indicators: After making a diagnosis of the main problems associated with HRM, it is crucially important to solve them. For this purpose, a series of objectives and indicators to be fulfilled are proposed to eliminate the detected dysfunctions and to avoid their repetition, as well as to achieve the increase of the percentage of compliance with requirements of CN 3000: 2007.

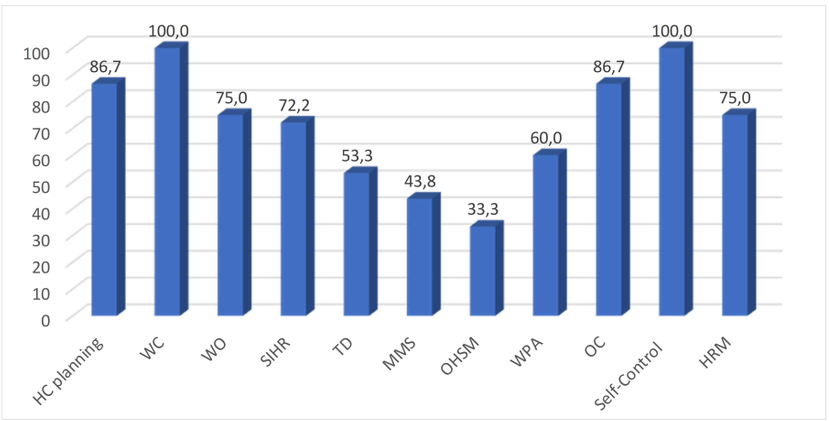

Figure 4. Percentage of existence of dysfunctions by processes.
Source: Authors

Table 1. Identification of Hidden Costs

Dysfunctions	Process	Hidden cost
Unproductive times due to technical-organizational issues	Organization of Work	Non-production
Underutilization of work study results		Over times
Poor time management		
Demotivation	Moral and Material Stimulation	Expenses for absences of workers
Labor Fluctuation	Selection and Integration	Risk

Source: Authors

Table 2. Quantification of Hidden Costs and Productivity Reserves

Process	Dysfunctions	Causes	Classification	Hidden cost
Organization of Work	Technical-organizational issues	Lack of clothing	No-production	3,5h/day*10days/month*11months/year*7,87MU/h=3 030UM/ year
		Work unrelated to task		2h/day*30days/month*11months/year*7,87MU/h=5 194,2UM/year
	Underutilization of work study results	Non-application of the tools proposed in the studies carried out	Over times	8h/day*6days/month*11months/year*1,96MU/hrs =1 034,88 MU/year
	Poor time management	Replacement of the minibar by the waitresses	Over times	0,49h/day*30days/month*11months/year*7,87MU/hrs =1 285,56MU/ year
Subtotal				10 544,61MU/year
Selection and Integration	Labor Fluctuation	Workers who resign after receiving training	Risk	2,5MU/h*150h/year=375MU/year 11,59MU/h-work*192h/year= 2 225,28 MU/year
Subtotal				2 705,28 MU/year
Total				13 249,89 MU/year

Source: Authors

1. General objective: To guarantee compliance with the premises by 95 % for the period 2016-2017.

Specific objectives: Design HRM processes and join business process improvement.

Indicator: The percentage (%) of compliance with the premises.

2. To achieve the satisfaction of external customers by reaching the required quality on HRM related to services provided.

Indicator: Customer satisfaction coefficient.

3. Ensure that 90 % of workers meet the requirements of job suitability and thus achieve excellence in service.

Indicator: Coefficient of suitability shown, coefficient of job satisfaction.

4. To guarantee 98 % of assistance to the services requested by the clients.

5. Indicator: Coefficient of assistance to implement 90 % of the proposed solutions from work organization studies.

Indicator: Coefficient of implementation of work organization studies.

Based on the diagnosis of the current situation of the processes integrated in HRM of the Hotel, it is corroborated that the requirements of NC 3002, 2007 are not met, as well as the existence of dysfunctions in the HRM processes. Hence a design of processes corresponding to Work Competences, Work Organization, Self-Control, Training and Development through process records was developed to diminish the existence of dysfunctions.

C2. Design of the Integral Command Table (ICT)

In order to evaluate the Human Capital Management based on designed processes and indicators, an Integral Command Table was created. Thus, a set of indicators linked to HRM were compilated, through four perspectives: financial, customer, process, and learning. The use of this tool allows visualizing the impact of the evaluation of indicators on the strategic results of the organization. Therefore, it is recommended that it is carried out with a Control Panel, as shown in Figure 5.

C3. Proposal of the corrective and preventive action plan: A set of preventive and corrective actions is designed, in which the actions to be performed, the compliance period and the responsible to meet the proposed objectives are defined. The purpose of the plan is to eradicate the dysfunctions detected.

Discussion

C3. Assessment of compliance with the requirements of CN 3002, 2007: Following the previous design of the sub-processes, the evaluation of compliance with the requirements of CN 3000: 3002, 2007 is carried out again, allowing the comparison of a "Before" and an "After" of the fulfillment of these requirements of the HRM sub-processes. At first sight, there is an increase in the compliance with the mentioned requirements, as shown in Figure 6.

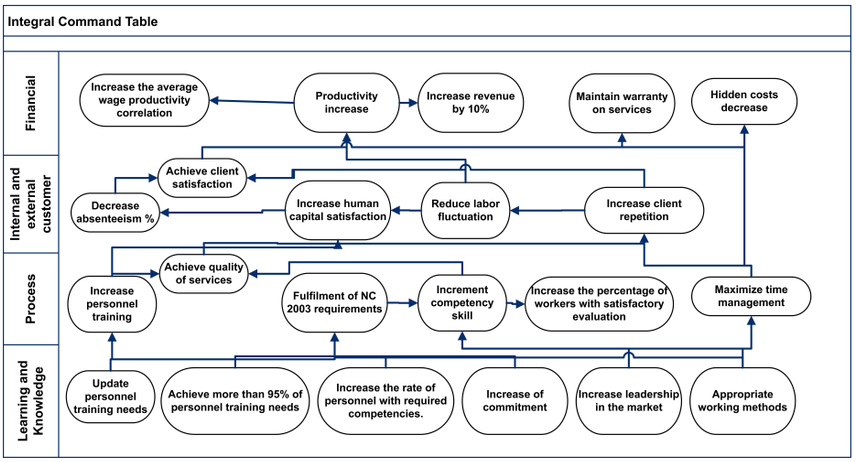

Figure 5. Integral Command Table.
Source: Authors

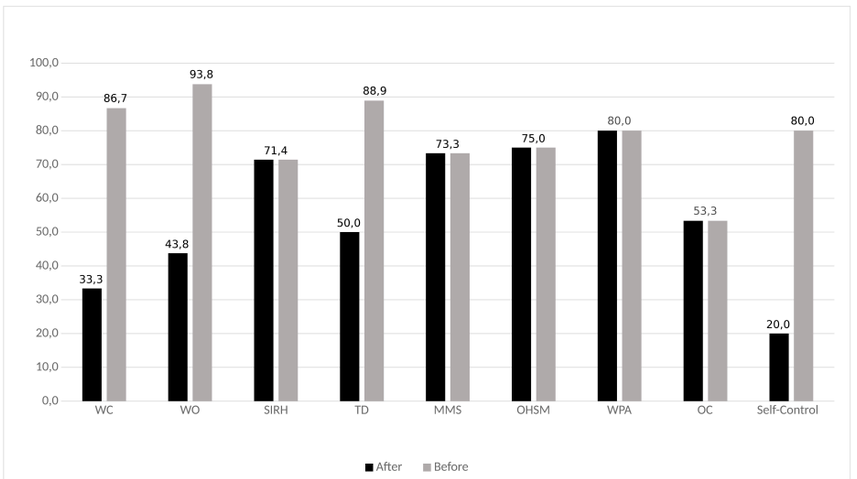

Figure 6. Percentage of compliance with the requirements of the standard after the improvements were applied.
Source: Authors

Figure 6 shows that the compliance with the requirements of CN 3000: 3002, 2007 in Self-Control processes is improved by 60 %, Work Competencies by 53 % and Work organization by 45 %.

C4. Evaluation of the economic impact of hidden costs in the Hotel.

Currently, the hotel quantifies the tangible costs in the Human Capital Management, that is, social security, vacations, etc. However, it does not take into account the hidden costs, which generate an expense of 13 249,89 MU/year due to the detected malfunctions.

Through the diagnosed problems and the proposed solutions, two alternatives are presented:

1. Failure to implement the proposed corrective actions would result in an expenditure of 13 249,89 MU/year.
2. Implementing the proposed corrective actions would enable to improve HRM in the Hotel, increase customer satisfaction, and eliminate the identified malfunctions. That would save hidden costs of 10 544,61 MU/year and an investment of 1 500,00 MU to 3 000,00 MU to acquire the Clothes mount.

After evaluating the cost-benefit relationship, alternative 2 is chosen taking into account its economic impact on the company.

C5. Evaluation of the results of the procedure for the continuous improvement of HRM.

Once the procedure is applied, it is possible to eliminate a series of problems that undermine the proper human resource management, namely, dysfunctions, non-fulfillment of requirements of the family of CN 3002: 2007. Nevertheless, the constant monitoring of the HRM is necessary. A good

practice is to establish comparisons between the periods in which continuous improvement is conducted. Besides, it is also necessary to keep a record of them so that there is a feedback and to avoid thinking that by complying with the proposed corrective measures, these problems cannot emerge in the future.

Results attributed to this research validate the application of the procedure to other hotels in the city, since it promotes the evaluation and rate of the causal relations between dysfunctions and hidden costs, based on statistical tools.

Conclusions

A procedure of three stages is proposed for the continuous improvement of human resource management. It aims to achieve the continuous improvement of human resource management processes to raise organizational results and produce goods and services that meet the needs of customers, through a higher work performance and increased labor productivity.

The procedure for the continuous improvement of human resource management in the Hotel is applied with significant focus on the detection of dysfunctions related to: poor management of time, labor fluctuation and unproductive times due to technical and organizational problems. The hidden costs are quantified in value of 13 249,89 MU/year.

A comparison was made after applying the solutions in compliance with the requirements of the processes of the Cuban model covered by the CN 3000: 3002, 2007. An improvement from the design of the processes corresponding to Work Competences, Organization of Work, Self-control, training and Development was observed in a 53 %, 45 %, 60 % and 31 %, respectively.

This study will be applied in other hotels, emphasizing the specific technical aspects of each human resource process and will lead to a higher qualitative work performance in the continuous improvement of human resource management.

References

Agrawal, D. C. (2011). Management: Implementation of Policies and strategies in the planning process. *Bhartiyam International Journal of Education & Reserch*, *1*(1), 1-8. Retrieved from: http://www.gangainstituteofeducation.com/BhartiyamJournal/ManagementImplementationofPoliciesand.pdf

Alagaraja, M., and Githens, R. P. (2016). Capacity and Capability Building for National HRD. *Human Resource Development Review*, *15*(1), 77-100. DOI: 10.1177/1534484315623908

Bampoky, B. (2012). Les Dysfonctionnements Révélateurs De Coûts Cachés Dans Les Entreprises Sénégalaises: Quelles Perspectives Pour La Maximisation De La Valeur. *Revue Congolaise de Gestion*, *1-2* (15-16), 127-166. DOI: 10.3917/rcg.015.0127

Beltrán Martín, I., Escrig Tena, A. B., Bou Llusar, J. C., and Roca Puig, V. (2013). Influencia de las prácticas de recursos humanos en la flexibilidad de los empleados. *Cuadernos de Economía y Dirección de la Empresa*, *16*(4), 221-237. DOI: 10.1016/j.cede.2012.10.002

Blackman, A., Moscardo, G., and Gray, D. E. (2016). Challenges for the Theory and Practice of Business Coaching. *Human Resource Development Review*, *15*(4), 459-486. DOI: 10.1177/1534484316673177

Blaga, P., and Jozsef, B. (2014). Human resources, quality circles and innovation. *Procedia Economics and Finance*, *15*, 1458-1462. DOI: 10.1016/S2212-5671(14)00611-X

Boon, C., Eckardt, R., Lepak, D. P., and Boselie, P. (2018). Integrating strategic human capital and strategic human resource management. *The International Journal of Human Resource Management*, *29*(1), 34-67. DOI: 10.1080/09585192.2017.1380063

Chitescu, R. I., and Lixandru, M. (2016). The Influence of the Social, Political and Economic Impact on Human Resources, as a Determinant Factor of Sustainable Development. *Procedia Economics and Finance*, *39*, 820-826. DOI: 10.1016/S2212-5671(16)30259-3

Comas, R. (2013). *Integración de herramientas de control de gestión para el alineamiento estratégico en el sistema empresarial cubano. aplicación en empresas de Sancti Spiritus*. (PhD. thesis, Universidad de Matanzas Camilo Cienfuegos). Retrieved from: http://beduniv.reduniv.edu.cu/index.php?page=13&id=1201&db=1

Cuesta, A. (2012). Modelo integrado de gestión humana y del conocimiento: una tecnología de aplicación. *Revista Venezolana de Gerencia*, *17*(53).

Cuesta, A. (2015). Gestión de recursos humanos en la empresa, desempeño y sentido de compromiso. *Revista Brasileira de Gestao de Negócios*, *17*(56), 1134-1148. DOI: 10.7819/rbgn.v17i56.1736

Ferris, G. R., Perrewé, P. L., Ranft, A. L., Zinko, R., Stoner, J. S., Brouer, R. L., and Laird, M. D. (2007). Human resources reputation and effectiveness. *Human Resource Management Review*, *17*(2), 117-130. DOI: 10.1016/j.hrmr.2007.03.003

García-Alcaraz, J. L., Adarme-Jaimes, W., and Blanco-Fernández, J. (2016). Impact of human resources on wine supply chain flexibility, quality, and economic performance. *Ingeniería e Investigación*, *36*(3), 74-81. DOI: 10.15446/ing.investig.v36n3.56091

García Carbonell, N., Martín Alcázar, F., and Sánchez Gardey, G. (2014). El papel moderador de la percepción del sistema de dirección de recursos humanos y su influencia en los resultados organizativos. *Revista Europea de Dirección y Economía de la Empresa*, *23*(3), 137-146. DOI: 10.1016/j.redee.2014.03.002

González-Alvarez, R., Torres-Estévez, G., Pérez-DeArmas, M., and Varela-Izquierdo, N. (2012). Diseño de un procedimiento para realizar el autocontrol del sistema de gestión integrado de capital humano. *Ingeniería Industrial*, *33*(1), 41-49. Retrieved from http://rii.cujae.edu.cu/index.php/revistaind/article/view/354/441

Hernández, I., Fleitas, M. S., and Salazar, D. (2010). Experiencia de gestión del conocimiento para el sistema de gestión integrada de capital humano en empresas cubanas. *Entramado*, 6(2), 12-25.

King, K. G. (2016). Data Analytics in Human Resources. *Human Resource Development Review*, *15*(4), 487-495. DOI: 10.1177/1534484316675818

López Salazar, A., Ojeda Hidalgo, J. F., and Ríos Manríquez, M. (2017). La responsabilidad social empresarial desde la percepción del capital humano. *Estudio de un caso. Revista de Contabilidad*, *20*(1), 36-46. DOI: 10.1016/j.rcsar.2016.01.001

Matsumoto Nishizawa, R. (2014). Desarrollo del Modelo Servqual para la medición de la calidad del servicio en la empresa de publicidad Ayuda Experto. *Revista Perspectivas*, (34), 181-209.

Melián González, S., and Verano Tacoronte, D. (2008). Estilos de dirección de RRHH dentro de las empresas: Una cuestión de intensidad en la DRRHH. *Cuadernos de Economía y Dirección de la Empresa*, *11*(36), 151-177. DOI: 10.1016/S1138-5758(08)70066-5

Negrón González, A. M., Fleitas Triana, M. S., Gémar Castillo, G., Negrón González, J. C., García Fenton, V., and Trujillo Reyna, Y. (2018). Identificación de costos ocultos a partir de un estudio de organización del trabajo en una empresa del sector farmacéutico en Cuba. *Ingeniare. Revista Chilena de Ingeniería*, *26*(1), 6-20. DOI: 10.4067/S0718-33052018000100006

Nieves, J., and Quintana, A. (2016). Human resource practices and innovation in the hotel industry: The mediating role of human capital. *Tourism and Hospitality Research*, *18*(1), 72-83. DOI: 10.1177/1467358415624137

Pan, P. C. (2013). The evaluation of design supervision service Based on the method of SERQUAL. *Applied Mechanics and Materials*, 357-360, 2494-2497. DOI: 10.4028/www.scientific.net/AMM.357-360.2494

Pereda, S., and Berrocal, F. (2005). *Técnicas de gestión de recursos humanos por competencia*. Madrid: Editorial Universitaria Ramón Areces.

Savall, H. (2011). *Por un trabajo más humano*. Charlotte NC: IAP.

Sotolongo, M. (2005). *Procedimiento para la auditoria interna del Sistema de Gestión de Recursos Humanos en instalaciones turísticas hoteleras cubanas. Aplicación en pequeñas y medianas instalaciones turísticas hoteleras* (M.Sc. Thesis, Universidad Central "Marta Abreu" de las Villas).

Stone, D. L., and Deadrick, D. L. (2015). Challenges and opportunities affecting the future of human resource management. *Human Resource Management Review*, *25*(2), 139-145. DOI: 10.1016/j.hrmr.2015.01.003

Vardarlier, P. (2016). Strategic Approach to Human Resources Management During Crisis. *Procedia-Social and Behavioral Sciences*, 235(October), 463-472. DOI: 10.1016/j.sbspro.2016.11.057

Ingeniería e Investigación vol. 39 No. 1, April - 2019 (63-75)

DOI: http://dx.doi.org/10.15446/ing.investig.v39n1.73638

Modeling and simulation for mechanical behavior of modified biocomposite for scaffold application

Modelado y simulación para el comportamiento mecánico de un biocompuesto modificado para la aplicación de andamios

Jenan S. Kashan[1], and Saad M. Ali[2]

ABSTRACT

Bones in the human body are a natural composite material that can be fractured due to impact stress and excessive loads. Human bones become less dense and strong when age increases, thereby they become more susceptible to fracture. The present work aims to study the effect of adding nano-ceramic particles on the mechanical properties to fabricate four types of hybrids of Titanium dioxide (TiO_2) and Alumina (Al_2O_3) reinforced polyetheretherketone (PEEK) biocomposites. The objective of this study is to develop and improve the biomechanical properties of the fabricated biomaterials to withstand the loads of the daily human activities. Modeling and analysis of femur bone biomechanics were implemented by using the SOLIDWORKS 17.0 and the finite element ANSYS 15.0 software programs. The response surface methodology (RSM) technique and the Design Expert 11.0 software program were used to improve and verify the results of biomechanical performance of the fabricated biocomposites. From the current research results, it was deduce that the maximum equivalent (von-Misses) and shear stresses on the modeled femur bone are 120,93 and 60,80 MPa. The tensile for modeling the fabricated 20 vol. % TiO_2/5 vol. % Al_2O_3/PEEK biocomposite material is higher than the one of natural femur bone by 10 %. The maximum strain energy and the maximum equivalent elastic strain were reduced by 20 % and 26,09 %, respectively. The stress safety factor values increased in 5,81 %, and the fatigue life for the fabricated biocomposite is more than 40,43 %, when compared with natural femur bone material.

Keywords: Femur bone replacement, Nano PEEK, Titanium Oxide, Nano alumina, Biocomposite, RSM, ANSYS modeling, Femur bone fatigue life.

RESUMEN

Los huesos en el cuerpo humano son un material compuesto natural que puede fracturarse debido a la tensión de impacto y cargas excesivas. Los huesos humanos pierden densidad y fuerza al aumentar la edad, por lo que se vuelven más susceptibles a las fracturas. En el presente trabajo, se ha estudiado el efecto de la adición de partículas de nanocerámica en las propiedades mecánicas para fabricar cuatro tipos de híbridos de biocompuestos de polieteretercetona reforzada con dióxido de titanio (TiO_2) y alúmina (Al_2O_3). El objetivo de este estudio es desarrollar y mejorar las propiedades biomecánicas de los biomateriales fabricados para soportar las cargas de las actividades humanas diarias. El modelado y análisis de la biomecánica ósea del fémur se implementó utilizando los programas de software SOLIDWORKS 17.0 y de elementos finitos ANSYS 15.0. La técnica de metodología de superficie de respuesta (RSM) y el programa de software Design Expert 11.0 se utilizaron para mejorar y verificar los resultados de las propiedades de rendimiento biomecánico de los biocompuestos fabricados. Los principales resultados de la investigación actual deducen que el máximo equivalente (von-Misses) y las tensiones de cizallamiento en el hueso del fémur modelado son 120,93 y 60,80 MPa. La tensión para modelar el fabricado es 20 vol. % TiO_2/5 vol. El material biocompuesto % Al_2O_3/PEEK es más alto que el del hueso del fémur natural en un 10 %. La energía de tensión máxima y la máxima tensión elástica equivalente se redujeron en un 20 % y en un 26,09 %, respectivamente. Los valores del factor de seguridad de estrés aumentaron en un 5,81 %, y la vida de fatiga del biocompuesto fabricado es superior al 40,43 % en comparación con el material del hueso del fémur natural.

Palabras clave: Reemplazo del hueso del fémur, Nano PEEK, Óxido de titanio, Nano alúmina, Biocompuesto, RSM, ANSYS modelado, vida de fatiga ósea del fémur.

Received: July 22nd, 2018
Accepted: April 1st, 2019

[1]B. and M.Sc. in Production Engineering and Metallurgy, University of Technology, Baghdad, Iraq. Ph.D. in Biomaterials, University of Technology, Iraq and SPEME University of Leeds U.K. Affiliation: Full-time Assistant Professor and Scientific Assistant of the Head of Biomedical Engineering Department, University of Technology, Iraq. E-mail: 70010@uotechnology.edu.iq.
[2]B. in Production Engineering and Metallurgy, University of Technology, Iraq, M.Sc. Degree in Industrial Engineering, University of Baghdad, Iraq. Ph.D. Degree in Applied Mechanical Engineering, University of Technology, Iraq. Affiliation: Full-time Lecturer and Official Scientific and Cultural Division of Biomedical Engineering Department, University of Technology, Iraq. E-mail: 30249@uotechnology.edu.iq.

How to cite: Kashan, J. S., and Ali, S. M. (2019). Modeling and simulation for mechanical behavior of modified biocomposite for scaffold application. *Ingeniería e Investigación*, *39*(1), 63-73.
DOI: 10.15446/ing.investig.v39n1.73638

Introduction

Bones are natural composite living tissues supporting the softer parts of the human body (Maharaja *et al.*, 2013). They are approximately 60 % inorganic on a weight basis, 30 % organic, and 10 % water (Keaveny, Morgan and Yeh, 2004). Femur bone is the longest, strongest and heaviest bone in the human body with a length that is almost 26 % of the person height and a mass of about 0,455 kg (Popa, Gherghina, Tudor and Tarnita, 2006; Mughal, Khawaja and Moatamedi, 2015). The durability of biomaterials for prosthesis and orthopedic implants are of critical importance, mainly fabricated by using various alloys and metals to achieve the sufficient strength covered by the polymers biomaterials (Dhanopia and Bhargava, 2016).

Today the titanium, stainless steel, cobalt, chrome and zirconium are the most used biomaterials because of a favorable combination of corrosion resistance, mechanical properties and cost effectiveness (Shireesha, Ramana and Rao, 2013; Das and Sarangi, 2014). For artificial femur materials, different ceramic materials like alumina (Al_2O_3), hydroxyapatite, zirconia (ZrO_2), Ti6Al4V and Al_2O_3/Al FGM are widely researched for implant applications due to their good biocompatibility (Ahmed, Rahman and Adhikary, 2013; Reddy *et al.*, 2016).

Different synthetic hybrid biocompatible polymer-based matrices materials like polyethylene (PE), polyether ether ketone (PEEK), hydroxyapatite (HA), and poly methyl methacrylate (PMMA) are being used for bone scaffolds for potential load-bearing bone replacement and other biomaterial applications due to their durability, low cost, less weight, simple manufacturing, high strength and corrosion resistance. These biocomposites have also the advantages of high strength to weight-ratio, besides high specific modulus and superior fracture toughness (Bernhardt, Lode, Peters and Gelinsky, 2011; Lee *et al.*, 2012; Mohammed *et al.*, 2013; Nautiyal, Nain and Kumar, 2014).

The polyether ether ketone (PEEK) thermoplastic is an organic colorless thermoplastic polymer with its own high mechanical, thermal properties and chemical stability. The high biocompatibility of titanium dioxide (TiO_2) has a wide range of applications, for orthopedic biomaterials. The bio-inert ceramic aluminum oxide (Al_2O_3) is a chemical compound of aluminum and oxygen with high abrasion resistance and high hardness. It is commonly called alumina. Due to its high melting point, Al_2O_3 is a refractory material that naturally appears in a crystalline polymorphic phase α-Al_2O_3.

Long bones have different mechanical properties in the transverse and longitudinal directions, while loaded along different directions (Toth-Tascau, Rusu and Toader, 2010). The mechanical properties and structure understanding of natural bone is vital for developing new biomaterial bone implants. The mean fluctuating loads on the hip joint in general are expected to increase the body weight three to five times during jogging and jumping, depending on the human activities such as running, standing, sitting, staircase climbing, etc. (Mohammed *et al.*, 2013).

Bone remodeling is a complex process that involves interactions between mechanical, biochemical, and mechanic-biological parameters to explain the relationship between mechanical forces and bone structure (Bougherara, Klika, Marsik, Marik and Yahia, 2010; Yousif and Aziz, 2012). Different efforts were made to analyze the stresses experienced by the human femur and CAD models were developed (Mughal *et al.*, 2015). The 3D models of human femur were constructed by reverse engineering method and using finite element model under single, expanded loads (Zakiuddin, Khan, Roshni and Hinge, 2016).

During normal activities, the femur bone is subjected to tensile, compressive, and shear stresses. Shear stress magnitudes are relatively small, but can become significant in long bones subjected to torsion. Bone will fail along the weakest plane and this fracture plane coincides with maximum tensile stresses (Turner, Wang and Burr, 2001). The literature show that there is still a lack of predictive models despite the progress in bone remodeling and simulation using the finite element (FE) method (Hambli, 2014). The use of specific finite element models in orthopedic biomechanics still represents a challenge in the prediction of fracture risk and stress-state induced in bones under various loading conditions (Schileo, Taddei, Malandrino, Cristofolini, and Vicecont, 2007).

A limited number of researchers have worked on 3D modeling of the femur bone. In biomechanics, specific problems of the FEM are still difficult to model (*Yousif and Aziz*, 2012; Nautiyal *et al.*, 2014). Research done by Nautiyal *et al.* (2014) has explored the replacement of defective bone for a perfect design and comfort of the patient including rotation, i.e. ease for changing direction, and weight for maximizing comfort, balance and speed (Nautiyal *et al.*, 2014).

In the present work, the remarkable and promising properties of Titanium dioxide (TiO_2) and Alumina (Al_2O_3) nano-ceramic particles were added for reinforcement of polyetheretherketone (PEEK) matrices to fabricate four types of hybrid bio-composites by using the powder metallurgy process. An attempt has been made to develop and study the effect of adding these nano-ceramic particles on the mechanical properties and inflammation behavior using animal model for the fabricated bio-composites systems. The aim of this study was to improve the biomechanical properties of these fabricated biomaterials to meet the wide demands for orthopedic application, particularly in bone and hip joint replacement.

The objectives of this study also included finding the best bio-material fatigue life and stress factor of safety to withstand the daily human normal walking, running and jumping activities loads. A three-dimensional femur bone geometry was initiated by using SOLIDWORKS 17.0 and it was modeled and analyzed by using finite element ANSYS 15.0 software programs. The response surface methodology (RSM) technique and the Design Expert software program were used to improve and verify the results of biomechanical properties of the fabricated biocomposites.

Experimental Procedure

Numerical analyses of biomaterial hard tissue are closely related to the selection of biomechanical properties and of biomaterials and implants (Sherekar and Pawar, 2013). In this study, four biocomposite materials were fabricated using a polymeric matrix of PEEK powder with an average particle size of 10 μm and a density of 1,3 g/cm^3. The first material used was TiO_2 ceramic filler of 99,9 % purity, average particle size of 40 nm and particle density equal to 4,23 g/cm3. The second material used was Al_2O_3 ceramic powder of 10 nm average particle size and a density of (3,890 g/cm^3). The powders were mixed by using the micro powder ball mill mixing and grinding machine type YLK, rotated at 180 RPM for 12 h. Then, they were hot pressed at 180, 190, and 200 °C and using a compounding pressure of 30, 60, and 90 MPa, respectively.

The four mixed biocomposites were prepared for implants with different compositions with composites of 10 vol. % of TiO_2 and 90 % PEEK, 20 vol. % of TiO_2 and 80 % PEEK, 10 vol. % of TiO_2 with 5 vol. % of Al_2O_3 and 85 % PEEK, and 20 vol. % TiO_2 with 5 vol. % of Al_2O_3 and 75 % PEEK. The mechanical and physical properties of the PEEK, TiO_2 and Al_2O_3 are presented in Table 1.

Then, the prepared biocomposites were compacted by using the hot-pressing powder metallurgical technique with an applied compression pressure of 50MPa under sintering temperatures of 370, 380, 390, and 400 °C. The fabrication process parameters with the experimentally obtained mechanical properties of the fabricated biocomposites and natural bones properties are given in Table 2.

For examining the implant biological reactivity of the highest mechanical properties of the fabricated biocomposite, i.e. 20 vol. % of TiO_2 with 5 vol. % of Al_2O_3 and 75 % of PEEK, *in vivo* tests were implemented with cylindrical shapes in four breed rabbits to study the implants inflammation behavior. X-Ray radiographical examinations were implemented in all animals after 2, 4, 6 and 8 weeks, using Shimadzu digital x-ray machine grid type 2016/CRX10.

Modeling and Analyzing of Femur bone

The longest bone in human body is the femur, which is subjected to maximum deformation and compressive stresses. Finding these deformation and stress concentrations zones is very important in the femur bone implant (Amalraju and Dawood, 2012). The biomechanical behavior research on the femur bone is a hard task, since it is a live part in constant change and very complicated in terms of material properties, geometry, porosity and density. Finite element analysis (FEA) is the most reliable method among all of them (Taheri *et al.*, 2012; Mohd Sheikh, Ganorkar and Dehankar, 2016). By using finite element analysis with different simulations, the weak points of the femur can be known, thus helping in the design and biomaterial selection (Zhang, Wang, Yu and Zheng, 2017).

Table 1. Mechanical and physical properties of the PEEK, TiO_2 and Al_2O_3

Property	TiO_2 (99,6 %)	PEEK	Al_2O_3
Molar mass (g.mol^{-1})	79,87	350-500	101,96
Appearance	White solid	black	White solid
Odor	odorless	Slight	odorless
Density (g/cm^3)	4,23	1,23-1,32	3,99
Young's modulus (E) (GPa)	230-288	3,7-3,9	372,32
Tensile strength (σ_t) (MPa)	333,3-367,5	90-100	172,37
Endurance Limit (MPa)	283,5-330,7	65	2100
Compressive Strength (MPa)	660,0-3675,0	138	344,74
Shear Modulus (GPa)	90,0-112,5	1,43	144,79
Fracture Toughness (KIC)	2,4-3,3	2,7-4,3	4,0
Poisson's Ratio	0,27-0,29	0,39	0,21
Glass temperature (°C)	708,0-723,0	143	645
Melting point (°C)	1,843	343	2,072
Boiling point (°C)	2,972	-	2,977
Thermal conductivity (W/m.K)	4,8-11,8	0,25	30
Thermal Expansion (10^{-6}/K)	8,4-11,8	0,5-0,6	6,9
Solubility in water	insoluble	Insoluble	insoluble
Water absorption, 24 hours (%)		0,1	0

Source: Authors from Burgal, Peeva, Marchetti and Livingston (2015)

In this work, the geometry of the human femur bone was implemented using the 3D Solidworks 17.0 software. The modeling dimensions of the bone were taken from a plastic copy of the adult bone. The modeling and analysis of human bone were done by using Ansys Workbench 15.7. The present bone model of the long femur was assumed to be homogeneous and isotropic. The suggested model for the real human bone was represented by two sections. The epiphysis part is made of spongy cancellous (trabecular) bone covered by a thin layer of compact trabecular bone. The bone model is also considered with two sections: the upper (epiphysis) edge part includes the head, neck and trochanters and the lower (diaphysis) edge is defined as the condyles (Dash, Kishor and Panda, 2013).

Table 2. Mechanical properties obtained for the fabricated biocomposites and natural bones properties

Sp. compositions	Compact Temp. °C	Density (g/cm^3)	Modulus of elasticity (GPa)	Tensile strength (MPa)	Compressive strength (MPa)
Cortical bone (compact)	-	1,60	17,5 (**)	208(*)	195 (*)
Cancellous bone (trabecular)	-	2,08	0,1 (***)	50–100	68 (*)
10 vol.% TiO_2/PEEK	370	1,89	6	140	156
	380	1,894	6,8	150	159
	390	1,90	7	155	163
	400	1,92	7,4	162	168
20 vol.% TiO_2/PEEK	370	1,93	10	170	182
	380	1,94	11	176	185
	390	1,946	12,5	178	189
	400	1,95	13	180	194
10 vol.% TiO_2/5 vol.% Al_2O_3 /PEEK	370	2,1	15	184	203
	380	2,14	15,7	188	209
	390	2,27	17	191	212
	400	2,31	17,3	192	215
20 vol.% TiO_2/5 vol.% Al_2O_3/PEEK	370	2,32	19	210	240
	380	2,34	19,8	215	243
	390	2,36	20	218	252
	400	2,4	21	220	260

((*) MIT, 2006); ((**) Carter, Caler, Spencler and Frankel, 2017); ((***) Ibrahim, Daud, Zain, Izzawati and Bajuri, 2017)

Source: Authors

For modeling the natural femur bone composite, the process for creating the outer cortical bone part and the inner trabecular-bone part of the femur was done after importing the 3D model by creating a new part and using the freeze commands in ANSYS workbench. Then, the femur bone will appear as a complete femur bone (one piece) as shown in Figures 1a and b. The 3D finite element analysis (FEA) model of the femur bone was discretized by using a fine size volumetric meshing. To avoid unrealistic stress concentration points a mesh refinement was performed in the desired segments of the bone with higher gradients. The aim was to magnify the accuracy and ensure the quality of results, as shown in Figure 1c for modeling the natural femur bone composite and 1d and 1e for modeling the fabricated femur biocomposite bone. The number of created nodes is 39 957 and 19 480 elements.

In the present study, the stress analysis called multiphysics static structural analysis is used to determine the dynamic response of loads on the head of the femur during the hardest activity of the gait cycle (Qasim *et al.*, 2016). The bone was analyzed for stresses/forces during running and jumping activities. The femur bone was considered as an inflexible and solid condition. The resulting loads at the hip joint contact for these complicated activities are applied on the femoral head contact area and the other end lower part surface of the bone, i.e. the lateral condyle installed by a fixed support (free clamped for all degrees of freedom).

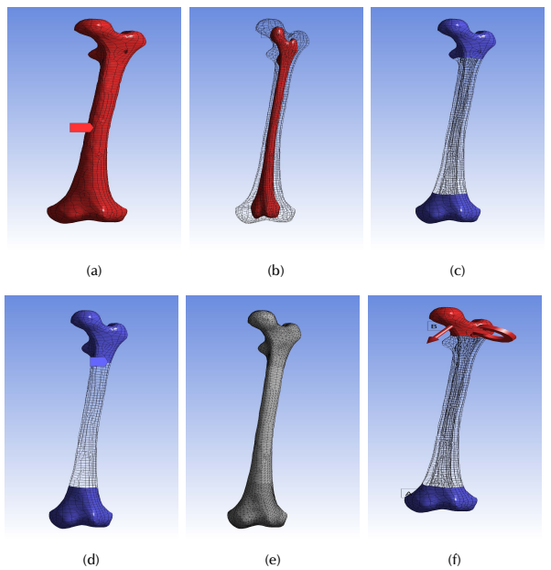

Figure 1. Modeling of femur bone: (a) natural outer part as cortical bone part; (b) natural inner part as trabecular bone; (c) mesh refinement of the natural bone; (d) mesh refinement of the fabricated biocomposite bones; (e) the resulted mesh refinement of the bones; (f) mesh refinement of the fabricated biocomposite bones.
Source: Authors

At walking activities with a speed of more than 5 km/h and during running and jumping activities, a longitudinal compressive load was simulated for an average adult male patient. Weight of 750 N was applied on the femoral head eccentrically and concentrically at the extremes with a maximum inclined angle of knee joint considered as a couple torque force (moment) of 10 N.mm applied normal to the long edge of the implant (Toth-Tascau *et al.*, 2010; Ahmed *et al.*, 2013). The applied loads components in $-x$, $-y$ and $-z$ directions are the human weight * cos 30° * tan 30°, weight * cos 30° * sin 30° and weight * cos 30° * cos 30°, respectively. The applied moment components were calculated in the same manner and directions using a moment value of 10 N.mm. The boundary conditions of the modeled femur bone are shown in Figure 1f.

Results and Discussion

The main contribution of this study is to create a simulation model that can demonstrate the highest stresses, strains distribution and fatigue failure of the natural femur bone and for the fabricated nano-composites for bones replacements. The performance of the mechanical properties in the modeling results for the natural femur bone and all the fabricated biocomposites are given in Table 3.

Table 3. Results of the performance of mechanical properties for the natural femur bone and the fabricated biocomposite materials

Sp. compositions	Compact Temp. °C	Strain Energy (m.J.)	Equivalent Elastic Strain (mm/mm)	Stress Safety Factor	Fatigue Life ($x10^6$ Cycles)
Natural femur bone	-	15,612	0,0069	1,72	51,51
10 % vol. TiO_2/PEEK	370	45,54	0,0202	1,16	4,18
	380	40,18	0,0178	1,24	6,53
	390	39,03	0,0173	1,28	8,06
	400	36,92	0,0164	1,34	10,68
20 % vol. TiO_2/PEEK	370	27,32	0,0121	1,41	14,49
	380	24,84	0,0110	1,46	18,02
	390	22,86	0,0097	1,47	19,34
	400	21,02	0,0093	1,49	20,73
10 % vol. TiO_2/5 % vol. % Al_2O_3/PEEK	370	18,21	0,0081	1,52	23,77
	380	17,40	0,0069	1,56	27,17
	390	16,07	0,0071	1,58	29,96
	400	15,79	0,0070	1,59	30,94
20 % vol. TiO_2/5% vol. Al_2O_3/PEEK	370	14,38	0,0064	1,74	53,54
	380	13,80	0,0061	1,78	61,74
	390	13,66	0,0061	1,80	67,13
	400	13,01	0,0058	1,82	70,93

Source: Authors

The resulting maximum equivalent (von-Mises) and shear stresses for the applied force and moment on the modeled femur bone is 120,93 and 60,80 MPa, respectively, as shown in Figures 2a and b. These stresses increased in the middle uniform part of the bone, where fractures are expected, as confirmed by most cases of injury and fractures in various accidents. Senthil Maharaj, Maheswaran and Vasanthanathan reported that the maximum equivalent stress is generated at the middle section of the femur. It reached 65,35 MPa in the study of Maharaja *et al.* (2013), while Ahmed *et al.* (2013) concluded that the von-Mises stress distributions on the surface of the implanted femur are 128,05 MPa in stance and 1 127,8 MPa in fall.

In the present work, the experiments were designed using the response surface methodology (RSM) and the full factorial method (FFM). The results were analyzed using an analysis of variance (ANOVA) technique. Table 4 presents the ANOVA analysis of the tensile strength resulting from changing the compact temperature and the density of the fabricated biocomposite materials. The F-value of 258,81 implies that the model is significant. The 3D graphs for the tensile strength of the fabricated biocomposite materials are shown in Figure 3. These graphs show that the maximum tensile strength reached 220 MPa when modelling the fabricated 20 vol. % TiO_2/5 vol. % Al_2O_3/PEEK biocomposite material.

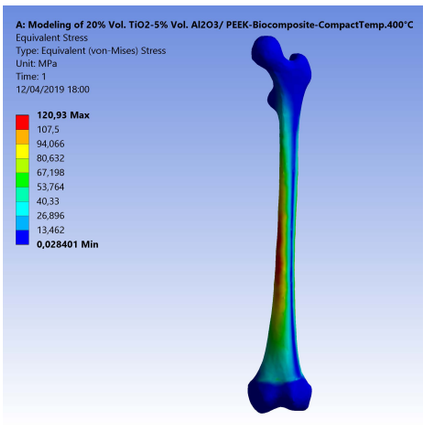

(a)

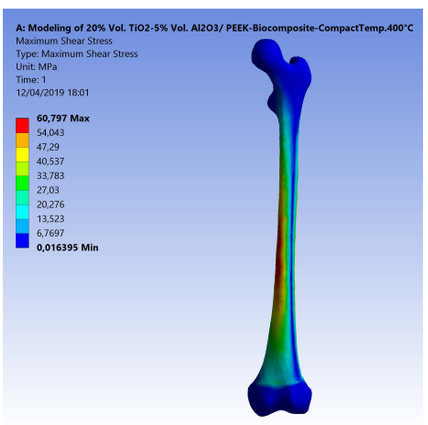

(b)

Figure 2. (a) Maximum equivalent (von-Misses) stress on the modeled femur bone; (b) Maximum shear stress.
Source: Authors

Table 4. ANOVA analysis of the tensile strength for the fabricated biocomposite materials

Source	Sum of Squares	df	Mean Square	F-value	p-value
Model	9 457,33	6	1 576,22	258,81	< 0,0001*
A-Compact Temp.	244,04	1	244,04	40,07	< 0,0001
B-Density	15,24	1	15,24	2,50	0,1448
C-Type of bio-composite	2 354,60	4	588,65	96,66	< 0,0001
Residual	60,90	10	6,09		
Cor Total	9 518,24	16			

*significant

Source: Authors

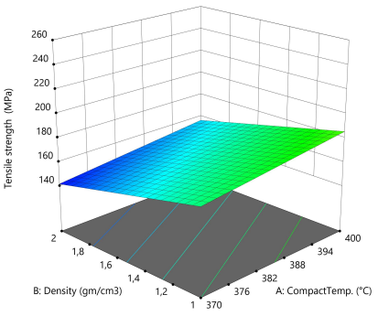

(a) 10 vol. % TiO_2/PEEK

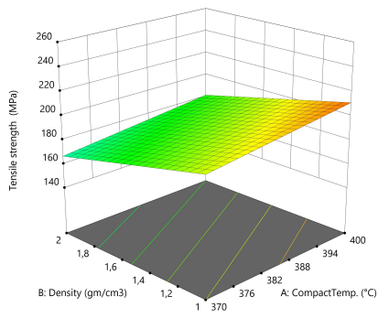

(b) 20 vol. % TiO_2/PEEK

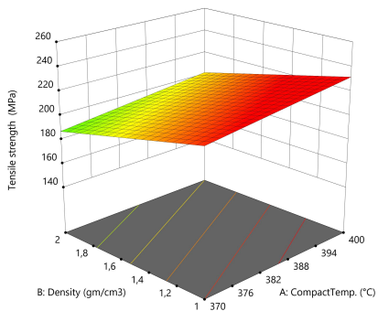

(c) 10 vol. % TiO_2/5 vol. % Al_2O_3/PEEK

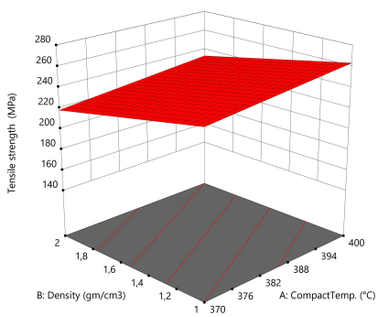

(d) 20 vol. % TiO_2/5 vol. % Al_2O_3/PEEK

Figure 3. 3D graphs for the tensile strength of the fabricated biocomposite materials.
Source: Authors

This value is higher than for natural femur bone by 10 %. The tensile strength value increased with the compact temperature during the powder metallurgical process. The increase in the density also helped to obtain higher tensile strength values because it means an increase in the molecular bouncing of the crystal structure. Increasing the proportion of titanium dioxide nano-ceramic material to the base PEEK material also increased the durability, as these materials possess high mechanical properties such as the tensile strength, endurance limit and compressive strength. This strength increased considerably by increasing the alumina particle ratios because its endurance limit and fracture toughness improved significantly. This conclusion agrees with Mohammed *et al*. (2013), whose study showed that the tensile strength of biocomposite materials increase with higher filler contents percentage of Al_2O_3 and of TiO_2.

The external mechanical work causes the elastic deformation of the femur bone structure in daily human activities, as movement is transformed into internal strain energy. The bone failure occurs when the maximum shear strain energy component is equal to the corresponding value at the yield point in the tensile test. The ANOVA analysis of the internal strain energy of the fabricated biocomposite materials are given in Table 5. The F-value of 195,28 implies that the model is significant. The 3D graphs show that the strain energy values increased with the biomaterial density and vice versa, with the tensile strength, the elastic strain and compact temperature, as shown in Figure 4.

Table 5. ANOVA analysis of the internal strain energy of the fabricated biocomposite materials

Source	Sum of Squares	df	Mean Square	F-value	p-value
Model	1 818,01	6	303,00	195,28	< 0,0001*
A-Compact Temp.	41,77	1	41,77	26,92	0,0004
B-Density	5,58	1	5,58	3,59	0,0872
C-Type of bio-composite	649,57	4	162,39	104,66	< 0,0001
Residual	15,52	10	1,55		
Cor Total	1 833,53	16			

*significant

Source: Authors

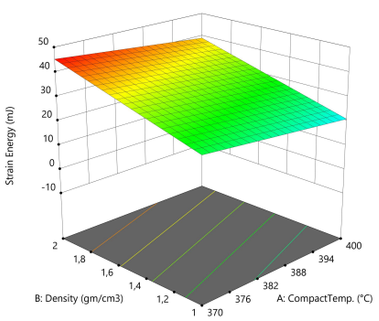

(a) 10 vol. % TiO_2/PEEK

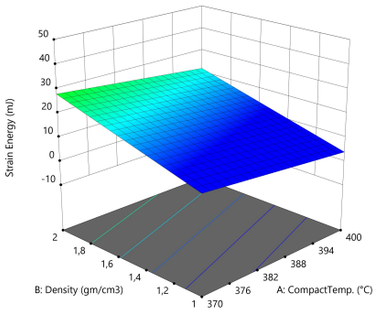

(b) 20 vol. % TiO_2/PEEK

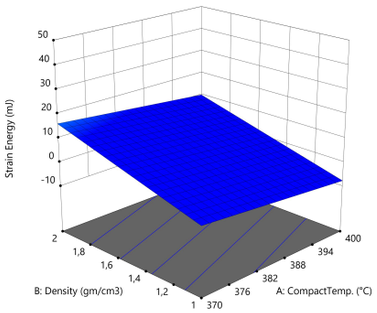

10 vol. % TiO_2/5 vol. % Al_2O_3/PEEK

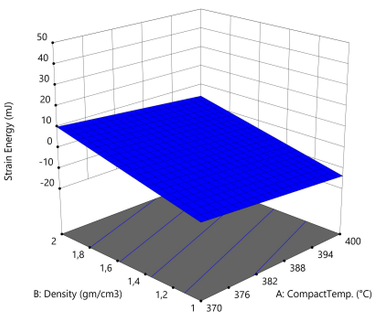

(d) 20 vol. % TiO_2/5 vol. % Al_2O_3/PEEK

Figure 4. 3D graphs for the internal strain energy of the fabricated biocomposites materials.
Source: Authors

These graphs show that the lower maximum strain energy values are due to external loadings for these complex states of stress systems. This was obtained with the model of the natural femur bone and the best fabricated biocomposite material (20 % vol. TiO_2/5 % vol. Al_2O_3/PEEK) at the highest compact temperature of 400 °C. Strain energy values were equal to 15,61 and 13,01 m.J., as shown in Figures 5a and b. The strain energy was reduced by 20 %, when compared with the natural femur bone material. This means that for this type of fabricated biocomposite material, the required value of the strain energy conversion into mechanical kinetic energy and the rising in the temperature generated is the lowest. This is in favor of patients who are fractured and injured and undergo partial repair or replacement of femur bone. For the same human weight, the maximum displacement that Amalraju *et al.* (2012) found was 0,0012 mm, and values of 0,0012 for Ti6Al4V and 0,0036 for Al_2O_3/Al FGM were reported by Ahmed *et al.* (2013).

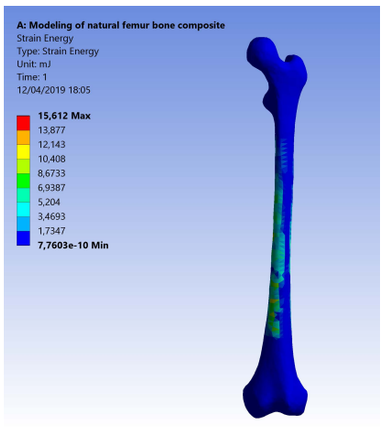

(a)

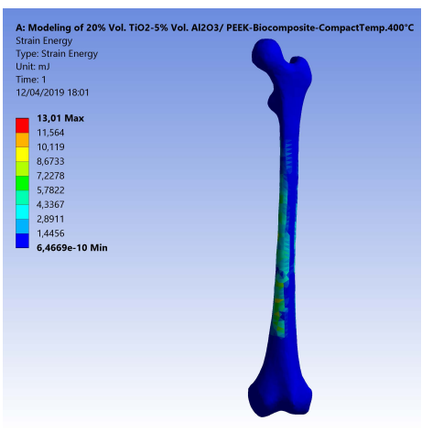

(b)

Figure 5. (a) Maximum strain energy of the natural modeled femur bone; (b) for the fabricated (20 % vol. TiO_2/5 % vol. Al_2O_3/PEEK) biocomposite at compact temperature of 400 °C.
Source: Authors

ANOVA analysis of the equivalent elastic strain and the stress safety factor values for all the examined biomaterials are listed in Tables 6 and 7. The F-values of 185,14 and 252,14 imply that the models are significant. The 3D graphs show that the equivalent elastic values increased with the decrease in the biomaterial density and in compact temperature, as shown in Figure 6. Figure 7 shows the 3D graphs of the stress safety factor values, which decreased with the increase in the biomaterial density and in compact temperature.

The maximum equivalent elastic strain and the stress safety factor values for the best fabricated (20 % vol. TiO_2/5 % vol. Al_2O_3/PEEK) biocomposite material were obtained at compact temperature of 400 °C in the simulation model, resulting from the external loads applied on the femur. These values are the lowest of all types of the fabricated biocomposite materials and for all the compact temperatures used, reaching 0,0051 mm/mm and 1,82. These equivalent elastic strain and stress

Table 6. ANOVA analysis of the equivalent elastic strain of the fabricated biocomposite materials

Source	Sum of Squares	df	Mean Square	F-value	p-value
Model	0,0004	6	0,0001	185,14	< 0,0001*
A-Compact Temp.	9,351E-06	1	9,351E-06	28,69	0,0003
B-Density	1,865E-06	1	1,865E-06	5,72	0,0378
C-Type of biocomposite	0,0001	4	0,0000	103,23	< 0,0001
Residual	3,260E-06	10	3,260E-07		
Cor Total	0,0004	16			

*significant

Source: Authors

Table 7. ANOVA analysis of the stress safety factor of the fabricated biocomposite materials

Source	Sum of Squares	df	Mean Square	F-value	p-value
Model	0,6465	6	0,1077	252,14	< 0,0001*
A-Compact Temp.	0,0157	1	0,0157	36,76	0,0001
B-Density	0,0009	1	0,0009	2,10	0,1781
C-Type of biocomposite	0,1613	4	0,0403	94,36	< 0,0001
Residual	0,0043	10	0,0004		
Cor Total	0,6508	16			

*significant

Source: Authors

safety factor values are better than the values obtained for the modeled natural composite femur bone, which reached 0,0069 mm/mm and 1,72, by 26,09 % and 5,81 %, as shown in Figures 8a and b and 9a and b, respectively. These values are highly important for helping the patient's replaced femur bone to carry higher external loads and weights and withstand any sudden dynamic movement events, which are expected to occur within the daily activities of life.

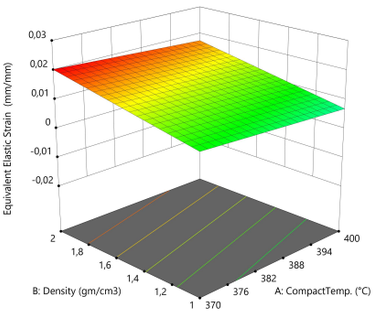

(a) 10 vol. % TiO_2/PEEK

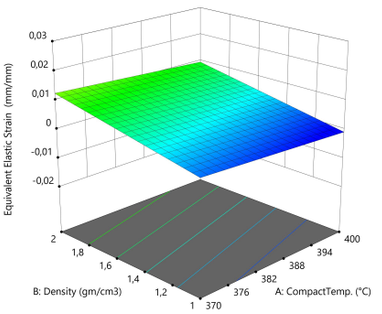

(b) 20 vol. % TiO_2/PEEK

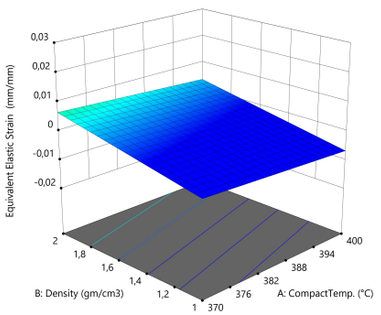

(c) 10 vol. % TiO_2/5 vol. % Al_2O_3/PEEK

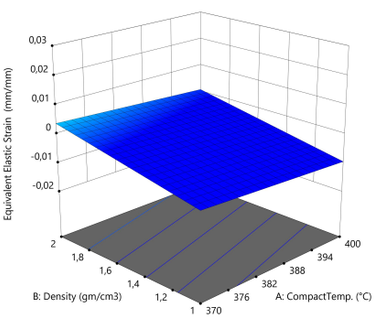

(d) 20 vol. % TiO_2/5 vol. % Al_2O_3/PEEK

Figure 6. 3D graphs for the equivalent elastic strain of the fabricated biocomposite materials.
Source: Authors

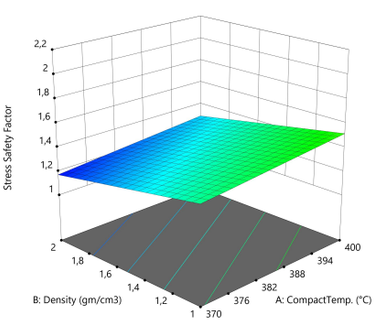

(a) 10 vol. % TiO_2/PEEK

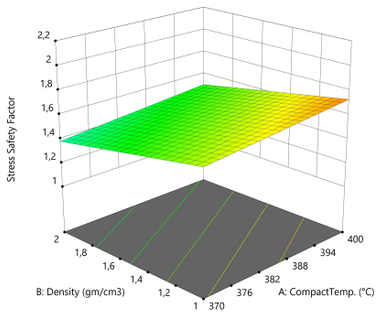

(b) 20 vol. % TiO_2/PEEK

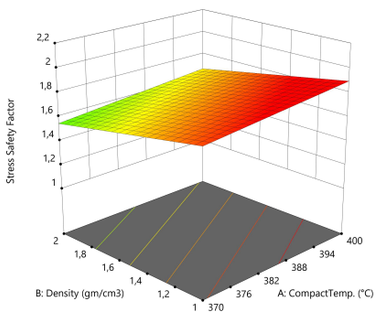

(c) 10 vol. % TiO_2/5 vol. % Al_2O_3/PEEK

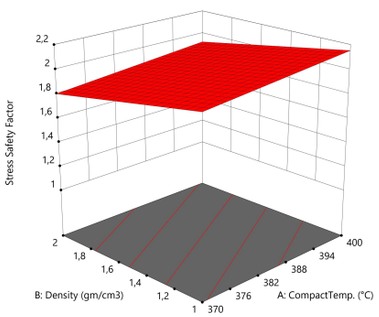

(d) 20 vol. % TiO_2/5 vol. % Al_2O_3/PEEK

Figure 7. 3D graphs for stress safety factor of the fabricated biocomposite materials.
Source: Authors

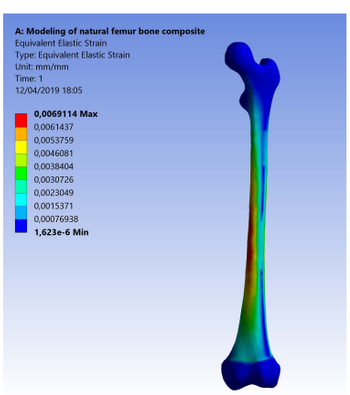

(a)

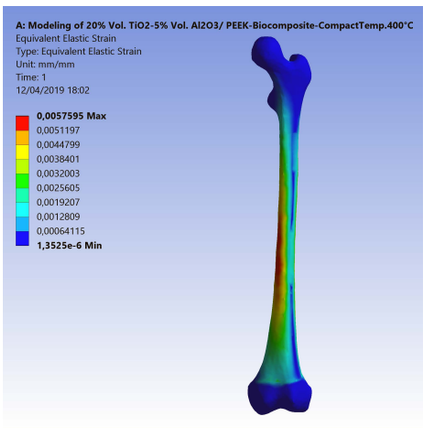

(b)

Figure 8. (a) Maximum equivalent elastic strain of the modeled natural femur bone; (b) for the fabricated biocomposite (20 % vol. TiO_2/5 % vol. Al_2O_3/PEEK) at compact temperature of 400 °C.
Source: Authors

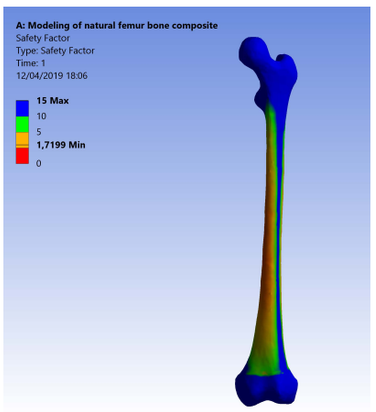

(a)

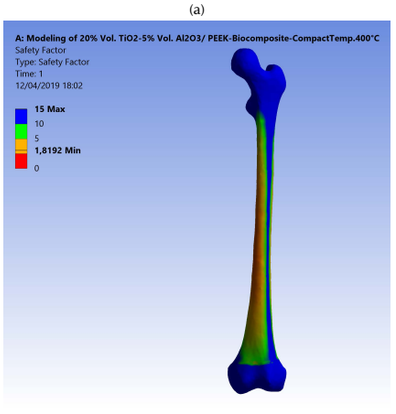

(b)

Figure 9. (a) Maximum stress safety factor of the modeled natural femur bone; (b) for the fabricated biocomposite (20 % vol. TiO_2/5 % vol. Al_2O_3/PEEK) at compact temperature of 400 °C.
Source: Authors

To calculate the fatigue lives in cycles for the natural femur bone, all the four fabricated biocomposites at all compact temperatures are used. Firstly, endurance (S'_e) should be calculated from the ultimate tensile stress (S_{ut}) values limit by using the following equation (Shigley and Mischke, 2006):

$$Endurance\ limit\ (S'_e) = 0,5 * S_{ut} \quad (1)$$

The modified endurance limit (S_e) can be found as:

$$Modified\ Endurance\ Limit\ (S_e) = S'_e * k_a * k_b * k_c * k_d * k_e * k_f \quad (2)$$

where the Surface Condition Factor (k_a) for grinding surface is equal to:

$$(k_a) = a\, S_{ut}^{b} = 1,58 * 150^{-0,085} \quad (3)$$

The size Factor (k_b) for bending and torsion (assuming that the mean diameter of the femur bone is equal to 25 mm) is:

$$(k_b) = 1,23d^{-0,107} \quad (4)$$

The loading factor (k_c) for bending and torsion is:

$$(k_c) = 1,0\ (\text{for bending load}) + 0,85\ (\text{for axial load})/2 \quad (5)$$

The temperature factor for human life (k_d) = 1. For 99 % reliability, the reliability factor corresponds to 8 % standard deviation of the endurance limit (k_e) = 0,82. The miscellaneous-effects factor (k_f) = 1. Then, the modified endurance limit (S_e) can be obtained by using equation (2). The fatigue life, i.e. the number of cycles to the failure (N) at a given fatigue stress (σ), is found as:

$$N = (1/a)^{1/b} \quad (6)$$

where:

$$a = (f\, S_{ut})^2/S_e \quad (7)$$

For $S_{ut} < 490$ MPa; $f = 0,9$:

$$B = -1/3 \log (f * S_{ut}/S_e) \quad (8)$$

The fatigue lives (σ) and the results of all the fabricated biocomposite materials were calculated for all fatigue stresses, as well as for the natural femur bone for all the stress rates, starting from the tensile strength to the endurance limit stress values with a difference of 5 MPa.

These results with the mechanical properties obtained from the experimental tests, presented in Table 2, have been introduced in the engineering date of the ANSYS 15,7 software program.

The ANOVA analyses of the values of fatigue life for the fabricated biomaterials are listed in Table 8. The model F-value of 227,69 implies that the model is significant. The 3D graphs show that the fatigue life values increased with the biomaterial density and compact temperature, as shown in Figure 10. Figure 11 shows the maximum values of fatigue lives of the modeled natural femur bone and for the best result of the fabricated biocomposite (20 % vol. TiO_2/5 % vol. Al_2O_3/PEEK) at compact temperature of 400 °C, reaching 50,51 and 70,93 x 10^6 cycles, respectively.

Table 8. ANOVA analysis of the stress safety factor of the fabricated biocomposite materials

Source	Sum of Squares	df	Mean Square	F-value	p-value
Model	7 720,65	6	1 286,77	227,69	< 0,0001*
A-Compact Temp.	92,10	1	92,10	16,30	0,0024
B-Density	0,0190	1	0,0190	0,0034	0,9549
C-Type of biocomposite	1 989,70	4	497,43	88,02	< 0,0001
Residual	56,51	10	5,65		
Cor Total	7 777,16	16			

*significant

Source: Authors

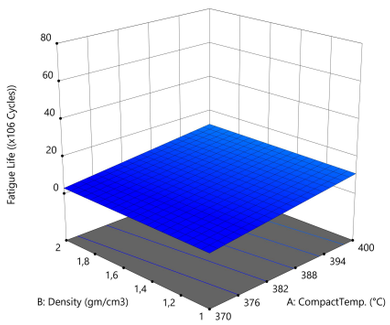

(a) 10 vol. % TiO_2/PEEK

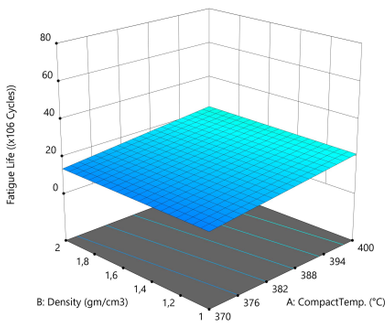

(b) 20 vol. % TiO_2/PEEK

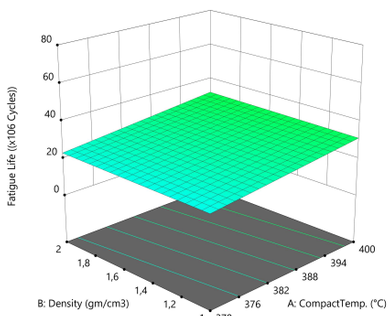

(c) 10 vol. % TiO_2/5 vol. % Al_2O_3/PEEK

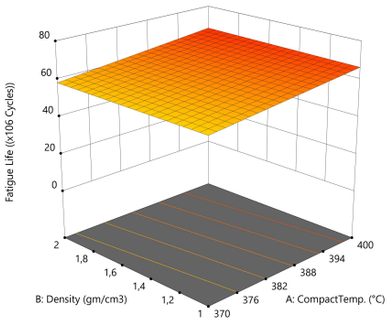

(d) 20 vol. % TiO_2/5 vol. % Al_2O_3/PEEK

Figure 10. 3D graphs for stress safety factor of the fabricated biocomposite materials.
Source: Authors

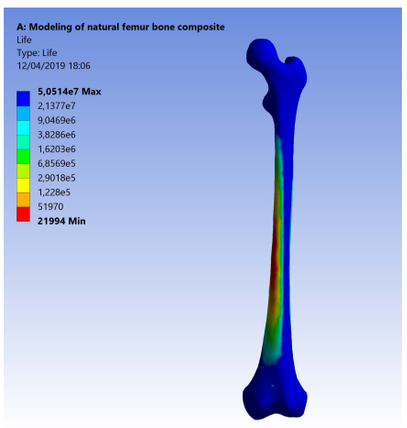

(a)

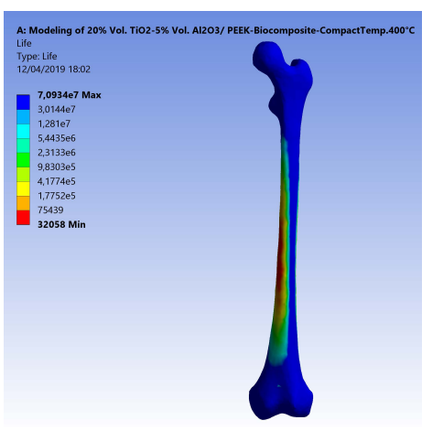

(b)

Figure 11. (a) Maximum fatigue life of the modeled natural femur bone; (b) for the fabricated biocomposite (20 % vol. TiO_2/5 % vol. Al_2O_3/PEEK) at compact temperature of 400 °C.
Source: Authors

These results show that the fatigue life for the fabricated biocomposite is 40,43 % more than that of the natural femur bone life. These results give hope to bone fractures and osteoporosis patients to use successful biocomposite substances in the *in vitro* and *in vivo* tests with good durability, flexibility and a better life performance.

Conclusions

The maximum equivalent (von-Misses) and shear stresses on the modeled femur bone are 120,93 and 60,80 MPa.

The tensile strength increased with the compact temperature and the density. The maximum tensile strength reached 220 MPa when modeling the fabricated biocomposite of 20 vol. % TiO_2/5 vol. % Al_2O_3/PEEK material. This value is higher than that for natural femur bone by 10 %.

The lower maximum strain energy values obtained with the modeled the natural femur bone and the best fabricated biocomposite (20 % vol. TiO_2/5 % vol. Al_2O_3/PEEK) at the highest compact temperature of 400 °C are equal to 15,61 and 13,01 m.J., respectively. The strain energy was reduced in 20 %, when compared with natural femur bone material.

The maximum equivalent elastic strain and the stress safety factor values for the best fabricated biocomposite (20 % vol. TiO_2/5 % vol. Al_2O_3/PEEK) at compact temperature of 400 °C reached 0,0051 mm/mm and 1,82, respectively. These equivalent elastic strains and these values are better than those obtained for the modeled natural femur bone composite by 26,09 % and 5,81 %, respectively.

The maximum values of fatigue lives for the modeled natural femur bone and for the best fatigue life result of the fabricated biocomposite (20 % vol. TiO_2/5 % vol. Al_2O_3/PEEK) at compact temperature of 400 °C reached 50,51 and 70,93 x 10^6 cycles, respectively. These results show that the fatigue life for the fabricated biocomposite is 40,43 % more than that of the natural femur bone life.

References

Ahmed, T., Rahman, M.Z. and Adhikary, D. (2013). Analysis of Al_2O_3/Al FGM as Biomaterial of Artificial Human Femoral Bone and Compare with Ti6Al4V Alloy through Computational Study. *Global Journal of Researches in Engineering*, *13*(3), 1-8. Retrieved from: https://engineering research.org/index.php/GJRE/article/view/811

Amalraju, D. and Dawood, A. K. (2012). Mechanical Strength Evaluation Analysis of Stainless Steel and Titanium Locking Plate for Femur Bone Fracture. *Engineering Science and Technology: An International Journal, 2* (3), 381-388.

Bernhardt, A., Lode, A., Peters, F. and Gelinsky, M. (2011). Novel ceramic bone replacement material Osbones in a comparative in vitro study with osteoblasts. *Clinical Oral Implants Research, 22*(6), 651-657. DOI: 10.1111/j.1600-0501.2010.02015.x

Bougherara, H., Klika, V., Marsik, F., Marik, I. A. and Yahia, L. (2010). New Predictive Model for Monitoring Bone Remodeling. *Journal of Biomedical Materials Research*, *95*(1). 9-24. DOI: 10.1002/jbm.a.32679

Budynas, R. G. and Nisbett, J. K. (2006). *Shigley's Mechanical Engineering Design* (8th ed.). New York: McGraw-Hill.

Burgal, J. S., Peeva, L., Marchetti, P. and Livingston, A. (2015). Controlling molecular weight cut-off of PEEK nanofiltration membranes using a drying method. *Journal of Membrane Science*. *493*(1), 524-538. DOI: 10.1016/j.memsci.2015.07.012

Carter, D. R., Caler, W., Spencler, D. M. and Frankel, V. H. (2009). Fatigue Behavior of Adult Cortical Bone: The Influence of Mean Strain and Strain Range. *Acta orthop Scand 52*, 481-490. DOI: 10.3109/17453678108992136

Dash, P. P., Kishor, K. and Panda, S. K. (2013). *Biomechanical Stress Analysis of Human Femur Bone*. Paper presented at the International Conference on Computer Aided Engineering, Madras, Indian Institute of Technology.

Das, S. and Sarangi, S. K. (2014). Finite Element Analysis of Femur Fracture Fixation Plates. *International Journal of Basic and Applied Biology 1*(1), 1-5.

Dhanopia, A. and Bhargava, M. (2016). Three Dimensional Virtual Modeling of Human Femur Bone with Prosthetic Plate and Screws. *International Journal of Advanced Engineering, Management and Science*, *2*(9), 1489-1494. Retrieved from: https://ijaems.com/ upload_images/issue_files/14 %20IJAEMS-SEP-2016-11-3 %20Dimensional %20Virtual %20Modelling %20of %20 Human %20Femur %20Bone %20with %20Prosthetic %20 Plate %20and %20Screws %20.pdf

Hambli, R. (2014). Connecting mechanics and bone cell activities in the bone remodeling process: an integrated finite element modeling. *Frontiers Bioengineering and Biotechnology*, *2*(6), 1-12. DOI: 10.3389/fbioe.2014.00006

Ibrahim, N. F., Daud, R., Zain, N. A., Izzawati, B. and Bajuri, Y. (2017). *Stress Interaction Analysis of Uniaxial Fixator Pins-Diaphysis Femur Bone Interface Subjected to Four-Point Bending*. Paper presented at the International Medical Device and Technology Conference, Kuala Lumpur, Universiti Teknologi Malaysia. Retrieved from: http://www.utm.my/imeditec2017/files/2017/10/P14_Stress-Interaction-Analysis-of-Uniaxial-Fixator-Pins-Diaphysis-Femur-Bone-Interface-Subjected-to-Four-Point-Bending.pdf

Keaveny, T. M., Morgan, E. F. and Yeh, O. C. (2004). Bone Mechanics. In: Kutz, Myer. *Standard Handbook of Biomedical Engineering and Design*. Bone Mechanics. New York: McGraw-Hill.

Kumar, N., Tandon, T., Silori, P. and Shaikh, A. (2015). *Biomechanical stress analysis of a Human Femur bone using ANSYS*. Paper presented at the 4th International Conference on Materials, Hyderabad, Institute of Engineering and Technology. DOI: 10.1016/j.matpr.2015.07.211

Lee, S., Porter, M., Wasko, S., Lau, G., Chen, P., Novitskaya, E. E., Tomsia, A. P., Almutairi, A., Meyers, M. A. and McKittrick, J. (2012). *Potential Bone Replacement Materials Prepared by Two Methods*. Paper presented at the Symposium LL/MM – Gels and Biomedical Materials, Warrendale, Pa, Materials Research Society. DOI: 10.1557/opl.2012.671

Massachusetts Institute of Technology – MIT (Producer) (2006). Topic 21: Biomaterials for Organ Replacement. In: 3.051J/20.340J - *Materials for Biomedical Applications* [Online course]. Retrieved from: https://ocw.mit.edu/courses/materials-science-and-engineering/3-051j-materials-for-biomedical-applications-spring-2006/index.htm

Mohammed, H., Fazlur, R., Mohammed, Y., Syed, Z., Shanawaz, P. and Tajuddin, Y. (2013). Hybrid Polymer Matrix Composites for Biomedical Applications. *International Journal of Modern Engineering Research*, *3*(2), 970-979.

Mohd Sheikh, S. A., Ganorkar, A. P. and Dehankar, R. N. (2016). Finite Element Analysis of Femoral Intramedullary Nailing. *Journal for Research*, *02*(10), 1-8. Retrieved from: http://www.journal4research.org/Article.php?manuscript=J4RV2I10003

Mughal, U. N., Khawaja, H. A. and Moatamedi, M. (2015). Finite element analysis of human femur bone. *International Journal of Multiphysics*, *9*(2), 101-108. DOI: 10.1260/1750-9548.9.2.101

Nautiyal, A. N., Nain, P. K. S. and Kumar, P. (2014). Study of Knee-Joint Mechanism before Implanting a Knee Prosthesis by Modeling and Finite Element Analysis of Knee-Joint Bones. *International Journal of Advanced Mechanical Engineering*, *4*(7), 721-727.

Popa, D., Gherghina, G., Tudor, M. and Tarnita, D. (2006). A 3D Graphical Modeling Method for Human Femur Bone. *Journal of Industrial Design and Engineering Graphics*, *1*(2), 37-40. Retrieved from: https://doaj.org/article/4545cc912b034022a5d6ff84e03880d5

Qasim, M., Farinella, G., Zhang, J., Li, X., Yang, L., Eastell, R. and Viceconti, M. (2016). Patient-specific finite element estimated femur strength as a predictor of the risk of hip fracture: the effect of methodological determinants. *Osteoporosis International 27*(9), 2815-2822. DOI: 10.1007/s00198-016-3597-4

Reddy, V. K. Ganesh, B. K. Bharathi K. C. ChittiBabu, P. (2016). Use of Finite Element Analysis to Predict Type of Bone Fractures and Fracture Risks in Femur due to Osteoporosis. *Journal of Osteoporosis and Physical Activity, 4*(3), 1-8. DOI: 10.4172/2329-9509.1000180

Schileo, E., Taddei, F., Malandrino, A., Cristofolini, L. and Vicecont, M. (2007). Subject-specific finite element models can accurately predict strain levels in long bones. *Journal of Biomechanics*, *40*(13), 2982-2989. DOI: 10.1016/j.jbiomech.2007.02.010

Senthil Maharaj, P. S., Maheswaran, R. and Vasanthanathan, A. (2013). Numerical Analysis of Fractured Femur Bone with Prosthetic Bone Plates. *Procedia Engineering*, *64*, 1242-1251. DOI: 10.1016/j.proeng.2013.09.204

Sherekar, R. M. and Pawar, A. N. (2013). Numerical Analysis of Human Femoral Bone in Different Phases. *International Journal of Engineering and Innovative Technology*, *2*(12), 76-80.

Shireesha, Y., Ramana, S. V. and Rao, P. G. (2013). Modelling and static analysis of femur bone by using different implant materials. *Journal of Mechanical and Civil Engineering*, *7*(4), 82-91. DOI: 10.9790/1684-0748291

Taheri, N. S., Blicblau, A. S. and Singh, M. (2012). Effect of different load conditions on a DHS Effect of different load conditions on a DHS Effect of different load conditions on a DHS implanted human femur. GSTF *Journal of Engineering Technology*, *1*(1), 141-146. Retrieved from: http://dl6.globalstf.org/index.php/jet/article/view/37

Toth-Tascau, M., Rusu, L. and Toader, C. (2010). Biomechanical Behavior of Implanted Long Bones. *Annals of the Oradea University. Fascicle of Management and Technological Engineering*, [*XIX* (*IX*)] 2. 283-288. DOI: 10.15660/auofmte.2010-2.1891

Turner, C. H., Wang, T. and Burr, D. B. (2001). Shear Strength and Fatigue Properties of Human Cortical Bone Determined from Pure Shear Tests. *Calcified Tissue International*, *69*(6), 373-378. DOI: 10.1007/s00223-001-1006-1

Yousif, A. E. and Aziz, M. Y. (2012). Biomechanical Analysis of the human femur bone during normal walking and standing up. *IOSR Journal of Engineering*, *2*(8), 13-19.

Zakiuddin, K., Khan, I. A., Roshni, A. and Hinge, A. (2016). A review Paper on Biomechanical Analysis of Human Femur. *International Journal of innovative research in Science and Engineering, 2*(3), 356-363.

Zhang, B., Wang, X., Yu, Y. and Zheng, J. (2017). Heterogeneous modelling and finite element analysis of the femur. *MATEC Web of Conferences*, *139*(55), 1-4. DOI: 10.1051/matecconf/201713900055

Suscripción a la Revista *I&I*

Instrucciones de Suscripción:

1. Consignar **$54 000 COP**, valor correspondiente a **1 año** y **tres ejemplares** de la revista en la cuenta **No. 01272007- 4** (No. Concepto **20181015**) a nombre del Fondo Especial de la Facultad de Ingeniería — Suscripción Revista, en cualquier oficina del **Banco Popular** .
2. Enviar una copia del recibo de consignación junto con los siguientes datos:

   Suscripción a nombre de:

   Email:

   Dirección de envío (País, ciudad,...):

   Teléfono celular:

   Fecha: dd/mm/yyy

INGENIERÍA E INVESTIGACIÓN

"*Tecnología e innovación con tradición y excelencia*"

ISSN: 0120-5609 (print)
ISSN: 2248-8723 (online)
E-mail: revii_bog@unal.edu.co
Página web: http://revistas.unal.edu.co/index.php/ingeinv

UNIVERSIDAD NACIONAL DE COLOMBIA

Suscripción a la Revista *I&I*

Instrucciones de Suscripción:

1. Consignar **$54 000 COP**, valor correspondiente a **1 año** y **tres ejemplares** de la revista en la cuenta **No. 01272007- 4** (No. Concepto **20181015**) a nombre del Fondo Especial de la Facultad de Ingeniería — Suscripción Revista, en cualquier oficina del **Banco Popular** .
2. Enviar una copia del recibo de consignación junto con los siguientes datos:

   Suscripción a nombre de:

   Email:

   Dirección de envío (País, ciudad,...):

   Teléfono celular:

   Fecha: dd/mm/yyy

INGENIERÍA E INVESTIGACIÓN

"*Tecnología e innovación con tradición y excelencia*"

ISSN: 0120-5609 (print)
ISSN: 2248-8723 (online)
E-mail: revii_bog@unal.edu.co
Página web: http://revistas.unal.edu.co/index.php/ingeinv

UNIVERSIDAD NACIONAL DE COLOMBIA

Instructions for Authors

Editorial Committee reserves the copyright to printing any material and its total or partial reproduction, as well as the right to accept submitted material or reject it. It also reserves the right to make any editorial modification which it thinks fit. In such event, the author of the submitted material in question will receive the evaluators' recommendations for changes to be made in writing. If an author accepts them, the revised (or rewritten) article must be submitted with the suggested changes having been made by the date fixed by the journal to guarantee its publication in the programmed issue.

The process to be followed for publishing an article in the journal

The article must be uploaded into the journal's OJS website, see the guidelines for article submission in the Authors guide section in our website http://www.revistas.unal.edu.co/index.php/ingeinv/article/view/59291/56815. Any manuscript must be sent using journal's template (6 pages length max.) and must be accompanied by the license agreement, addressed to the journal's editor, Prof. Andrés Pavas, stating that all authors involved in the work in question agree to it being submitted for consideration in the *Ingeniería e Investigación journal*.

Article and License templates are available on:
http://www.revistas.unal.edu.co/index.php/ingeinv/index

Once an article has been received by the journal, the corresponding author will be notified by e-mail and the peer-review process will be begun. Following this evaluation, authors will then be informed whether their article has been accepted or not. If accepted, authors must deal with the respective corrections recommended by the evaluators and the Editorial Committee's final decision. If it is to be published.

Content

All articles being considered by the committee for possible publication in the *Ingeniería e Investigación journal* must consist of the following parts:

- Title, abstract and keywords must be written in Spanish and English. The title must clearly explain the contents of the article in question, written in normal title form and be preferably brief. The abstract should contain around 200 words in Spanish and English, as well as including the methods and materials used, results obtained and conclusions drawn.
- An Introduction must be given. It must describe article's general purpouse, including its main objective, referring to any previous work and the scope of the current article.
- Conclusions must be drawn. This section must provide the implication of the results found and their relationship to the proposed objective.
- Bibliographical references must be given (an explanation and example of how to set them out is given later on).
- Acknowledgements (Optional). These should be brief and mention any essential support received for carrying out the work being reported.
- Appendix (Optional).

Scientific and technological research articles must also include:

- Experimental development. This must be written giving sufficient details for the subject to be fully understood by readers, including descriptions of any procedures involved.
- Results. These must give a clear explanation and interpretation of the findings. If it is necessary, a brief, focused discussion about how given results can be interpreted.

It is required that the bibliographical references for all articles are included at the end of the article, given in alphabetical order of first authors' surnames and mentioned in the text and, since May 2014, it is asked that the authors use the American Psychological Association (APA) style for citation and references:

- Articles published in journals:

Author, A. A., Author, B. B., & Author, C. C. (year). Article title. Journal Title, volume number(issue number), page numbers.

Del Sasso, L. A., Bey, L. G. & Renzel, D. (1958). Low-scale flight ballistic measurements for guided missiles. Journal of the Aeronautical Sciences, 15(10), 605-608

Author, A. A., & Author, B. B. (year). Article title. Journal Title, volume number(issue number), page numbers. Retrieved from http://www.xxxxxxxxxxxxxxxx

Gaona, P. A. (2014). Information visualization: a proposal to improve search and access digital resources in repositories. Ingeniería e Investigación, 34(1), 83-89. Retrieved from http://www.revistas.unal.edu.co/index.php/ingeinv/article/ view/39449

- Books:

Author, A. A. & Author, B. B. (year). Title of work. Location: Publisher.

Turner, M. J., Martin, H. C. & Leible, R. C. (1964). Further development and applications of the stiffness method, Matrix Methods of Structural Analysis. New York: the Macmillan Co.

- Conference papers and symposium contributions:

Uribe, J. (1973, September). The effects of fire on the structure of Avianca building, Paper presented at National Seminar concerning Tall Buildings, Bogotá, Colombian School of Engineering.

- Theses or undergraduate projects:

Patton, F. D. (1906). Multiple modes of shear failure in rock-related materials (PhD thesis, University of Illinois).

Further information can be obtained by:

Contacting the Editorial Team (Email: revii_bog@unal.edu.co) or Prof. Andrés Pavas (Editor-in-Chief.
Email: fapavasm@unal.edu.co)

The *Ingeniería e Investigación* journal's office is located at: Ciudad Universitaria, Facultad de Ingeniería, Edificio CADE. Telefax: (57-1) 3165000 Ext. 13674. Bogotá - Colombia.